NADPH-Cytochrome P450 Oxidoreductase: Extraction of the Full-Length Protein and Methyl-TROSY NMR of the Soluble Mutants

Sara Ali Jamal Arafeh
Marquette University

NADPH-CYTOCHROME P450 OXIDOREDUCTASE: EXTRACTION OF THE FULL-LENGTH PROTEIN AND METHYL-TROSY NMR OF THE SOLUBLE MUTANTS

by

Sara Ali Jamal Arafeh, B.Sc.

A Thesis submitted to the Faculty of the Graduate School,
Marquette University,
in Partial Fulfillment of the Requirements for
the Degree of Master of Science

Milwaukee, Wisconsin

May 2018

ABSTRACT
NADPH-CYTOCHROME P450 OXIDOREDUCTASE: EXTRACTION OF THE FULL-LENGTH PROTEIN AND METHYL-TROSY NMR OF THE SOLUBLE MUTANTS

Sara Ali Jamal Arafeh

Marquette University, 2018

NADPH-cytochrome p450 oxidoreductase (CYPOR) is a membrane-bound protein in living cells. CYPOR delivers electrons to cytochrome p450 proteins (CYPs) to catalyze metabolism of drugs and synthesis of steroids. Extraction and solubilization of CYPOR from the membrane is typically done with the TritonX-100 detergent. The amount of the solubilized protein by this detergent, however, remains relatively low to structurally analyze CYPOR with NMR spectroscopy. The goal of the first project in this thesis was to optimize the amount of the extracted CYPOR from the *E. coli* membrane using various detergents and additives. To this aim, non-ionic detergents with variable hydrophobicity (TritonX-100, X-114, and X-405) and binding strength to the extracted protein (TritonX-100, TWEEN20, and Brij35) were evaluated. Besides, the combinations of TritonX-100 with CHAPS or polyamine and alkylamine additives were assessed. None of these detergents and additives extracted more of CYPOR than the typical amount extracted by TritonX-100. Thus, it was concluded that this detergent extracts all of the available and functional CYPOR. The remaining protein is probably in an unusual and aggregated form.

Understanding the details of CYPOR dynamics can be achieved by solution NMR spectroscopy. The initial step towards this goal requires NMR signal assignments of crucial residues in the protein. In this contribution, NMR analysis was performed on the soluble form of CYPOR lacking its N-terminal hydrophobic anchor (**Δ**56). Two dual cysteine mutants of this form of the protein (Q157C/Q517C and Q157C/N271C) were reacted with ^{13}C-methyl-methanethiosulfonate (^{13}C-MMTS). The resulting residue, which is ^{13}C -methylthiocysteine (^{13}C-MTC) gave strong signals in the ^{1}H-^{13}C HSQC and ^{1}H-^{13}C HMQC spectra of the mutants. The new assignment of MTC-271 at 2.46 ppm ^{1}H, 25.42 ppm ^{13}C was established besides the existing assignments of MTC-157 and MTC-517. The NMR spectra of the two mutants were highly resolved, and they lacked the middle peak. This peak was previously reported in the ^{1}H-^{13}C HMQC spectra of several **Δ**56 CYPOR mutants. It was concluded that this unspecific peak is due to sample preparation rather than the NMR technique.

ACKNOWLEDGMENTS

Sara Ali Jamal Arafeh

First and foremost, I praise and thank Allah (God) for giving me the strength, patience, and optimism to successfully complete this thesis. I cannot deny that Allah's blessings have been showered on me throughout my life. Allah emphasizes the importance of knowledge in the Holy Qur'an, and this was the primary reason for my decision to pursue my master's studies. Allah says in the Holy Qur'an: "Allah will raise the believers among you, and those given knowledge, to high ranks; and Allah is aware of your deeds." (Quran 58:11). Besides, Prophet Mohammed, peace be upon him, said: "A person who follows a path for acquiring knowledge, Allah will make easy the passage to paradise for him."

I would like to express my deepest appreciation to my advisor, Dr. Evgenii Kovrigin, for his guidance, support, and kindness throughout my graduate career in Marquette University. Dr. Kovrigin has given me a golden opportunity to master my biochemical and biophysical skills in his lab by conducting several vital projects. His constant supervision and weekly lab meetings have boosted my troubleshooting skills in the lab.

Furthermore, I am grateful to my committee members, Dr. Nicholas Reiter, Dr. Chieu Tran, and Dr. Qadir Timerghazin, for their valuable insight and feedback. Additionally, I would like to express my gratitude to my current and past group members, Azamat Galiakhmetov and Dr. Anna Shishina, for their advice and friendship during my time in Marquette University.

A very special gratitude goes out to my mother, Dr. Alia Arafeh, for providing me with unfailing support and continuous encouragement throughout my years of study, both bachelor's and master's, in the United States. I strongly believe that my accomplishments and successes would have been impossible without her blessing prayers and innumerable sacrifices since I was born.

My sincere thanks go out to my father, Dr. Ali Arafeh, and my brother, Jamal Arafeh, for encouraging me to pursue my graduate studies in the United States. I would remiss if I did not express my special appreciation to my lovely grandmother, Amneh Samarah, and all of my relatives in Jordan for their warm welcome when I visit them.

TABLE OF CONTENTS

LIST OF TABLES

LIST OF FIGURES

Chapter 1

INTRODUCTION

1.1 STRUCTURE OF CYPOR

NADPH-cytochrome p450 oxidoreductase (CYPOR, CPR, or POR) is a 78 kDa membrane-bound protein that is found in the cytoplasmic side of the endoplasmic reticulum (ER) of the living cell.[1] It is a flavoprotein because it contains the flavin mononucleotide (FMN) and the flavin adenine dinucleotide (FAD) cofactors (**Figure 1.1., A** and **B**, respectively**)** in its structure.[2] CYPOR (**Figure 1.2.**) is composed of three structural domains: the FMN domain, the connecting domain, and the FAD domain, which contains a binding site for the nicotinamide adenine dinucleotide phosphate (NADPH) (**Figure 1.1., C**).[1] Thus, throughout the following text, the FAD/NADP(H) domain will be used instead of the FAD domain for the sake of accuracy. There is also a flexible hinge region in CYPOR that connects the FMN domain to the rest of the domains in this enzyme.[3] CYPOR is connected to the ER membrane via a hydrophobic N-terminal anchoring region. The molecular weight of the three main domains of CYPOR is 72 kDa, while that of the hydrophobic N-terminal anchor is 6 kDa.[4]

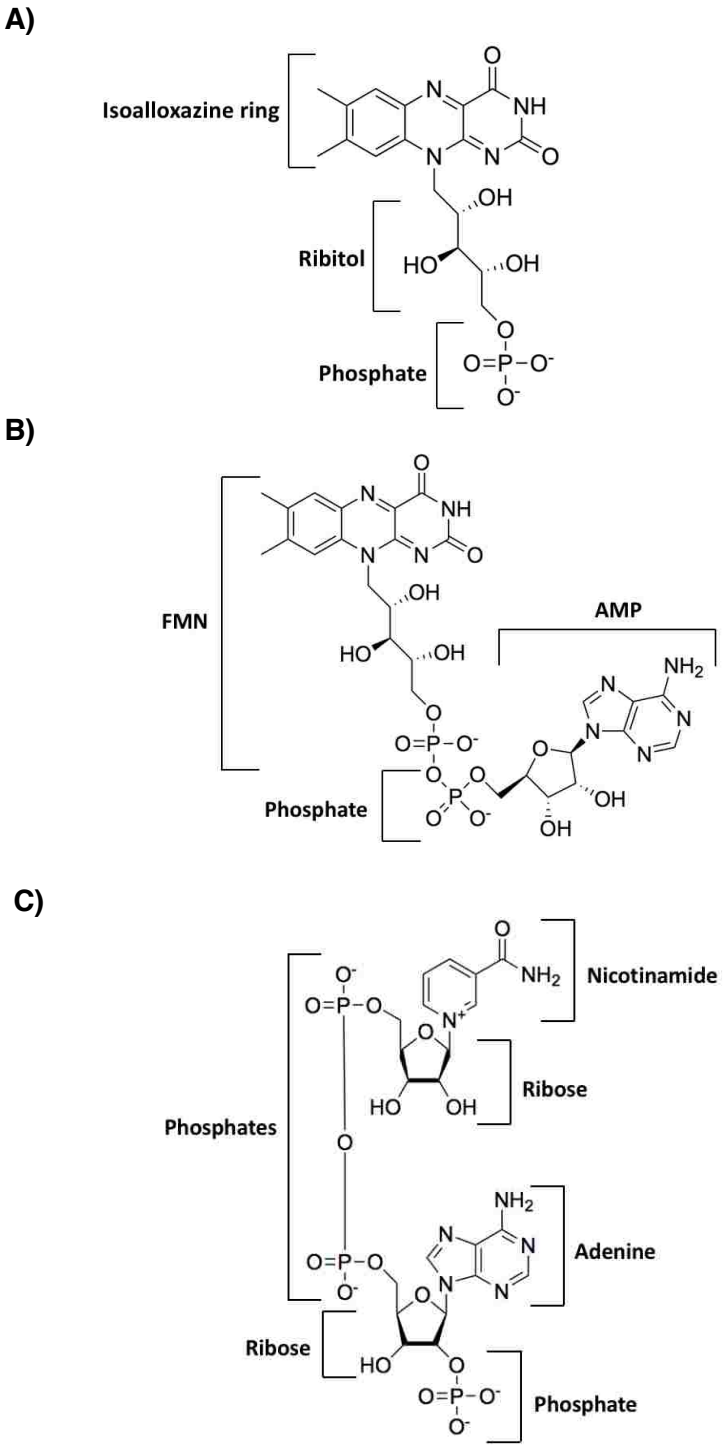

Figure 1.1. Molecular structures of the flavins and NADPH. FMN (**A**) is composed of an isoalloxazine ring, a ribitol group, and a phosphate. FAD (**B**), is made of an FMN cofactor bridged with adenosine monophosphate (AMP) through a phosphate group.[5] NADPH (**C**) is composed of three phosphate groups, two ribose carbohydrates, an

adenine nucleobase, and a nicotinamide ring. The structures were constructed using the ChemDraw molecular editor.

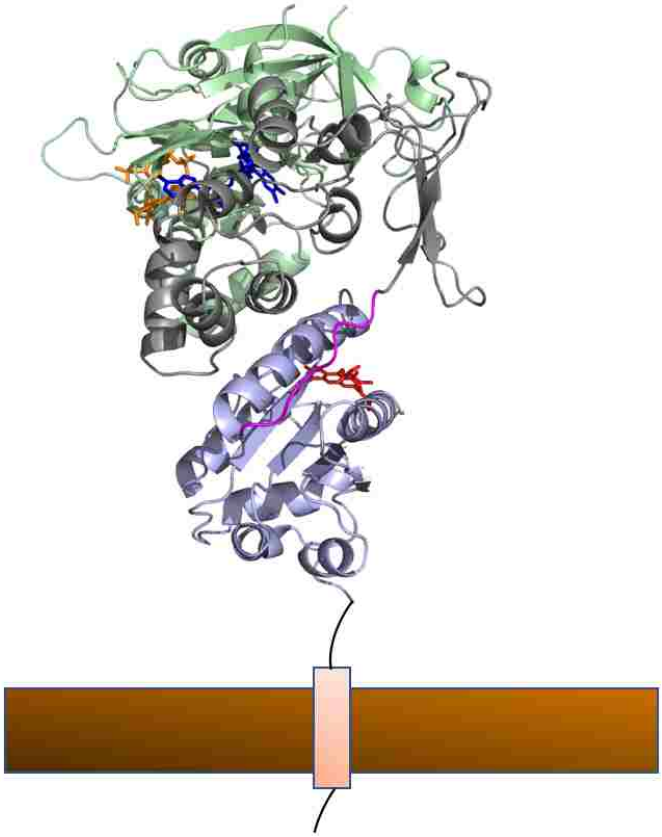

Figure 1.2. Structure of CYPOR. This protein is composed of the FMN domain (light blue), the connecting domain (grey), and the FAD/NADP(H) domain (green). The flexible hinge region (magenta) connects the FMN domain in CYPOR to the rest of the protein. The lipid bilayer is schematically depicted as a brown rectangle. The N-terminal hydrophobic anchor of the protein (absent from crystal structures) is shown as a black line outside the membrane and as a light salmon rectangle when it spans the membrane.[3] The flavins are shown in stick models: FMN (red), FAD (dark blue), and $NADP^+$ (orange). The structure was obtained from PDB ID 3ES9 and was modified using the PyMOL software.

When the amino acid sequences of rat and human CYPOR proteins were analyzed, it was suggested that this protein evolved from the fusion of two genes. One gene codes for a protein related to the FMN-containing flavodoxin (Fld), and the other codes for a protein similar to the FAD-containing ferrodoxin-$NADP^+$ oxidoreductase

(FNR).[6] Flds are electron transfer proteins which are involved in photosynthetic reactions in bacteria.[7] FNRs mediate electron transfer between $NADP^+$ and ferrodoxin during photosynthesis in plants.[8] The structures of Fld and FNR with their bound flavins (FMN and FAD, respectively) are shown in **Figure 1.3., A**. They are similar to the structures of the FMN-and FAD/NADP(H) domains of CYPOR with their bound FMN and FAD, respectively (**Figure 1.3., B**). An overlay of Fld, FNR, and CYPOR structures along with their bound flavins (**Figure 1.3., C**) confirms this fact. In some texts, the FAD/NADP(H) domain of CYPOR is referred to as the FNR-like domain.[1]

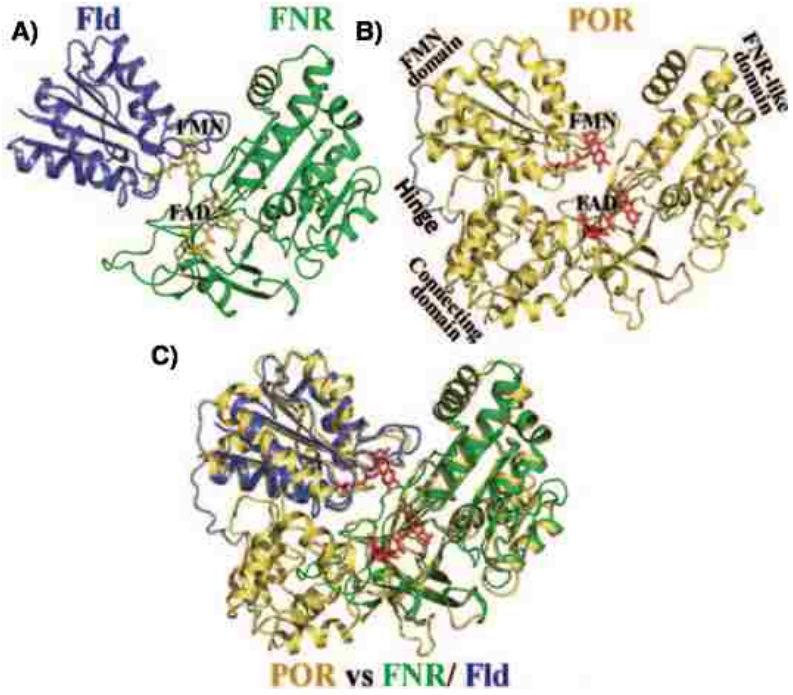

Figure 1.3. Structures of Fld, FNR, and CYPOR. Structures of Fld and FNR (**A**) are similar to the FMN and FNR-like domains of CYPOR (**B**). An overlay of these structures (**C**) confirms this fact. FAD and FMN cofactors are depicted as stick models; those bound to Fld and FNR are colored yellow, while those bound to CYPOR are colored red. Note: in this figure, CYPOR is referred to as "POR".[1] Adapted from reference 1.

In CYPOR, the first 55 amino acids correspond to its N-terminal hydrophobic anchor, while amino acids 77-228 correspond to the protein's FMN domain.[6] The

FAD/NADP(H) domain corresponds to amino acids 267-325 and 450-678. The amino acids 244-266 and 326-450 are found in the protein's connecting domain, which is interspersed within the FAD/NADP(H) domain.[6] This means that the FMN domain of CYPOR is located at the N-terminus, while the FAD/NADP(H) domain is found at the C-terminus of the protein.[4] **Figure 1.4.** illustrates the topology (**Figure 1.4., A**) and linear (**Figure 1.4., B**) diagrams for the amino acid positions and domain arrangements in CYPOR.[4] From the N-to the C-termini in both diagrams, there are: the FMN domain, the connecting domain, and the FAD/NADP(H) domain.

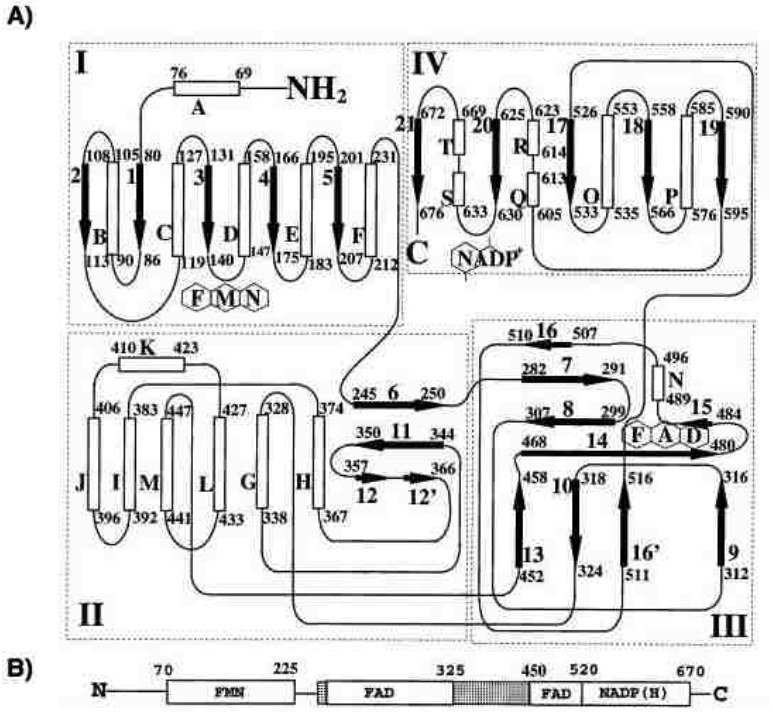

Figure 1.4. Amino acid sequence and domain arrangement in CYPOR. In the topology diagram (**A**), the numbered filled arrows are beta sheets, while the lettered empty cylinders are alpha helices. The lines that connect these secondary structural elements represent random coils. From the N-to the C-termini in this diagram, there are the FMN domain (**I**), the connecting domain (**II**), and the FAD/NADP(H) domain (**III** and **IV**). In the linear diagram (**B**), the FMN and FAD/NADP(H) domains are shown as boxes, and the connecting domain is shown as stippled boxes. The numbers above these boxes illustrate the amino acid positions in these domains. Adapted from reference 4.

In the topology diagram (**Figure 1.4., A**), the FMN domain starts at the N-terminus of the protein in a region around alpha helix "A" (**Figure 1.4., A**, panel **I**)**.** Then, the amino acid sequence of the connecting domain starts with beta sheet "6" (**Figure 1.4., A**, panel **II**), but after a few amino acids, the sequence for the FAD/NADP(H) domain starts with beta sheet "7" (**Figure 1.4., A**, panel **III**). The sequence of this domain ends temporarily in a region around beta sheet "10" so that the connecting domain sequence starts again via alpha helix "G". The sequence of the connecting domain ends around alpha helix "M" so that the sequence of the FAD/NADP(H) domain resumes with beta sheet "13". The final amino acids of this domain form beta sheet "16'", and the sequence of the $NADP^+$ binding site starts with beta sheet "17" (**Figure 1.4., A**, panel **IV**). After passing through many amino acids in this site, the sequence of CYPOR ends with beta sheet "21" at the C-terminus of the protein.

The idea from the topology diagram is simplified in the linear diagram (**Figure 1.4., B**). The FMN domain is located between amino acids 70-225, and after that, the connecting and FAD/NADP(H) domains start to loop into each other several times. The amino acids 325-450 of the connecting domain are located in the middle of the FAD/NADP(H) domain's amino acid sequence. The $NADP^+$ binding site in the protein is composed of amino acids 520-670.[4] From these two diagrams, it is evident that domain arrangement in CYPOR is not just "beads on a string" but rather a more complicated structure.

1.2 ELECTRON TRANSFER IN CYPOR

The main function of CYPOR is to deliver a pair of electrons from NADPH, through the flavins, to cytochrome p450s (CYPs or P450s) and other electron acceptors.[9] Examples of these electron acceptors include cytochrome c (an artificial electron acceptor), cytochrome *b5,* and heme oxygenases. Discussions throughout this text, however, will focus on CYPs as the ultimate electron acceptors since interactions of these proteins with CYPOR are the ones generally considered for CYPOR function.

Electrons are transferred in CYPOR in three different steps: (1) NADPH to FAD, (2) FAD to FMN, and (3) FMN to CYPs.[9] **Scheme 1.1.** shows the chemical mechanism of electron transfer in CYPOR. First, NADPH binds to the FAD/NADP(H) domain of the enzyme and delivers a pair of electrons in a form of a hydride ion to the FAD cofactor, which turns into the FAD hydroquinone ($FADH_2$). $NADP^+$ forms and remains bound to the protein. Then, $FADH_2$ delivers one electron at a time to the FMN cofactor so that both FAD and FMN semiquinones (FADH and FMNH) form in a state called quasi-equilibrium (QE). In that state, the electrons are equilibrated between the flavins. After that, FADH delivers the second electron to FMNH so that the FMN hydroquinone ($FMNH_2$) forms. With excess of NADPH, FAD can be further reduced so that both $FADH_2$ and $FMNH_2$ exist in the enzyme at the same time.[10]

Scheme 1.1. Chemical mechanism of electron transfer in CYPOR. NADPH binds to the protein and delivers a hydride ion to its FAD cofactor, which delivers the electrons one at

a time to FMN. During this transfer, both flavins reach the QE state. Another NADPH can bind to the protein and reduce FAD again.[10] Scheme from reference 10.

In-depth details of this electron transfer process, which starts in the FAD/NADP(H) domain of CYPOR are discussed in **Scheme 1.2.** In this domain, the amino acids serine 457 (S457), cysteine 630 (C630), and aspartate 675 (D675) interact with each other via hydrogen bonds and salt bridges.[2] Besides, the indole ring of tryptophan 677 (W677) covers the *re*-face of the isoalloxazine ring of FAD (**Scheme 1.2.,** Panel **I**). The negatively charged 2'-phospho-AMP region of NADPH binds to the positively charged amino acids that line its binding site in the domain via electrostatic interactions. Subsequently, the nicotinamide ring of NADPH displaces the indole ring of W677, and it anchors itself in the active site of the enzyme against the *re-face* of the FAD isoalloxazine ring. The amino acids S457 and D675 form hydrogen bonds with the carboxamide group of the nicotinamide ring, while C630 forms van der Waal interactions with it (**Scheme 1.2.,** Panel **II**). These interactions facilitate cofactor binding and the orientation necessary for hydride transfer. Upon oxidation of NADPH, the nicotinamide ring of $NADP^+$ is displaced by the indole ring of W677. This allows D675 to return to its original position, where it forms hydrogen bonds with S457 and C630 (**Scheme 1.2.,** Panel **III**). Then, the electrons are transferred to the FMN cofactor one at a time. Afterwards, the bound $NADP^+$ in the enzyme (**Scheme 1.2.,** Panel **IV**) is released, and this recycles CYPOR back to the NADPH-free state. The water molecules (WAT) in this scheme form hydrogen bonds with N-1 and O-2 atoms of the FAD isoalloxazine ring. This facilitates protonation and deprotonation during catalysis, and it stabilizes the FAD seqmiuonone.[2]

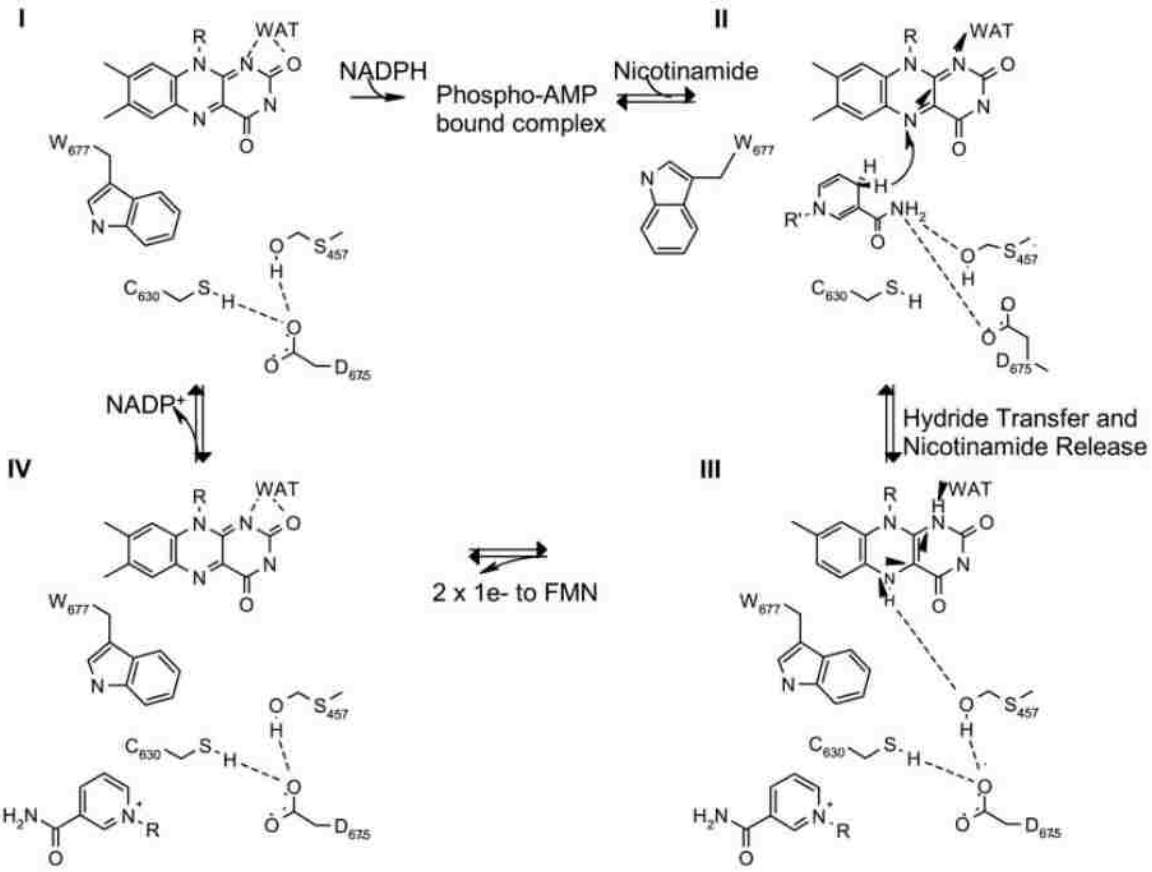

Scheme 1.2. Electron transfer in the FAD/NADP(H) domain of CYPOR. In the NADP(H)-free state of the protein, S457, C630, and D675 form hydrogen bonds and salt bridges with each other, and the indole ring of W677 is at the *re*-face of the isoalloxazine ring of FAD (**I**). The nicotinamide ring of NADPH displaces the indole ring of W677 and delivers its electrons to the FAD isoalloxazine ring (**II**). Electron transfer continues along this ring in FAD, and the indole ring of W677 displaces the nicotinamide ring of $NADP^+$ (**III**). Following electron transfer to FMN, the bound $NADP^+$ (**IV**) is released so that the enzyme returns to its NADP(H)-free state. The water molecules (WAT) facilitate electron transfer during catalysis.[2] Scheme from reference 2.

The FMN cofactor delivers the electrons it receives to CYPs, which use them to catalyze the oxidation of endogenous and exogenous substrates such as metabolism of drugs and vitamins.[11] It is worth to mention that electrons are delivered to CYPs one at a time because the iron (III) protoporphyrin-IX (heme) (**Figure 1.5.**) in the active site of these proteins is a one electron acceptor.[1] The ferric iron (Fe^{3+}) of heme is linked to CYP

via the sulfur atom of a cysteine residue in the protein.[12] The first electron reduces Fe^{3+} of CYPs into the ferrous form (Fe^{2+}), which binds to a molecular oxygen (O_2) to form the oxyferrous protein (Fe^{3+}-O^{-}_2). The other electron reduces the oxyferrous form into the peroxo species (Fe^{3+}-O^{2-}_2).[11] In the catalytic cycle of CYPs, the oxygen-oxygen bond of this species is split by two protons (H^+).[13] One oxygen atom is inserted into the hydrocarbon substrate (RH) to form the oxidized product (ROH), while the other oxygen is reduced to a water moelcule (H_2O) as shown in **Equation 1.1.**[6]

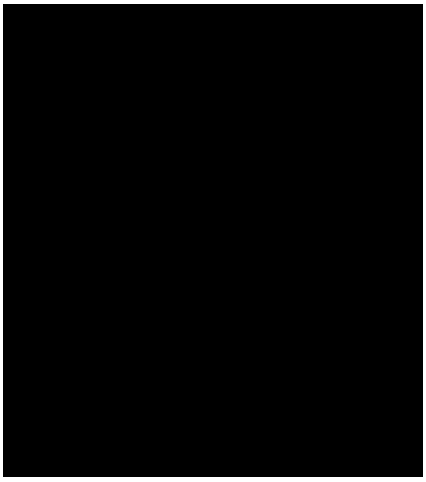

Figure 1.5. Structure of iron (III) protoporphyrin-IX in CYP.[12] Fe^{III} in this heme is attached to the sulfur atom of a cysteine residue in CYP. Figure from reference 12.

$$NADPH + RH + O_2 + H^+ \rightarrow NADP^+ + ROH + H_2O$$

Equation 1.1. Substrate oxidation by CYP proteins. These proteins utilize the electrons from NADPH as well as protons (H^+) to activate O_2. One oxygen atom is inserted into the substrate (RH) to form the oxidized product (ROH), while the other is reduced to H_2O.[6] Equation from reference 6.

1.3 CYPOR CONFORMATIONS

The electron transfer process in CYPOR requires a large domain motion, and this was confirmed by Xia et al. in 2011. This group engineered a disulfide bond between the

FMN and FAD/NADP(H) domains of CYPOR in order to restrict its domain motion.[11] This mutant CYPOR exhibited ≥ 90% inhibition of electron transfer between the flavins as well as electron transfer from $FMNH_2$ to cytochrome c and CYPs. The group confirmed that the rotation of the FMN domain away from the FAD/NADP(H) domain is essential for CYPOR to transfer electrons from FAD to CYPs.[11] As a result of this domain motion, CYPOR adopts two major conformations (**Figure 1.6.)**.

The first one is the closed conformation, which is induced by NADPH binding. In this conformation, the hydride ion is transferred from NADPH to FAD and from FAD to FMN (inter-flavin electron transfer).[1] Here, the FAD and FMN cofactors are close to each other, and the distance between the dimethyl benzene rings of the flavins is ~ 4Å (**Figure 1.7.**).[1] In the closed conformation, FMN is buried in the core of the protein, so it is not accessible to electron acceptors.[9] The open conformation is induced by the release of $NADP^+$, and this conformation is suitable for electron transfer from FMN to CYPs.[1] Inter-flavin electron transfer is inhibited when CYPOR is in the open conformation.[10]

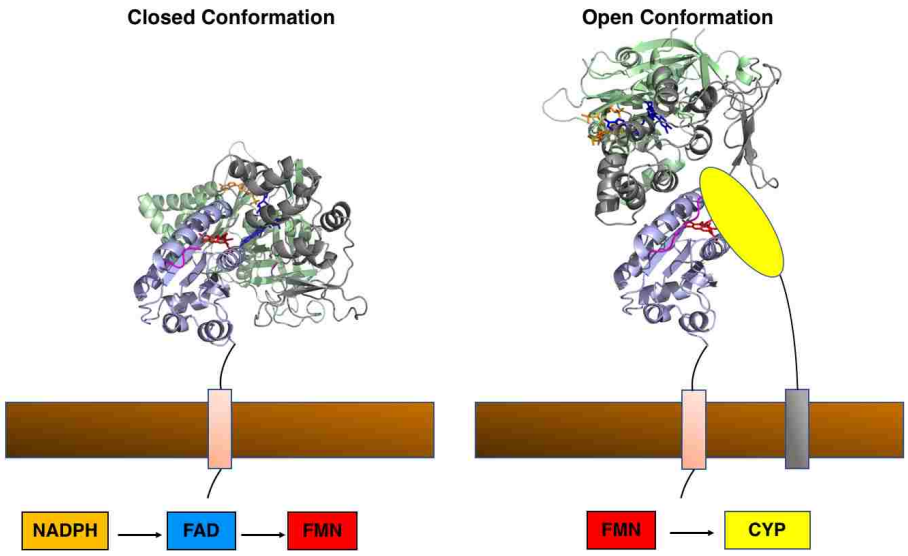

Figure 1.6. Conformations of CYPOR. When CYPOR is in the closed conformation (left), electrons are transferred from NADPH to FAD, and finally to FMN. When the

protein is in the open conformation (right), electrons are transferred from FMN to the protein's electron acceptors such as CYPs.[9] There are no crystal structures for CYPOR while it is interacting with CYPs. Thus, CYP is depicted here as an oval object that is attached to a black line, which spans the membrane via a grey rectangle. The closed and open conformations of CYPOR were obtained from PDB ID 1AMO and PDB ID 3ES9, respectively. Both conformations were modified using the PyMOL software.

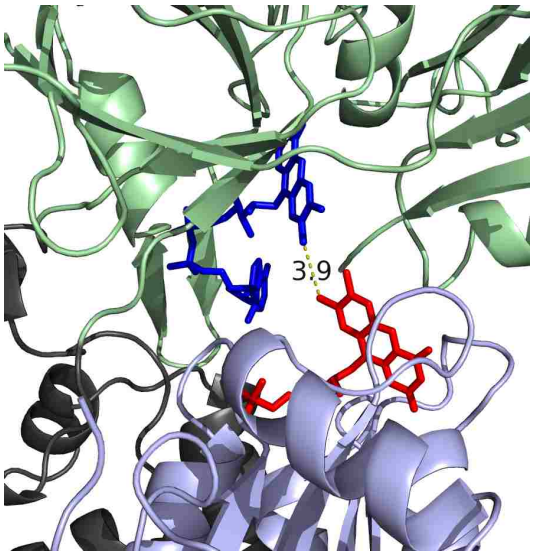

Figure 1.7. Orientation of FAD and FMN in the closed conformation of CYPOR. The distance between the dimethyl benzene rings of FAD (dark blue) and FMN (red) is ~ 4Å.[1] This diagram is adapted from the closed conformation of CYPOR, which was obtained from PDB ID 1AMO and modified using the PyMOL software.

1.4 CONFORMATIONAL CHANGES AND ELECTRON TRANSFER IN CYPOR

CYPOR must repeatedly cycle between the open and closed conformations in order to allow the un-interrupted electron transfer from NADPH to its electron acceptors.[14] NMR and X-ray scattering studies confirm that the oxidized CYPOR exists as an equilibrium between the open and closed conformations, while the reduced protein exists predominately in the closed conformation.[15] **Figure 1.8.** illustrates the relationship between CYPOR's conformational transitions and electron transfer in this enzyme. NADPH binds to the oxidized protein (oxidized CYPOR) in the closed conformation, and

this results in the formation of the oxidized (CYPOR.NADPH) complex. This is followed by the hydride ion transfer from NADPH to this enzyme. The protein becomes 2-electron reduced ($CYPOR^{2e-}$) in the closed conformation, while $NADP^+$ is still bound to it forming the reduced ($CYPOR^{2e-}$. $NADP^+$) complex. When, $NADP^+$ leaves, the reduced protein adopts the open conformation, which is able to deliver one electron at a time to CYPs.[3]

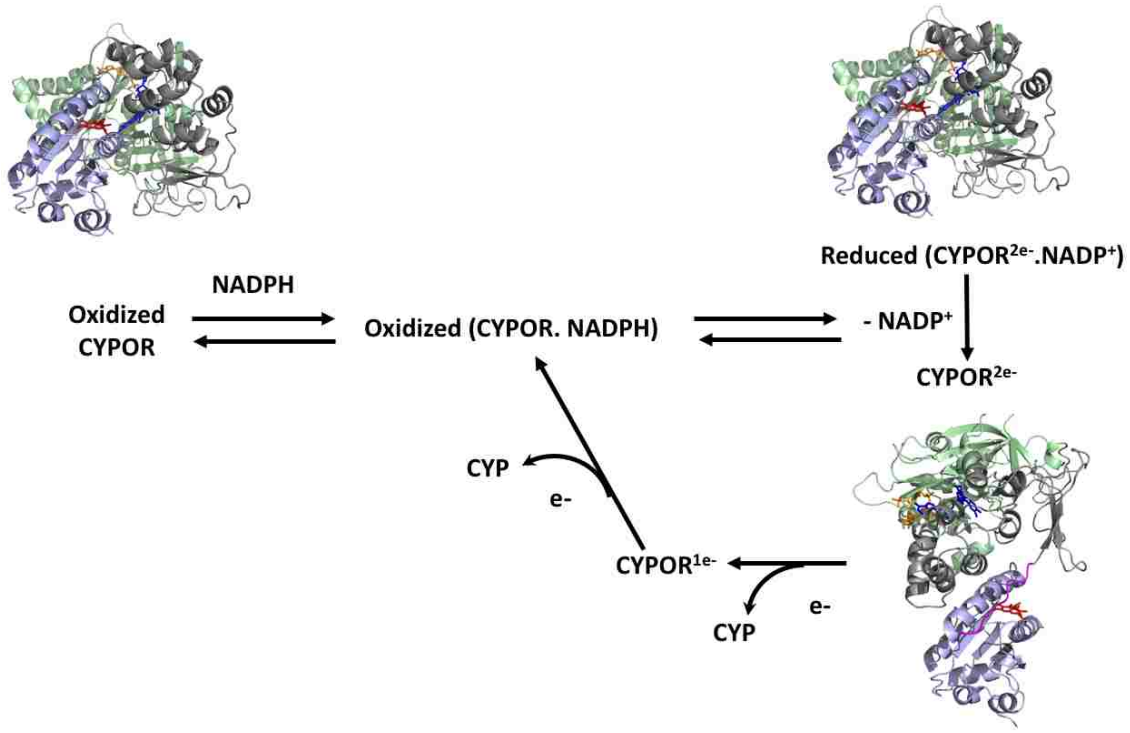

Figure 1.8. Electron transfer in CYPOR and its conformational transitions. Starting from the left, NADPH binds to the oxidized protein, which is in the closed conformation so that the oxidized (CYPOR. NADPH) complex forms. NADPH delivers two electrons to the enzyme so that the reduced ($CYPOR^{2e-}$. $NADP^+$) complex forms. When $NADP^+$ leaves, $CYPOR^{2e-}$ adopts the open conformation, which delivers one electron at a time to CYPs.[3] The structures were obtained from PDB ID 1AMO and PDB ID 3ES9 and were modified using the PyMOL software. Adapted and modified from reference 3.

Chapter 2

EXTRACTION OF RECOMBINANT FULL-LENGTH CYPOR FROM BACTERIAL MEMBRANES: OPTIMIZATION STUDY

2.1 INTRODUCTION

A. Biological Membranes

Living cells are surrounded by biological membranes (**Figure 2.1.**) which separate the interior of the cells (cytosol) from their extracellular environment.[5] These membranes are comprised mainly of lipids and proteins, and some of these biomolecules are attached to sugars.[16] Lipids are amphipathic organic compounds that have a hydrophilic head and a hydrophobic fatty acid tail. In an aqueous solution, they self-associate into a lipid bilayer where their polar head groups face the hydrophilic environment (cytosol and outside of the cell), while the hydrophobic tails form the core of the membrane.[17] Lipids exist in the membrane in three different forms: phospholipids, glycolipids, and cholesterol. The embedded proteins in this lipid bilayer regulate the flow of materials across the membrane.[16]

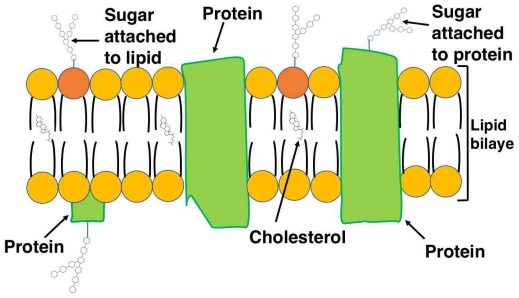

Figure 2.1. Structure of a biological membrane. The membrane is composed of lipids and proteins. Some of which are attached to sugar molecules. Lipids exist in the membrane in forms of phospholipids, glycolipids, and cholesterol molecules.[16]

B. Phospholipids, Glycolipids, and Cholesterol

Phospholipids are the major class of membrane lipids, and they contain one or two hydrophobic fatty acid chains and a hydrophilic head group.[5] This head group consists of a platform that supports the hydrophobic tails, a phosphate group, and an alcohol. When the platform is glycerol, phosphoglycerides form, which have, along with the glycerol moiety, two fatty acid tails and a phosphorylated alcohol. This alcohol group can be serine, choline, ethanolamine, inositol, or glycerol (**Figure 2.2.**). Consequently, phosphatidyl serine, phosphatidyl choline, phosphatidyl ethanolamine, phosphatidyl inositol, and diphosphatidyl glycerol form, respectively (**Figure 2.3.**). On the other hand, when the platform is sphingosine, a sphingomyelin (**Figure 2.4.**) forms which contains one fatty acid tail and a phosphorylated choline along with the sphingosine.[5]

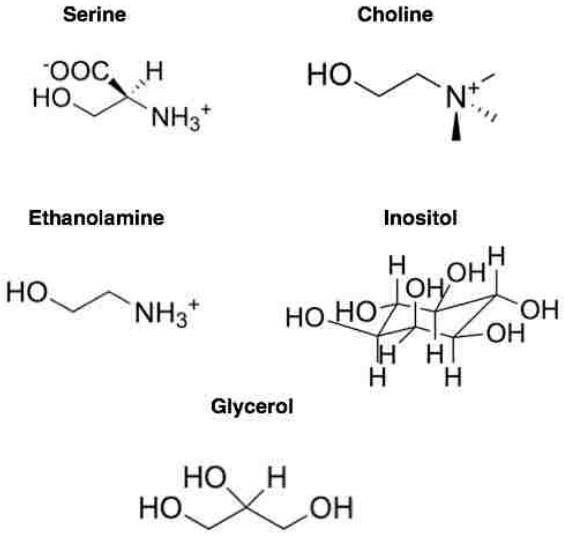

Figure 2.2. Molecular structures of alcohol moieties in phosphoglycerides. The possible alcohol groups that can be found in phosphoglycerides are serine, choline, ethanolamine, inositol, or glycerol.[5] The structures were built using the ChemDraw molecular editor.

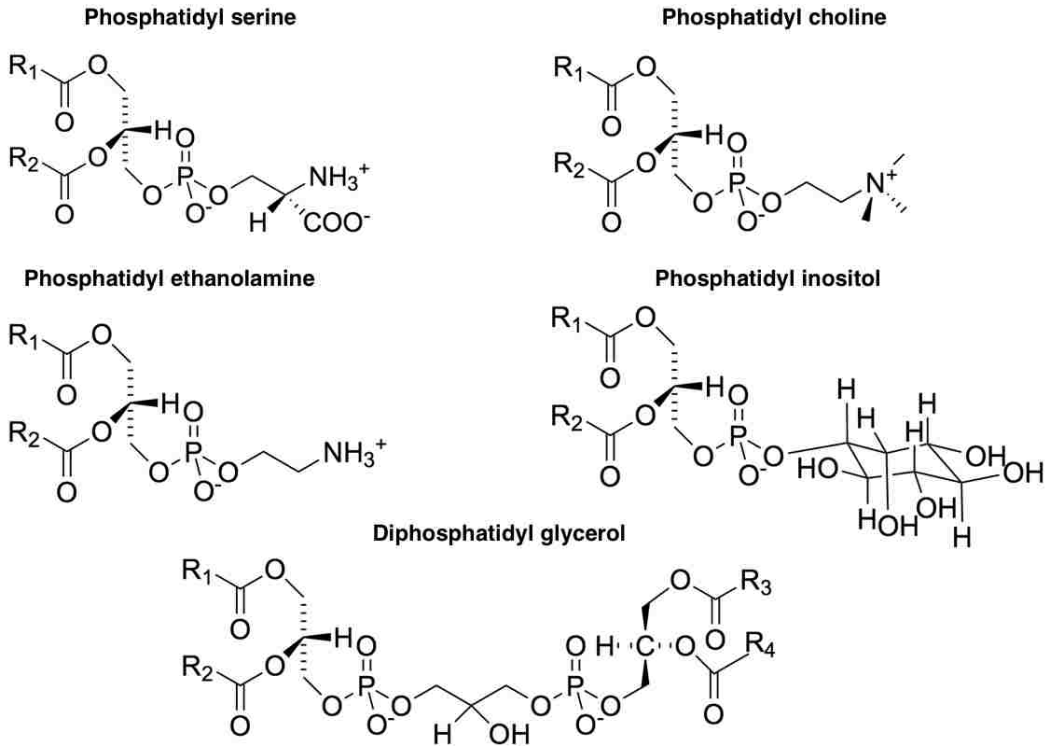

Figure 2.3. Molecular structures of phosphoglycerides. Phosphatidyl serine, phosphatidyl choline, phosphatidyl ethanolamine, phosphatidyl inositol, and diphosphatidyl glycerol have two hydrophobic fatty acid tails, a glycerol platform, a phosphate group, and an alcohol, which varies among them.[5] The structures were created using the ChemDraw molecular editor.

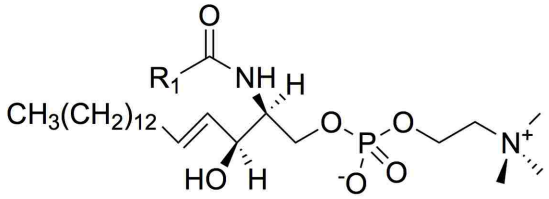

Figure 2.4. Molecular structure of a sphingomyelin. This molecule is composed of one fatty acid tail, a sphingosine platform, a phosphate group, and choline.[5] The structure was constructed using the ChemDraw molecular editor.

Glycolipids contain one fatty acid tail, a sphingosine group, as in sphingomyelin, and one or two sugars. Cerebroside is a simple glycolipid that contains a single sugar unit, which can be either glucose or galactose (**Figure 2.5.**).[5] Cholesterol, on the other hand, has a different structure from those of phospholipids and glycolipids. It contains

four linked hydrocarbon rings, a hydrophobic tail, and a hydroxyl group (**Figure 2.6.**).[5] Cholesterol molecules are found in almost all animal membranes. They are inserted in the lipid bilayer in a way where their polar hydroxyl groups interact with the hydrophilic head groups of phospholipids.[5]

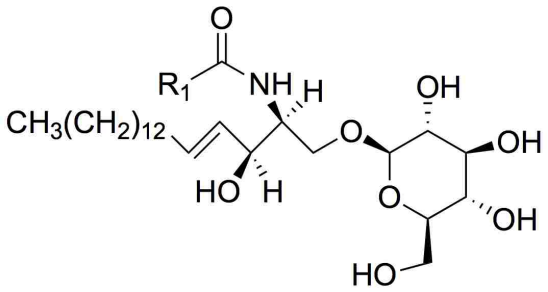

Figure 2.5. Molecular structure of cerebroside. This glycolipid contains one fatty acid chain, a sphingosine, and a single sugar unit such as glucose or galactose.[5] The structure was built using the ChemDraw molecular editor.

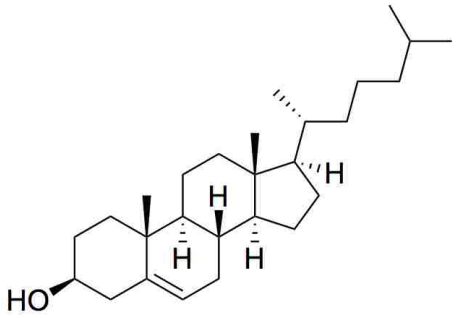

Figure 2.6. Molecular structure of cholesterol. This steroid contains four hydrocarbon rings connected to each other along with a hydrocarbon tail and a hydroxyl group.[5] The structure was constructed using the ChemDraw molecular editor.

C. Membrane Proteins

In general, proteins in the human body are classified into two major classes: soluble and membrane bound.[18] Soluble proteins are found in a watery hydrophilic environment,[19] and it is easy to express and purify them in high yields. These proteins are

relatively stable during their biophysical characterization.[18] Membrane proteins, on the other hand, are embedded in the lipid bilayer, so they are hydrophobic and have a poor solubility in aqueous solutions.[18]

Membrane proteins (**Figure 2.7.**) are encoded by ~30% of all genes in most living organisms,[20] and they fall into two major classes: peripheral (extrinsic proteins) and integral (intrinsic proteins).[5] Peripheral membrane proteins (**Figure 2.7., A**) loosely attach to the membrane via hydrophobic and electrostatic interactions with the polar head groups of their integral counterparts or the membrane lipids.[19] Integral membrane proteins (**Figure 2.7., B**), however, span the lipid bilayer via hydrophobic α helices or β sheets, which form α helical or β-barrel membrane proteins, respectively.[19]

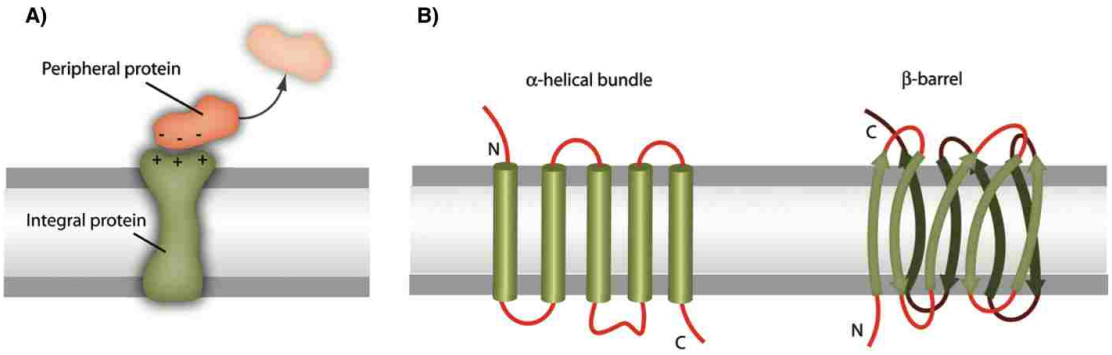

Figure 2.7. Major types of membrane proteins. Peripheral membrane proteins (**A**) form electrostatic interactions with their integral counterparts. Integral membrane proteins (**B**) span the membrane via α helices (to form the α-helical bundle) or β sheets (to form the β-barrel structure).[19] Figure from reference 19.

Membrane proteins have a variety of functions (**Figure 2.8.**) including transduction of signals in and outside the cell, transport of ions and metabolites across the membrane,[21] and cell recognition and communication.[22] Despite their importance, membrane proteins are not well-studied and characterized as much as soluble proteins. In fact, there is not much information about the three-dimensional structure of membrane

proteins and their behavior in the lipid bilayer.[23] Chae et al. estimated that there are only a few hundred resolved membrane protein structures compared to the tens of thousands of resolved soluble protein structures.[22]

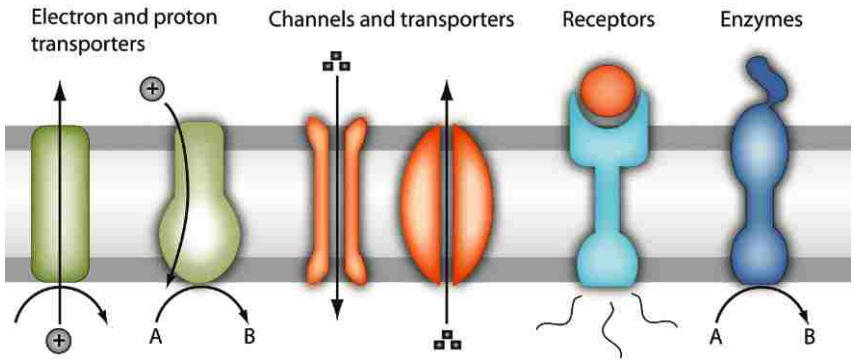

Figure 2.8. Functions of membrane proteins. These proteins transport electrons, protons, metabolites, and large molecules across the membrane. They also send signals in and outside the cell, and they catalyze various biochemical reactions.[19] Figure from reference 19.

One of the reasons that account for the relatively little knowledge on membrane proteins is their instability outside their native lipid bilayer environment.[23] In order to study the structure and function of membrane proteins, they have to be extracted and isolated from the lipid bilayer and studied in their native form and in a highly purified state.[24] The hydrophobic nature of these proteins makes them difficult to be solubilized in aqueous solutions.[22] Specifically, the hydrophobic effect minimizes the number of water molecules that are in contact with the hydrophobic transmembrane region of these proteins. As a result, these hydrophobic regions interact with each other, and this leads to the aggregation and precipitation of membrane proteins.[25]

Despite the challenges associated with studying membrane proteins, biochemists have found ways to keep such proteins soluble outside their native lipid bilayer

environment. The main idea is to provide a stable hydrophobic mimic of the lipid bilayer that is able to interact with the hydrophobic surfaces of membrane proteins. The commonly used mimics for this purpose are detergents.[21]

D. Detergents

Detergents are soluble amphipathic molecules with a hydrophilic head group and a hydrophobic tail (**Figure 2.9.**). Depending on the type of their head group, detergents can be ionic, non-ionic, or zwitterionic.[26] Ionic detergents have a charged head group (cationic or anionic) and either alkyl chain or steroidal hydrophobic structures. An example is sodium dodecyl sulfate (SDS) (**Figure 2.10., A**), which has a negatively charged sulfate head group and a hydrocarbon chain. These detergents effectively extract membrane proteins from the lipid bilayer, but they are denaturing because they disrupt the protein structure.[24]

Non-ionic detergents have a neutral head group, which contains either polyoxyethylene chains or glycosidic groups. Dodecyl glucoside (**Figure 2.10., B**) is a non-ionic detergent which has a neutral glucoside head group and a hydrocarbon chain. These detergents are non-denaturing because they disrupt the protein-lipid and lipid-lipid interactions rather than the interactions within the protein.[24] Another reason for the non-denaturing property of non-ionic detergents is recognized from the solubilization of Ca^{2+}-ATPase. Non-ionic detergents interact with and solubilize the lipid bilayer before extracting Ca^{2+}- ATPase, while ionic detergents, like SDS, extract the protein before they solubilize the lipid bilayer.[27]

Zwitterionic detergents have a neutral head group that carries negative and positive charges such as Fos-choline-8 (**Figure 2.10., C**).[24] This detergent has a positively- charged trimethylammonium group and a negatively-charged phosphate in its hydrophilic head besides the hydrocarbon tail.[28] Zwitterionic detergents are less denaturing than their ionic counterparts.[24] The overall charge of some zwitterionic detergents depends on the solution's pH and the pK of their charged groups, while others remain zwitterionic over the entire pH range.[29]

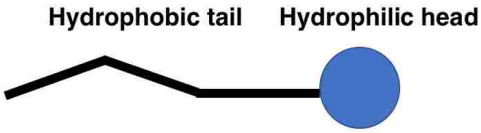

Figure 2.9. Structure of a detergent monomer. This monomer contains a hydrophilic head group and a hydrophobic tail.[24]

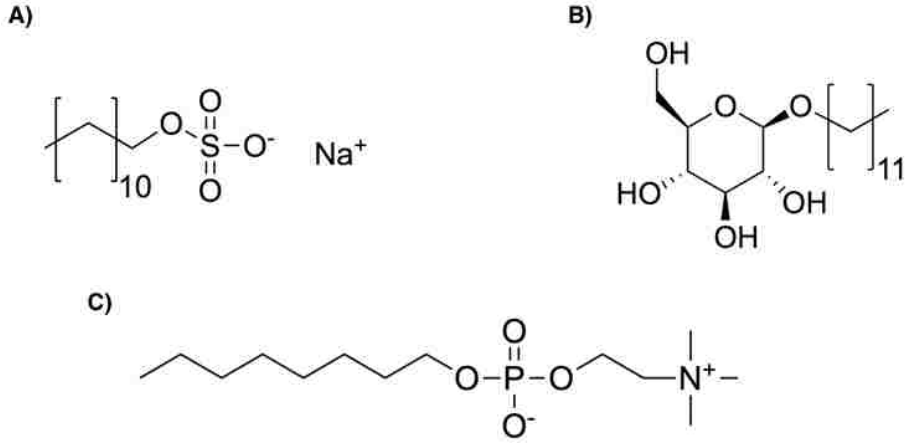

Figure 2.10. Molecular structures of various detergents. These detergents have hydrophobic hydrocarbon chains of various lengths along with different head groups. SDS (**A**) has a negatively charged sulfate head group. Dodecyl glucoside (**B**) has a neutral head group (glucose). Fos-choline-8 (**C**) has a negatively-charged phosphate and a positively-charged trimethylammonium in its head group. The structures were created using the ChemDraw molecular editor.

When detergent molecules are added to an aqueous solution, they self-associate into micelles through the hydrophobic effect (**Figure 2.11.**).[30] Particularly, their nonpolar hydrophobic tails disrupt the intermolecular hydrogen bonding network between the water molecules. Consequently, water molecules arrange around the detergent hydrophobic tails (**Figure 2.11., A**), and this decreases the system's entropy, which is thermodynamically unfavorable. As more detergent monomers are added, they self-associate into micelles (**Figure 2.11., B**), which limit the contact between the water molecules and the detergent hydrophobic tails. As a result, water molecules are dispersed, and this increases entropy in the system.[30]

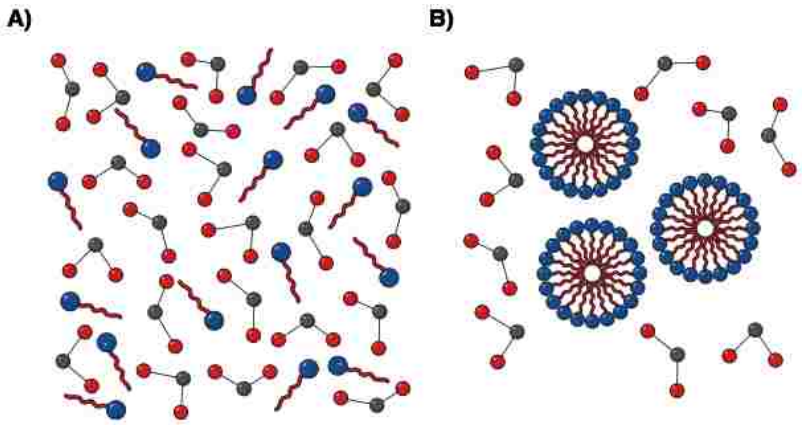

Figure 2.11. Hydrophobic effect and micelle formation. In an aqueous solution, water molecules surround the hydrophobic entities of detergent monomers (**A**). As more of these monomers are added, they self-associate into micelles and the water molecules are dispersed (**B**).[30] Adapted and modified from reference 30.

The tendency of a detergent to form micelles depends on the overall shape of its monomers, which is known as the packing parameter (P).[31] This value can be calculated for each detergent monomer using **Equation 2.1.** The P value depends on the volume and length of the detergent hydrophobic tail (v and l, respectively) as well as the volume of the hydrophilic head group (a). Detergents with small P values ($P < 1/3$) form spherical

micelles, while those with large values (P >1) form non-micellar structures. The P value explains the idea of detergent aggregation into micellar or lamellar structures. To better understand detergent behavior in aqueous solutions, other parameters are used as will be discussed. It is worth to mention that the structure of a micelle also depends on the pH, temperature, and ionic strength conditions of the surrounding medium.[31]

$$P = \frac{v}{al}$$

Equation 2.1. Calculation of the packing parameter of a detergent. The value of this parameter depends on the volume (v) and length (l) of the hydrophobic tail as well as the cross-sectional area of the hydrophilic head group (a) of a detergent monomer.[31]

The balance between the hydrophobic and hydrophilic moieties of a detergent monomer is described by the hydrophile-lipophile balance (HLB) number. This number ranges from 12-15 for detergents.[32] HLB is used to determine the hydrophilicity of a particular detergent, and its value is not measured but is calculated using **Equation 2.2.**[31] The value of HLB depends on the size and strength[33] of the hydrophilic (L) and hydrophobic (H) moieties of a detergent monomer. Detergents with low HLB values are more hydrophobic and are insoluble in water, while those with high HLB values are more hydrophilic and are soluble in water. The HLB number is inversely related to the P value; the lower the HLB, the higher the P value. For example, detergents with long hydrophobic chains (low HLB) tend to form lamellar-like structures.[34]

$$HLB = 7 + \mathcal{E}L - \mathcal{E}H$$

Equation 2.2. Calculation of the HLB value of a detergent. This value depends on the contribution from the hydrophilic region of a detergent (L) and the contribution from its hydrophobic entity (H). The values of L and H should be provided for a particular detergent before doing the calculation.[34]

The minimum concentration at which detergents form micelles is called the critical micelle concentration (CMC). Micelles form over a narrow concentration range rather than at a single concentration value.[30] The phase diagram (**Figure 2.12.**) shows that detergents exist as monomers when they are in low concentrations (below their CMC) in aqueous solutions.[32] At higher concentrations (above their CMC), they exist as micelles which are in equilibrium with the monomers. Detergent micelles aggregate into the so called "phase separation" at high temperatures. This means that detergents start to aggregate and become insoluble in water,[32] so two phases form, one is rich in detergents and the other is not.[30] When the detergent concentration is very high, lamellar and other non-micellar structures (like liquid crystalline) form. This phase diagram emphasizes the fact that temperature and detergent concentrations have a great effect on micelle formation.[32]

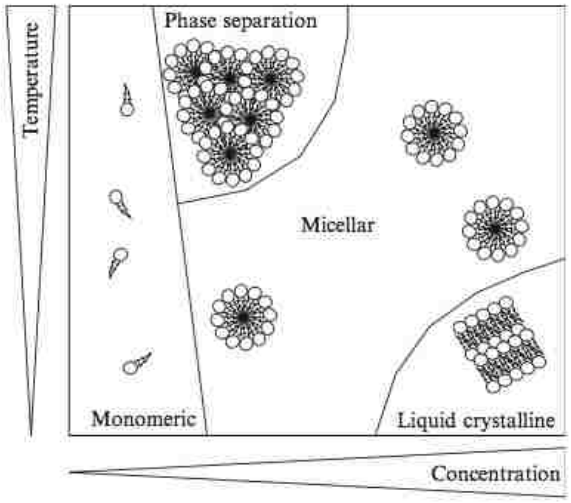

Figure 2.12. Phase diagram for dependence of micellization on temperature and detergent concentration. Detergents exist as monomers when they are at low concentrations in a solution, and they exist as micelles when they are at higher concentrations. At very high detergent concentrations, non-micellar detergent structures form like liquid crystalline. At high temperatures, detergent micelles aggregate into the "phase separation". [32] Illustration taken from reference 32.

Each detergent has its characteristic CMC, and, in general, low CMC values are common for detergents with neutral head groups (as in non-ionic and zwitterionic detergents) and those with long hydrocarbon chains.[30] These types of detergents require less monomers to form micelles. On the other hand, high CMC values are common for detergents with charged head groups (as in ionic detergents); the electrostatic repulsions between these groups require more detergent monomers to be added to form micelles.[30]

It is worth to mention that the size of a micelle can be described by the aggregation number (N).[26] This is the number of detergent monomers in a micelle, and it ranges from 50-100 for most detergents. A low N value is common for detergents with large hydrophilic groups, and they form spherical micelles. A high N value, on the contrary, is common for detergents with long hydrocarbon chains, and these form ellipsoidal micelles.[30]

The physical-chemical properties (P, HLB, CMC, and N) of detergents are important parameters in membrane protein solubilization. For example, the value of CMC indicates the binding strength between a detergent and a membrane protein.[35] In order to choose the right detergent for membrane protein solubilization, it is vital to understand how these amphiphiles interact with the membrane and membrane proteins.

E. Membrane Protein Extraction and Solubilization

The main principle of membrane protein extraction and solubilization is to disrupt the lipid bilayer where the proteins are embedded without irreversibly disrupting the structure of these proteins.[36] Upon their extraction, membrane proteins should be surrounded by a lipid-bilayer mimic to keep them solubilized in aqueous solutions. As

noted before, detergents are the commonly used means to provide a stable mimic for the lipid bilayer environment.[21] Following the formation of detergent micelles, membrane proteins incorporate into them through the hydrophobic effect. The hydrophobic regions of these proteins are surrounded by a layer of detergent molecules, while their hydrophilic groups are exposed to water.[24] Complete removal of detergents from the aqueous solution results in the dissociation of this layer. Consequently, the hydrophobic regions of membrane proteins cluster, which leads to their aggregation and precipitation.[24]

Membrane protein solubilization is hypothesized to occur in three different stages which all depend on the concentration of the detergent that is used in this process (**Figure 2.13.**). First, when the detergent concentration is below its CMC, some of the detergent monomers are free in solution.[30] Other detergent molecules, however, bind to the membrane and partition into the lipid bilayer through their hydrophobic regions.[37] Next, the lipid bilayer becomes saturated with detergent monomers, and it exists at a thermodynamic equilibrium with the detergent-lipid mixed micelles. Finally, at higher detergent concentrations (above CMC), the lipid bilayer is fully solubilized by the formation of detergent-lipid and detergent-protein mixed micelles.[37] Once membrane proteins are solubilized, the hydrophobic regions of detergents cover the hydrophobic moieties of these proteins. This prevents protein aggregation in aqueous solutions.[30]

Membrane protein extraction and solubilization by detergents are important processes that precede biochemical and physical characterization studies on the extracted proteins.[31] Considering the diversity of detergents and their different characteristics, a careful selection must be made for the appropriate detergent and solubilization conditions

to achieve an effective solubilization.[31] Making these decisions is not straightforward, however, and one must consider the compatibility of the detergents used with subsequent purification and characterization protocols.[31]

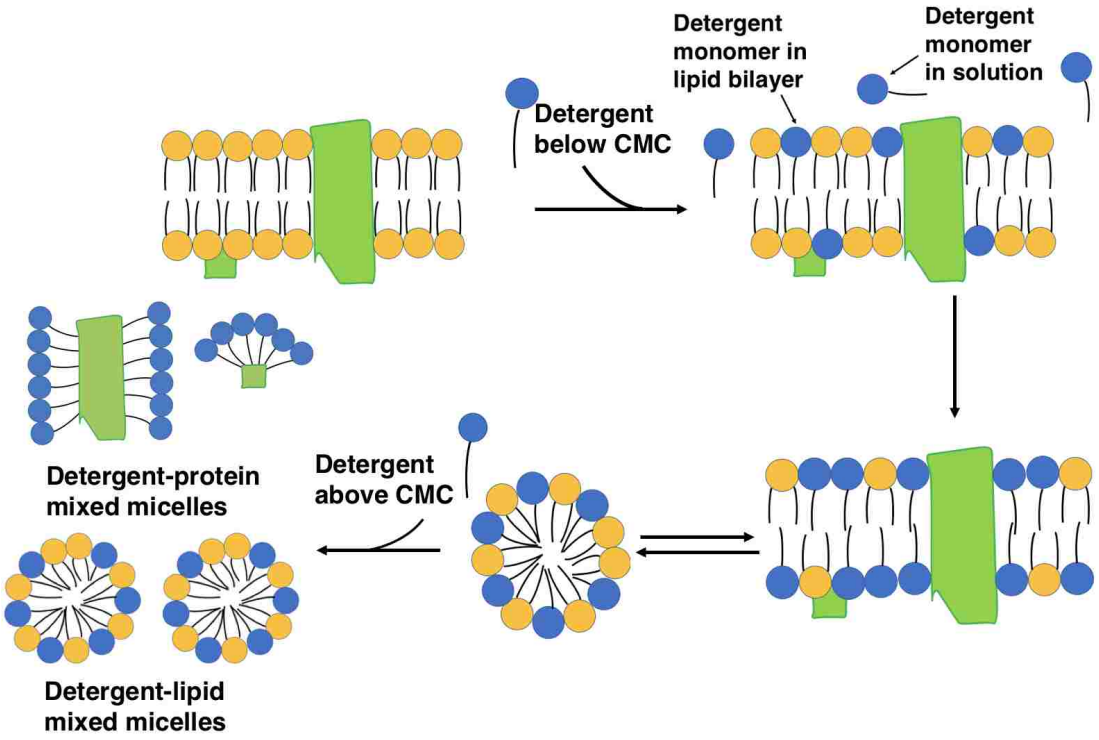

Figure 2.13. Stages of membrane protein solubilization. Below the detergent's CMC, some of its molecules penetrate into the lipid bilayer. At higher concentrations, the bilayer is saturated with detergent monomers. Above the detergent's CMC, detergent-lipid and detergent-protein mixed micelles form. In this figure, sugar and cholesterol molecules are omitted from the membrane for clarity.

F. Challenges in Membrane Protein Extraction and Solubilization

Solubilization of membrane proteins by detergents is complicated, and it carries out several challenges. First, there is no single and "magic" detergent that effectively solubilizes all membrane proteins.[26] In fact, these proteins require detergents with different properties for their optimal extraction and stability.[21] Besides, there are no standardized methods for solubilization of membrane proteins, and experimental

conditions must be optimized for every specific protein.[38] Furthermore, detergents can irreversibly denature the extracted membrane proteins.[39] Last but not least, developing a successful solubilization protocol for a particular membrane protein requires a lot of manipulations to temperature, solubilization time, and concentration of the detergents used.[36]

Despite these challenges and the variety of detergents to choose from for solubilization, there are some main points to consider when choosing detergents and the solubilization buffer conditions. When it comes to detergents, their type, concentration, and spectral properties are important parameters to take into account.[40] Regarding the type of a detergent, a special attention needs to be turned to its denaturing properties;[40] these properties can be determined by measuring the enzymatic activity of the solubilized protein. In most of the cases, it is desired to extract active and functional membrane proteins, so non-ionic detergents would be suitable for this purpose. During solubilization, the concentration of the detergent used should be above its CMC. If the detergent concentration drops below its CMC, the detergent layer around the hydrophobic region of the solubilized membrane protein dissociates leading to protein aggregation.[41] Besides, the detergent used for extraction should not interfere with the absorbance of the extracted proteins at 280 nm. For example, detergents with aromatic groups such as TritonX-100 should be avoided when the intention is to use absorbance at 280 nm to determine the concentration of the extracted protein.[40]

In regard to the solubilization buffer conditions, phosphate buffers are normally used in a concentration range of 0.1 to 0.5 M for an optimal solubilization of membrane proteins.[40] These buffers contain 100-150 mM of sodium chloride (NaCl) because

solubility of membrane proteins is affected by the ionic strength of solutions. Also, these buffers contain some percentage of polyols (5-50% v/v) such as glycerol in order to provide stability for membrane proteins in solution.[40] Besides, protease inhibitors such as phenylmethylsulfonyl fluoride (PMSF) along with ethylenediaminetetraacetic acid (EDTA) are added in order to reduce the protease activity.[40]

Keeping in mind the fact that solubilization of membrane proteins, in general, is a challenging task, a plan was developed for solubilization of the membrane-bound full-length CYPOR from *Escherichia coli* (*E. coli*) membranes. To effectively solubilize this membrane protein, a careful selection of detergents and solubilization buffer conditions was made.

G. Standard Procedures for Extraction of CYPOR

The full-length CYPOR with its N-terminal hydrophobic anchor is integrated in the lipid membrane. In order to purify this protein, it needs to be extracted from the membrane using proteases or detergents.[42] However, the use of proteases results in an un-functional CYPOR that is unable to interact with its partners and deliver electrons to them.[1,42,43] The common purification protocol for CYPOR is to solubilize the membrane with detergents such as TritonX-100 or cholate and then purify the protein through several chromatography steps.[44,45] Previous protocols for CYPOR solubilization utilized TritonX-100 along with EDTA and a protease inhibitor in the solubilization buffer.

In 1989, Shen et al. used EDTA, lysozyme, and aprotinin (a trypsin inhibitor) in Tris buffer for solubilization of the membrane-bound CYPOR.[44] Also, in 1997, Wang et al. reported using TritonX-100 for solubilization of the protein before its purification with

2',5'-ADP Sepharose 4B affinity column.[4] Furthermore, in 1997, Parikh et al. solubilized the human p450 1A2:rat NADPH-P450 reductase fusion protein from membranes using potassium phosphate buffer containing EDTA, dithiothreitol (DTT), and PMSF along with Emulgen 911 and sodium cholate detergents.[46] Based on these protocols, one can conclude that the most important reagents for solubilization of CYPOR would be a phosphate buffer containing protease inhibitors such as PMSF and EDTA along with TritonX-100.

2.2 GOAL AND PLAN

The recombinant full-length CYPOR including its soluble region and the N-terminal hydrophobic anchor (**Figure 1.2.**) is difficult to extract from the membrane of *E. coli* cells. This is a major challenge for studying this protein by NMR because a typical protein NMR experiment requires 10-20 mg of the protein to be analyzed.[47] Normally, to extract full-length CYPOR in sufficient quantities, large expression volumes have to be processed, and this is laborious and time consuming. In the lab, the capacity of the shakers and centrifuges limit us to express and process six liters of culture media at one time. Following expression, several purification steps have to be applied repeatedly to purify the protein from these six liters. After all, the amount of the protein obtained is still relatively low. The goal of this project was to optimize the extraction and solubilization of full-length CYPOR to facilitate future structural and dynamic studies on the protein by NMR.

To achieve that goal, several detergents and combination of detergents and additives were screened for their ability to extract full-length CYPOR from the *E. coli*

cell membrane. Most of the experiments and trials done for this purpose were based on previous successes of other labs in extracting several membrane proteins as will be discussed later. A total of four hypotheses were tested on four sets of detergents to examine their ability to extract the full-length CYPOR protein.

The initial selection of detergents was established based on two facts and a previous study that was done in 1976. The first fact is that the TritonX-100 detergent is commonly used for membrane studies.[48] This detergent can solubilize membranes and capture the embedded proteins in a native-like environment.[49] The other fact is that a more hydrophilic detergent weakly binds to the protein, leading to the protein's aggregation. In contrast, a more hydrophobic detergent tightly binds to the protein leading to its unfolding.[50] Hence, there should be a balance between the lipophilic and hydrophilic regions of the detergents used to optimize extraction and solubilization of the desired protein. A study was done by Slinde et al. in 1976 who examined the effect of the HLB value of the TritonX- series detergents on the solubilization of *b*-type cytochromes, which are integral membrane proteins. The group found, in general, that the solubilization efficiency of these detergents increased with decreasing the average length of their polar polyoxyethylene oxide chain.[51] Referring to this study and utilizing the two facts mentioned above, a set of three TritonX detergents (**Figure 2.14.**) with different HLB values were tested for their ability to extract the full-length CYPOR protein. The set contained: TritonX-100, TritonX-114, and TritonX-405.

These TritonX-series detergents are non-ionic with a constant hydrophobic moiety (octylphenyl) and a variable polar region (polyoxyethanol).[52] The only difference between these detergents is the number of the polar ethylene oxide units (n) in their

hydrophilic tail (**Table 2.1.**). TritonX-114 has the lowest number of the ethylene oxide units (n = 7-8), while TritonX-405 has the highest (n = 40).[51] The number of these units in TritonX-100 is intermediate (n = 9-10). As a consequence of the hydrophilic tail length variation, HLB also varies between these detergents. TritonX-114 has the lowest HLB (12.4), while TritonX-405 has the highest value (17.9). The HLB number for TritonX-100 is intermediate (13.5). In Slinde's work, it was noted that TritonX-114 with its low HLB was an efficient membrane solubilizer.[51] In this project, it was hypothesized that the shorter the hydrophilic tail of the TritonX detergent (and so lower HLB), the more it tightly binds to full-length CYPOR, and the more of this protein is extracted. Thus, it was expected that TritonX-114 would be the most efficient in extracting the protein.

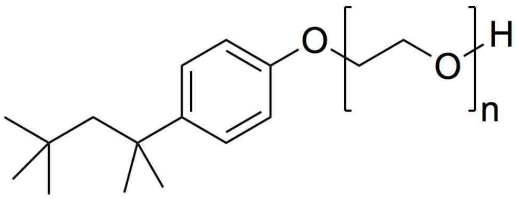

Figure 2.14. Structure of a TritonX detergent. The TritonX-series detergents have the same hydrophobic moiety (octylphenyl) and differ in the number of the ethylene oxide units (n) in their hydrophilic tail.[52] The structure was constructed using the ChemDraw molecular editor.

TritonX Detergent	Average Number of Ethylene Oxide Units (n)	Average HLB
TritonX-114	7-8	12.4
TritonX-100	9-10	13.5
TritonX-405	40	17.9

Table 2.1. HLB and n values of the TritonX-series detergents. TritonX-114 has the lowest n and HLB values, while TritonX-405 has the highest. These values for TritonX-100 are intermediate between the two detergents.[51]

The second set of detergents was selected based on the fact that detergents with low CMC values bind strongly to membrane proteins compared to those with high CMC.[35] In 2005, Berger et al. noted that using non-ionic detergents at concentrations near their CMC was efficient in extracting membrane proteins.[34] Combining this note from Berger's work and the fact mentioned above, the second set of detergents contained only the non-ionic types of these amphipathic compounds with different CMC values. These detergents were TritonX-100, TWEEN20 (**Figure 2.15.**), and Brij35 (**Figure 2.16.**).

These polyoxyethylene-type non-ionic detergents have a variable number of the ethylene oxide units and different CMC values. TWEEN20 contains fatty acid esters of polyoxyethylene sorbitan.[53] The 20 ethylene oxide units of this detergent provide the its hydrophilic nature, while lauric acid confers its hydrophobicity.[54] Brij 35 is composed of 23 ethylene oxide units that are attached to a lauryl alcohol.[55] The CMC values of TritonX-100, TWEEN20, and Brij35 are 0.2-0.9, 0.06, and 0.09 mM, respectively (**Table 2.3.).** It was hypothesized that the lower the CMC value, the more strongly detergent monomers bind to the transmembrane domain of full-length CYPOR. Thus, the more of the protein is extracted. Therefore, TWEEN20, with its lowest CMC, was expected to be the most efficient in extracting the protein.

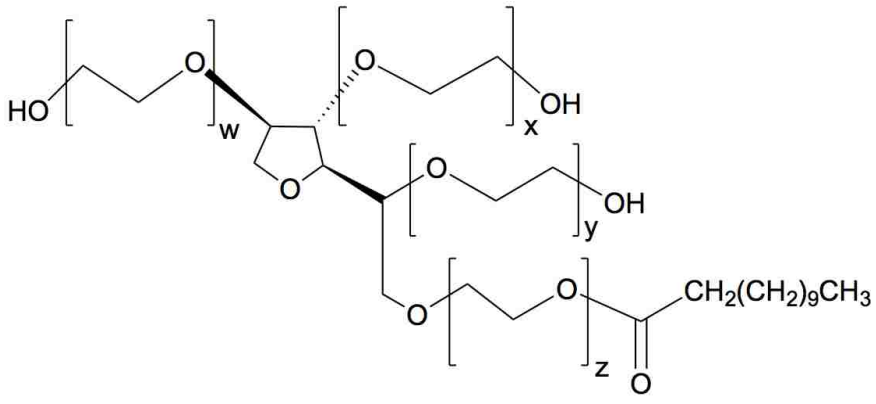

Figure 2.15. Structure of TWEEN20. This detergent has a total of 20 ethylene oxide units (x + y + w + z), a sorbitan, and a lauric acid tail.[53] The structure was created using the ChemDraw molecular editor.

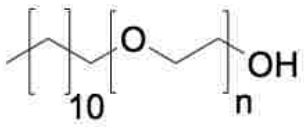

Figure 2.16. Structure of Brij35. This detergent has 23 ethylene oxide units (the "n" value varies among different Brij-type detergents) and a lauryl alcohol.[55] The structure was built using the ChemDraw molecular editor.

The third set of detergents that was tested in this project was an inspiration from the work done by Everberg et al. in 2006. This group combined the zwitterionic detergent, Zwittergent 3-10, and the non-ionic detergent, TritonX-114, to solubilize mitochondrial membrane proteins obtained from yeast *Saccharomyces cerevisiae.*[56] The extent of extraction by this combination of detergents was high and similar to that of SDS (~ 95% extraction of total membrane proteins). Everberg's study was very interesting because it combined detergents, which are neutral in different ways; TritonX-114 has an uncharged head group, while that of Zwittergent 3-10 has two opposite charges that cancel each other in its head group. Besides, Cladera et al. mentioned that CHAPS and CHAPSO zwitterionic detergents have been widely used to perturb the membrane structure and solubilize membrane proteins.[57] Therefore, in this work, CHAPS (**Figure 2.17.**) was used in combination with TritonX-100 to solubilize full-length CYPOR. Solubilization of the protein by TritonX-100 by itself was used as a reference.

These two detergents are from different classes; CHAPS is a zwitterionic detergent that is a derivative of bile salts. It is non-denaturing, and it can be used for membrane protein solubilization.[58] It has sulfonate and dimethylammonium polar groups

and bile salt in its hydrophobic region.[59] TritonX-100 is a non-ionic and mild detergent, and it is unlikely to cause protein denaturation.[23] It was expected that combining TritonX-100 and CHAPS detergents would enhance extraction and solubilization of full-length CYPOR. Accordingly, it was anticipated that the mixture of CHAPS and TritonX-100 detergents would solubilize more of the protein compared to TritonX-100 by itself.

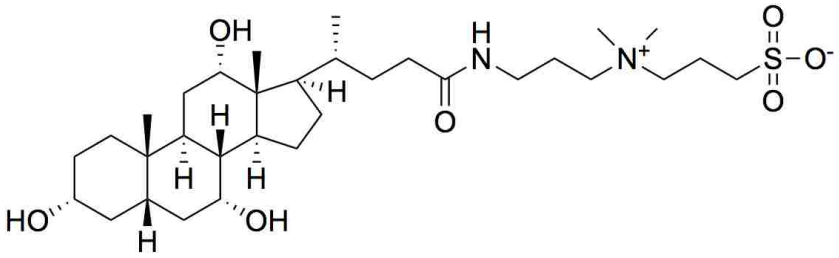

Figure 2.17. Structure of CHAPS. This detergent has a cholic group in its hydrophobic part and a dimethylammonium along with a sulfonate in its polar region.[59] The structure was constructed using the ChemDraw molecular editor.

Finally, the last detergent set to test contained only one detergent in addition to one of the alkylamine or polyamine additives. In 2010, Yasui et al. found that the addition of alkyl and polyamine additives to the solubilization buffer, containing a detergent, enhanced solubilization of several membrane proteins. These proteins include polygalacturonic acid synthase and NADH-dependent cytochrome c reductase. Solubilization of these membrane proteins was enhanced by up to 10-fold.[38] Based on that work, the last experimental set in this project comprised of TritonX-100 mixed with one of the alkylamines (**Figure 2.18.**) or polyamines (**Figure 2.19.**). The two alkylamines tested were propylammonium chloride (**Figure 2.18., A**) and ethylammonium chloride (**Figure 2.18., B**). The three polyamines tested were spermidine trihydrochloride (**Figure 2.19., A**), spermine tetrahydrochloride (**Figure 2.19., B**), and putrescine dihydrochloride

(**Figure 2.19., C**). As in the third set, solubilization of the protein by TritonX-100 by itself was used as a reference.

Figure 2.18. Chemical structures of alkylamines. Propylammonium chloride (**A**) and ethylammonium chloride (**B**) can be added to the solubilization buffer that contains a detergent. The structures were constructed using the ChemDraw molecular editor.

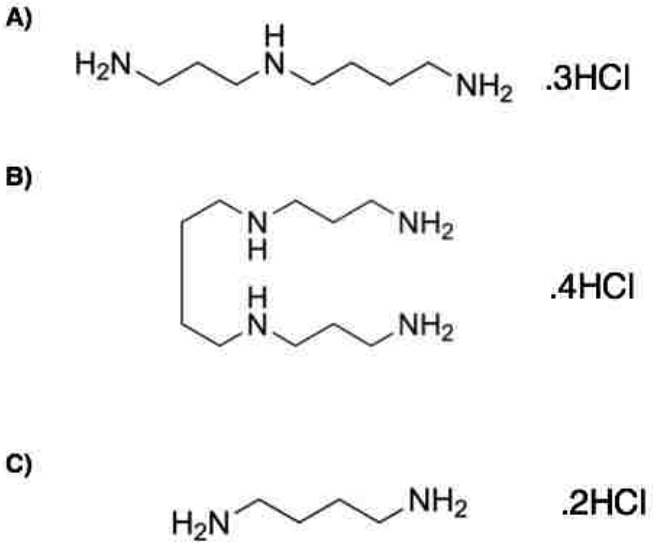

Figure 2.19. Chemical structures of polyamines. Spermidine trihydrochloride (**A**), spermine tetrahydrochloride (**B**), and putrescine dihydrochloride (**C**) can be added to the solubilization buffer that contains a detergent. The structures were constructed using the ChemDraw molecular editor.

As Yasui et al. suggested, the cationic character of these addiditves allows them to interact with the negatively charged phosphates in phospholipids.[38] Consequently, disrupting the phospholipids of membranes but not membrane proteins. Therefore, it was expected that the addition of these additives to the solubilization buffer containing TritonX-100 would enhance solubilization of full-length CYPOR. Thus, it was

hypothesized that these additives in combination with TritonX-100 would be better membrane solubilizers than TritonX-100 by itself.

2.3 EXPERIMENTAL

A. Reagents, Chemicals, and Biochemicals

All chemicals and reagents that were used in this project were purchased from commercial sources and used as received (**Table 2.2.**). Purified water from Branstead Water Mixed Bed Deionizer Filter was used when needed for dilutions and preparation of solutions. Yeast extract (24 g), trypton (12 g), and glycerol (0.4% v/v) were used to prepare one liter of Terrific Broth (TB) medium. Also, these reagents along with ampicillin sodium salt antibiotic (Amp) (100 ug/mL) and granulated agar (3 g) were used to prepare the Amp-TB agar plates. Potassium phosphate dibasic (K_2HPO_4) (72 mM) and potassium phosphate monobasic (KH_2PO_4) (17 mM) were used to prepare the TB salts solution. Isopropyl-β-$_D$-1-thiogalacto-pyranodside (IPTG) was used for inducing *E. coli* cells to overexpress the full-length CYPOR protein.

KH_2PO_4 (25 mM), sodium chloride (NaCl) (100 mM), and glycerol (10% v/v) were used to prepare the solubilization buffer at a pH of 7.2 (KEG buffer). PMSF, lysozyme from chicken egg white, and EDTA disodium salt dihydrate, were added to the solubilization buffer during cell lysis. TritonX-100, TritonX-114, TritonX-405, TWEEN20, Brij35, and CHAPS detergents were screened for extraction of full-length CYPOR. Spermidine trihydrochloride, spermine tetrahydrochloride, putrescine dihydrochloride, propylamine hydrochloride, and ethylammonium chloride were the additives used in combination with TritonX-100 for solubilization of full-length CYPOR.

Tris(2-carboxyethyl) phosphine (TCEP) and PMSF were added during extraction with the detergents.

Bromophenol blue and 2-mercaptoethanol were used to stain the protein samples for gel electrophoresis. Trizma (TRIS base), SDS, 30% bis-acrylamide solution, TEMED, and 10% ammonium persulfate (APS) were used to prepare the 10% separating and 4% stacking gels. Trizma (TRIS base), glycine, and SDS were used to prepare the gel running buffer. PhastGel® Blue R, 100% reagent alcohol, and glacial acetic acid were the main reagents in the preparation of stain for gels. Methanol (Methanol Optima) and glacial acetic acid were mainly used to prepare the destain solution for gels. Finally, 100% reagent alcohol and glycerol were the main components in the gel storage buffer. PageRuler Unstained Protein Ladder was used in order to establish the molecular weight ruler for all gels.

The expression vector, pOR263, which codes for full-length CYPOR was a gift from Dr. Jung-Ja Kim, the Medical College of Wisconsin (MCW). *E. coli* strains of DH5α and C41 (DE3) were used for plasmid amplification and protein expression, respectively.

Chemical / Reagent	**Manufacturer**	**Catalog Number**
Yeast extract	BD Biosciences	288620
Trypton	BD Biosciences	211705
Granulated agar	Becton Dickinson	11849
Glycerol	Sigma-Aldrich	G9012-1L
Ampicillin sodium salt antibiotic (Amp)	Sigma-Aldrich	A0166-25G
Potassium phosphate dibasic (K_2HPO_4)	Alfa Aesar	A11321-0B
Potassium phosphate monobasic (KH_2PO_4)	Fisher Scientific	P285-3

Isopropyl-β-$_D$-1-thiogalacto-pyranodside (IPTG)	OMEGA bio-tek	AC121
Sodium chloride (NaCl)	Sigma-Aldrich	S3014-1KG
Phenylmethylsulfonyl fluoride (PMSF)	Amresco	0754-25G
Lysozyme from chicken egg white	Sigma-Aldrich	L7651
EDTA disodium salt dihydrate	Amresco	M101-500G
TritonX-100	Sigma-Aldrich	T9284-500ML
TritonX-114	Sigma-Aldrich	93422-250ML
TritonX-405	Arcos Organic	215692500
TWEEN20	Arcos Organic	23336-2500
Brij35	Arcos Organic	329581000
CHAPS	Sigma-Aldrich	3023-5G
Spermidine trihydrochloride	Arcos Organic	215100010
Spermine tetrahydrochloride	Alfa Aesar	J63060
Putrescine dihydrochloride	MP Biomedicals	100450
Propylamine hydrochloride	Sigma-Aldrich	242543-25G
Ethylammonium chloride	EMD Millipore Corporation	800874
Tris(2-carboxyethyl)phosphine (TCEP),	Biosynth Chemistry and Biology	C-1818
Bromophenol blue	Sigma Aldrich	114391
2-mercaptoethanol	Sigma-Aldrich	M6250
Trizma (TRIS base)	Sigma-Aldrich	T1503-5KG
Sodium dodecyl sulfate (SDS)	ThermoFisher Scientific	28364
Bis-acrylamide solution, 30%	Hoefer, Inc	GR337500
TEMED	Bio-Rad	1610801
10% ammonium persulfate (APS)	Bio-Rad	161-0700
Glycine	Sigma-Aldrich	G7126-5KG
PhastGel® Blue R	Sigma-Aldrich	B4921-20TAB
100% reagent alcohol	Decon Laboratories, Inc	12R1001
Glacial acetic acid	Fisher Scientific	A38-212
Methanol (Methanol Optima)	Fisher Scientific	A454-1

PageRuler Unstained Protein Ladder	ThermoFisher Scientific	26614

Table 2.2. Manufacturers and catalog numbers for the chemicals and reagents used in this project (project 1).

B. Plasmid, Cell Growth, and Expression of Full-Length CYPOR

The ampicillin-resistant pOR263 plasmid, which contains the His-tagged full-length CYPOR (78 kDa)[60] was amplified in *E. coli* DH5α competent cells and was extracted and purified by Omega bio-tek E.Z.N.A. Plasmid Mini Kit I, (Q-spin) following the manual's protocol.

For protein expression, the plasmid was transformed into *E. coli* C41 (DE3) competent cells using a heat shock at 42°C for 40 seconds in the VWR 1224 Digital Water Bath. The transformed *E. coli* cells were incubated in a culture tube with TB medium. They were grown at 220 rpm and 37°C for 1 hour in the New Brunswick Stackable Incubator Shaker I2500 and I2500 KC. A 100 uL of the cell suspension was plated on an Amp-TB agar plate and incubated at 37°C overnight in the Precision Incubator. The next day, a single colony from the plate was inoculated into room-temperature sterile TB medium containing Amp (100 ug/mL). This starter culture was grown in the shaker at 220 rpm and 37°C for 3 hours. Later, the larger culture was prepared by transferring the starter culture into a larger volume of sterile TB medium containing Amp (100 ug/mL). This culture was grown in the shaker at 220 rpm and 37°C overnight.

On the following day, the OD_{600} of the overnight culture was measured using the Varian Cary 50 Bio UV-Visible Spectrophotometer. Then, this overnight culture was

transferred to a sterile TB medium containing TB salts and Amp (100 ug/mL) in order to make the expression culture. This culture was shaken at 220 rpm and 37°C for ~ 3 hours until the cells reached OD_{600} of ~ 0.9 au. Later, the growth culture was cooled on ice and was further shaken at room temperature for 10 minutes in the New Brunswick G25 Shaker Incubator. Then, small portions from that culture were taken to represent the non-induced cell culture. To the rest of the cells, IPTG (0.5 mM) was added in order to induce overexpression of full-length CYPOR. OD_{600} was measured for the non-induced and induced cell cultures before shaking them at 220 rpm and 18°C overnight.

C. Cell Membrane Preparation

In morning of the following day, OD_{600} was checked for the overnight cell cultures to ensure reaching OD_{600} of ~ 3-6 au. The cells were harvested by centrifugation at 5,000 g and 4°C for 15 minutes in the Sorvall LYNX 4000 Superspeed Centrifuge. The cell pellet was suspended in KEG buffer (25 mL per 1 L of the original cell culture). To this suspended pellet, PMSF (1 mM), EDTA (1 mM), and lysozyme (25 ug/mL) were added. Then, cell lysis was carried out at 4°C for 1 hour. These cells were further broken by sonicating the cell suspension on ice at 50% duty cycle, power setting of 8 for 30 seconds in the VWR Branson 450 Sonifier. This was followed by incubation on ice, and the sonication step was repeated 4 times.

Following that, the total cell lysate was passed through a series of centrifugation steps (**Figure 2.20.**). It was centrifuged at 5,000 g and 4°C for 15 minutes in the Eppendorf™ 5810R Centrifuge. The resulting pellet (Pellet 1) contained cell debris, unbroken cells, and insoluble proteins, so it was discarded. The supernatant (Supernatant

1) contained membrane particles (microsomes) and loosely associated membrane proteins. This solution was ultra-centrifuged at 30,000 g and 4°C for 1 hour. This separated the soluble proteins in the resulting supernatant (Supernatant 2) from the full-length CYPOR and other integral membrane proteins associated with microsomes in the resulting pellet (Pellet 2). This new pellet was re-suspended in KEG buffer.

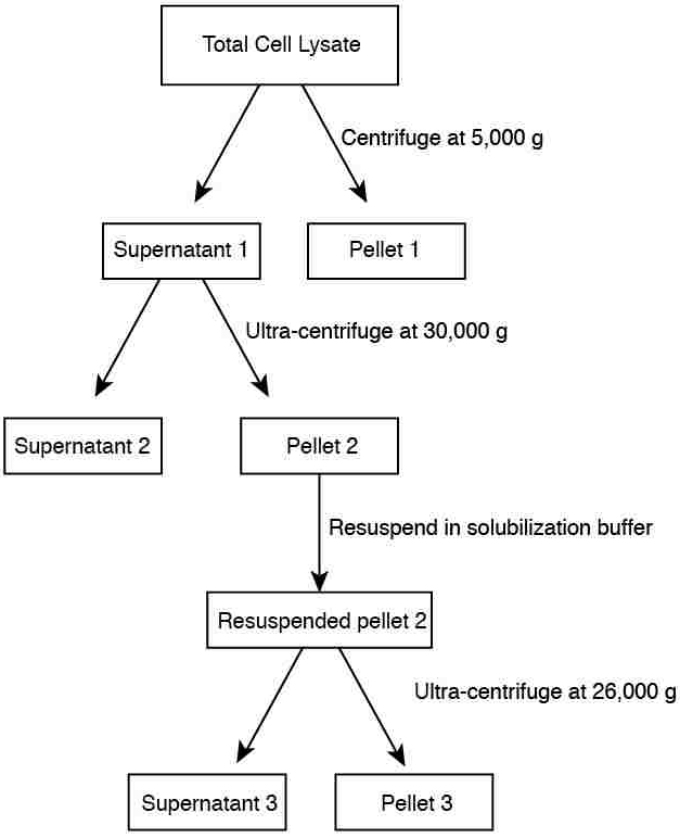

Figure 2.20. Workflow for full-length CYPOR solubilization. Centrifuging the total cell lysate at 5,000 g results in Pellet 1 and Supernatant 1, which is ultra-centrifuged at 30,000 g. The resulting Supernatant 2 is discarded, while Pellet 2 is re-suspended in the solubilization buffer and ultra-centrifuged at 26,000 g. This produces Supernatant 3 and Pellet 3, which are assessed for their content of full-length CYPOR.

D. Solubilization of Full-Length CYPOR

An aliquot of Pellet 2 was thawed with PMSF (1 mM) and TCEP (1 mM) and was sonicated two times with a total exposure time of 1 minute. This served as the starting material for all extraction trials. After sonication, 20 mL aliquots were made from this total cell lysate and were stored at -80ºC for later testing with various detergents and additives. All detergents were used at concentrations above their CMC (**Table 2.3.**) in order to prevent protein aggregation and precipitation.

Detergent	**CMC (mM)**	Reference
TritonX-100	0.2-0.9	61
TritonX-114	0.17	62
TritonX-405	0.32	63
TWEEN20	0.06	61
Brij35	0.09	61
CHAPS	6.4	39

Table 2.3. CMC values of the detergents used in this project (project 1).

The first set of detergents represented the TritonX-series non-ionic detergents: TritonX-100, TritonX-114, and TritonX-405. The second set contained TritonX-100, TWEEN20, and Brij35 non-ionic detergents. Detergents in these two sets were added to 2% (v/v) to the solubilization buffer. The third set comprised of TritonX-100 (used as a reference) and this detergent mixed with CHAPS. These detergents were added to 0.5% (v/v) and 0.5% (w/v) to the solubilization buffer, respectively. Finally, the fourth set was limited to 0.5% (v/v) TritonX-100 (used as reference) and this detergent mixed with spermidine trihydrochloride, spermine tetrahydrochloride, putrescine dihydrochloride, propylamine hydrochloride, or ethylammonium chloride. All additives were used to a final concentration of 50 mM, which was the optimal concentration for the maximum

solubilization of membrane proteins in the Yasui et al. study.[38] The extraction process was carried out overnight at 4°C.

On the next day, these overnight mixtures were ultra-centrifuged at 26,000 g and 4°C for 1 hour (**Figure 2.20.**). The resulting supernatant (Supernatant 3) contained the solubilized full-length CYPOR, while the pellet (Pellet 3) contained the un-solubilized protein along with other un-extracted membrane proteins. To determine the relative amount of the un-solubilized full-length CYPOR, Pellet 3 was re-suspended in KEG buffer and sonicated one time with a total exposure time of 30 seconds at the same sonication conditions as those used before. The extent of extraction by each single detergent, mixture of detergents, or detergents with additives was evaluated by gel electrophoresis in comparison to TritonX-100. The full length CYPOR protein found in the resulting Supernatant 3 indicated a successful extraction.

E. Gel Electrophoresis

To qualitatively trace the amount of full-length CYPOR from its expression in *E. coli* cells to its extraction from their membrane, samples for sodium dodecyl sulfate-polyacrylamide gel electrophoresis (SDS-PAGE) were taken. These samples were from the non-induced and induced cell cultures as well as Supernatant 1 and Supernatant 2. To assess the effect of detergents on the protein stability, a sample for gel electrophoresis was taken from Pellet 2 before and after incubating it overnight with detergents and additivities. Also, samples containing the un-extracted full-length CYPOR (Pellet 3) and the extracted protein (Supernatant 3) were resolved using SDS-PAGE. Electrophoresis

was carried out by Invitrogen Life Technology PowerEase 500. The settings that were used for running the gels were: 135 V, 90 mA, and 12.5 W for 95 minutes.

2.4 RESULTS

The overnight starter, induced, and non-induced cell cultures were growing at an expected rate (**Table 2.4.**). The overnight starter culture was grown to a high density (OD_{600} = 3.8) and was inoculated into fresh TB medium. During growth for three hours, the cells reached OD_{600} of 1.2 at which they were induced for full-length CYPOR overexpression with IPTG. When cells reached OD_{600} of 5.6, protein overexpression was confirmed by SDS-PAGE of the total cell lysate from the non-induced and induced cell cultures **(Figure 2.21.**). The amount of the protein in the non-induced cell lysate (**Figure 2.21., lane 2**) was lower than that in induced one (**Figure 2.21., lane 3**). This was very clear from the intensity of the 78 kDa band, which was less intense in **lane 2** compared to **lane 3** in this figure.

Sample	**OD_{600},** $\frac{au}{mL.cm}$
Overnight starter culture	3.8
Average growth at the start	0.21
Average growth after 1 hour	0.24
Average growth after 2 hours	0.53
Average growth after 3 hours	1.2
Average growth of induced cells before overnight	1.4
Average growth of non-induced cells before overnight	1.4
Average growth of induced cells after overnight	5.6
Average growth of non-induced cells after overnight	8.1

Table 2.4. OD_{600} values of the cultured cells. The concentration of the bacterial cell population of the larger, induced, and non-induced cell cultures is determined by their OD_{600}.

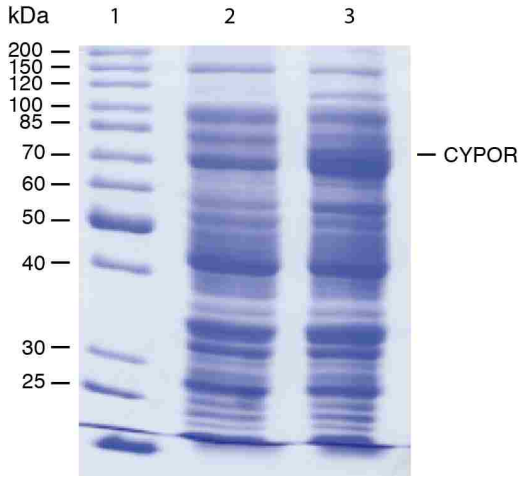

Figure 2.21. SDS-PAGE gel for overexpression of full-length CYPOR. **Lane 1** is the PageRuler Unstained Protein Ladder, **lane 2** is the total cell lysate of the non-induced cell culture, and **lane 3** is the total cell lysate of the induced culture. The band for full-length CYPOR is around 78 kDa, and it is more intense in **lane 3** compared to **lane 2**.

Upon centrifuging the induced total cell lysate, full-length CYPOR was present in Supernatant 1, and centrifuging this solution formed Supernatant 2, where the protein was absent (**Figure 2.22.)**. In this figure, the protein was present with membrane particles and loosely associated membrane proteins in Supernatant 1(**Figure 2.22., lane 2**), but it was absent from the sample where the soluble proteins were found in Supernatant 2 (**Figure 2.22., lane 3**).

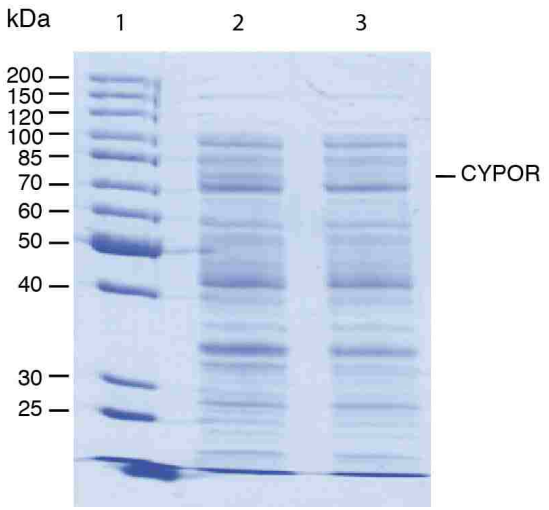

Figure 2.22. SDS-PAGE gel for Supernatant 1 and Supernatant 2. **Lane 1** is the PageRuler Unstained Protein Ladder, **lane 2** is Supernatant 1, and l**ane 3** is Supernatant 2. The 78 kDa band for full-length CYPOR is found in **lane 2** but not in **lane 3**.

The amount of the solubilized full-length CYPOR by the four sets of detergents was determined by SDS-PAGE gels. In all of these gels, **lanes 2** and **3** indicate Pellet 2 before and after overnight incubation with detergents, respectively. These lanes illustrate the effect of detergents on protein stability. **Lanes 4** and **5** feature the amount of the un-solubilized and solubilized protein in Pellet 3 and Supernatant 3, respectively.

The extent of solubilization of the protein by the TritonX-series detergents was comparable (**Figure 2.23.**). TritonX-114, however, solubilized the highest amount of the protein in this set; about 15% of the protein was extracted (**Figure 2.23., B**). TritonX-405 extracted the least amount of the protein, which was less than 10% (**Figure 2.23., C**). TritonX-100 extracted about 10% of the protein (**Figure 2.23., A**), and the extent of solubilization by this detergent was similar to that of TritonX-114.

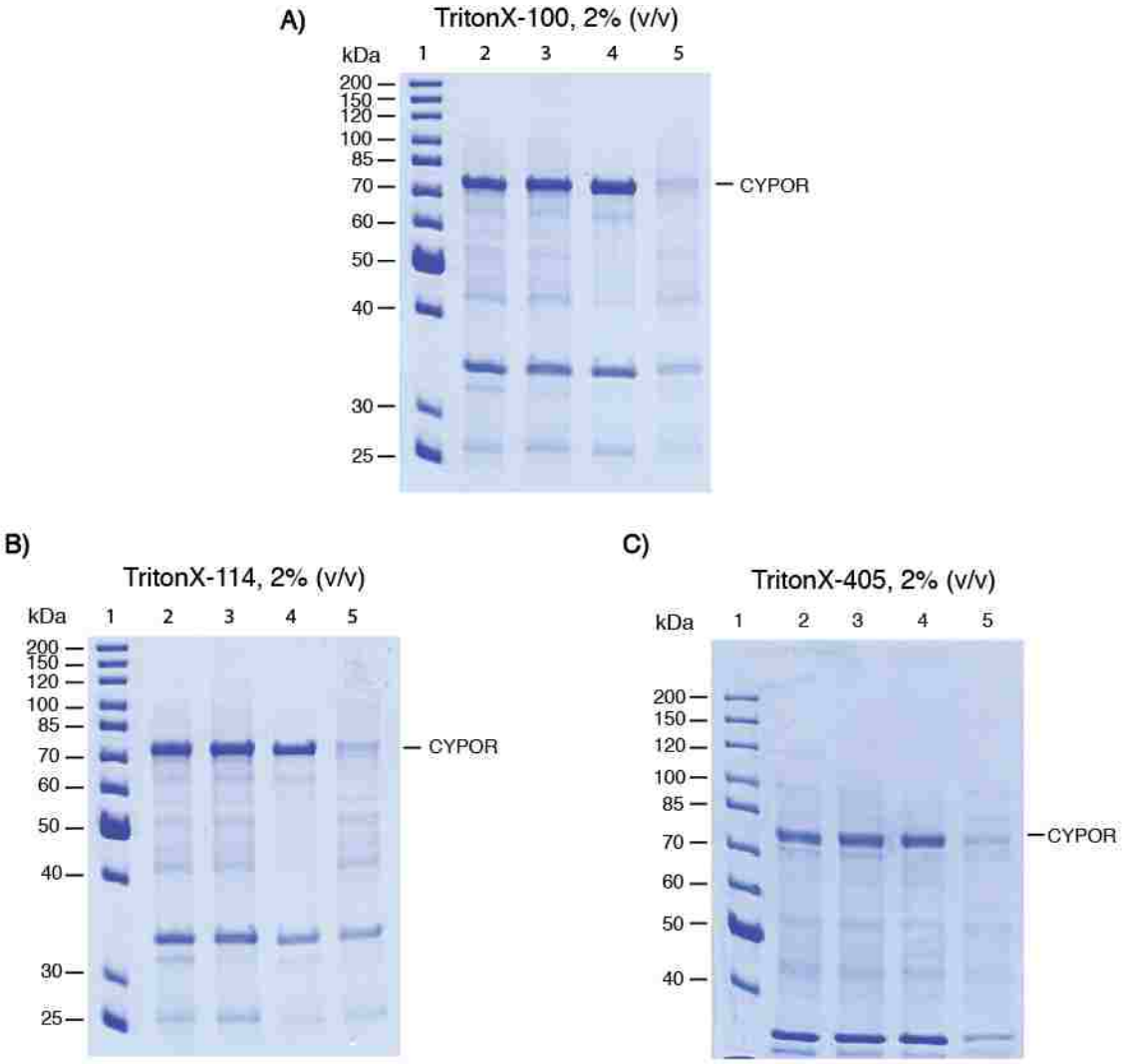

Figure 2.23. SDS-PAGE gels for solubilization of full-length CYPOR by the TritonX-series detergents: TritonX-100 (**A**), TritonX-114 (**B**), and TritonX-405 (**C**). In these gels, **lane 1** is the PageRuler Unstained Protein Ladder; **lanes 2** and **3** show Pellet 2 before and after overnight incubation with the detergents, respectively. **Lanes 4** and **5** represent the amount of the un-solubilized and solubilized protein, in Pellet 3 and Supernatant 3, correspondingly. The 78 kDa band in these gels indicates the presence of full-length CYPOR.

Extraction of full-length CYPOR by TritonX-100, TWEEN20, and Brij35 non-ionic detergents (**Figure 2.24.**) did not show any improvements from that by the TritonX-series detergents. The extent of extraction by TritonX100 (**Figure 2.24., A**) and Brij35

(**Figure 2.24., C**) was similar. These detergents extracted about 10% of the protein. Extraction by TWEEN20 was relatively weak; less than 5% of the protein was extracted by this detergent (**Figure 2.24., B**).

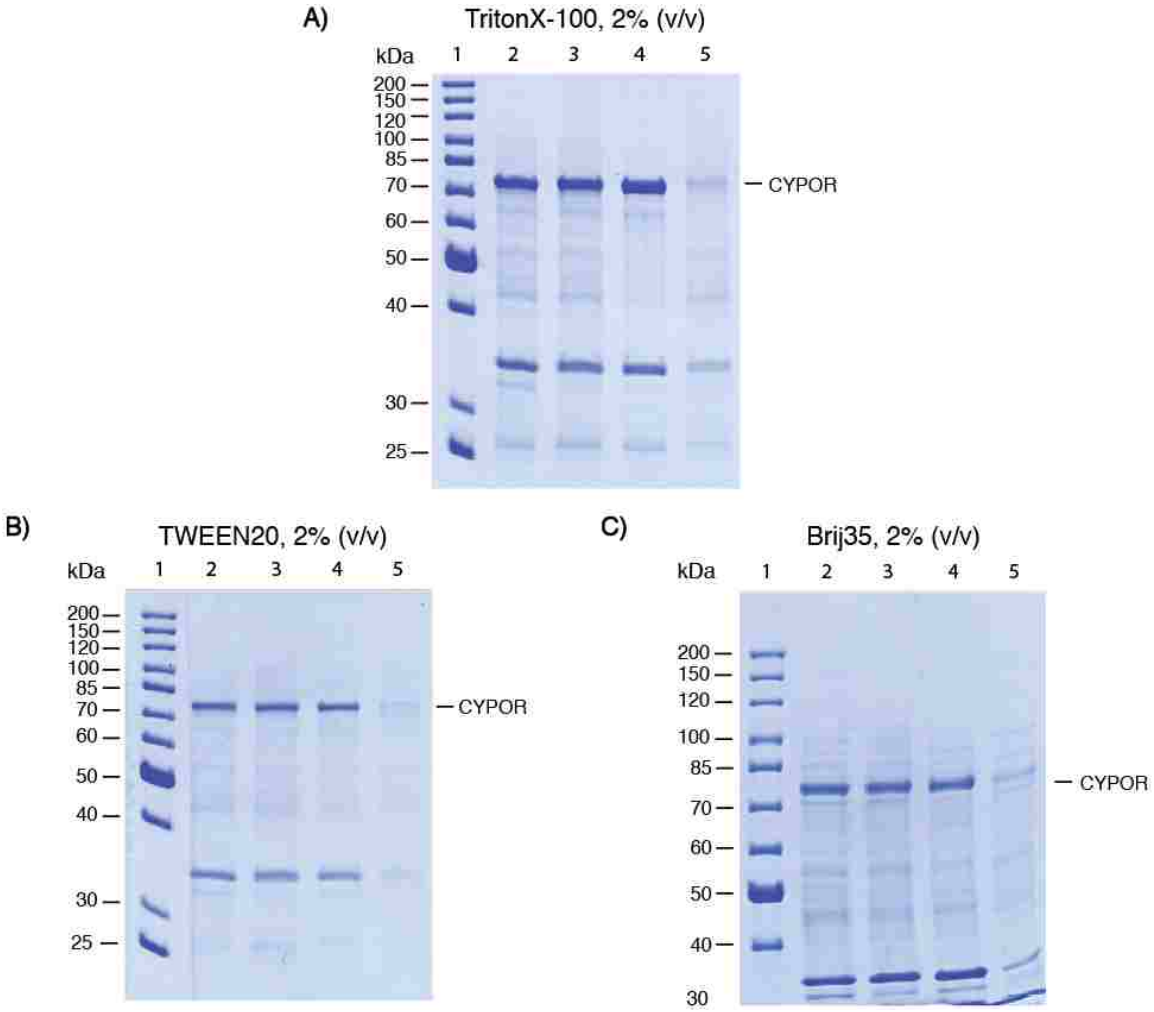

Figure 2.24. SDS-PAGE gels for solubilization of full-length CYPOR by various non-ionic detergents: TritonX-100 (**A**), TWEEN20 (**B**), and Brij35 (**C**). Lane assignments are the same as those in **Figure 2.23.** The 78 kDa band in these gels indicates the presence of full-length CYPOR.

Solubilization of full-length CYPOR by TritonX-100 and this detergent combined with CHAPS was different (**Figure 2.25.**). In fact, the combination of these two

detergents did not enhance solubilization of the protein. The reference, TritonX-100 by itself, extracted ~10% of the protein (**Figure 2.25., A**). However, when this detergent was mixed with CHAPS, only ~ 5% of the protein was extracted (**Figure 2.25., B**).

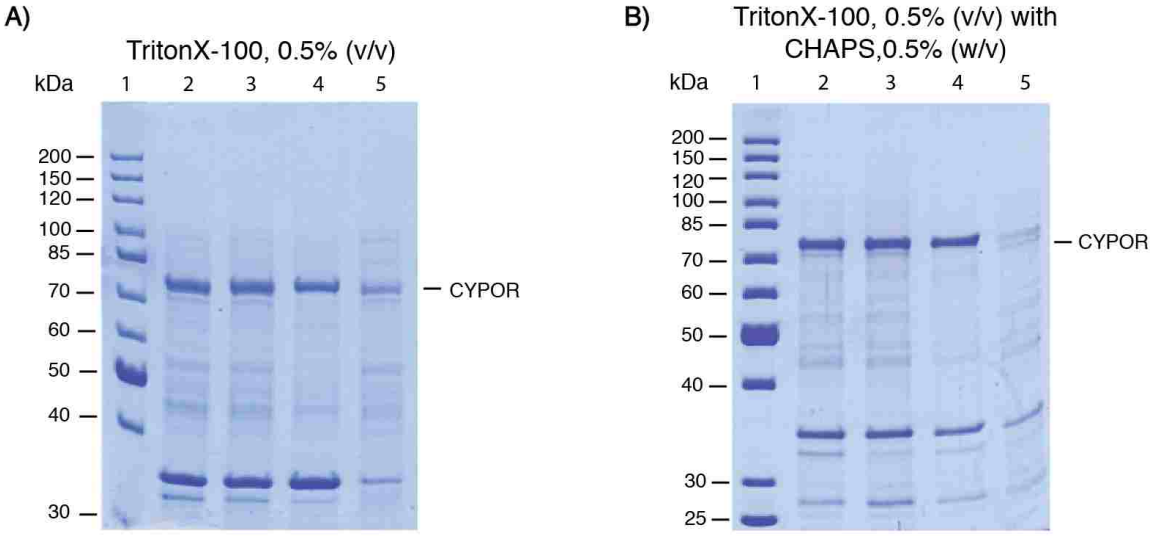

Figure 2.25. SDS-PAGE gels for solubilization of full-length CYPOR by TritonX-100 (**A**) and this detergent mixed with CHAPS (**B**). Lane assignments are the same those in **Figure 2.23.** The 78 kDa band in these gels indicates the presence of full-length CYPOR.

The amount of the solubilized full-length CYPOR by TritonX-100 alone and this detergent combined with polyamine and alkylamine additives was variable (**Figure 2.26.**). Different additives had different effects on the solubilization of the protein. The reference, TritonX-100 by itself, solubilized ~10% of the protein (**Figure 2.26., A**). The addition of spermidine trihydrochloride to this detergent reduced solubilization of the protein, and only less than 1% of it was extracted (**Figure 2.26., B**). The combination of TritonX-100 with spermine tetrahydrochloride did not extract any of the desired protein (**Figure 2.26., C**). About 2% of the protein was solubilized by TritonX-100 combined with putrescine dihydrochloride (**Figure 2.26., D**). When propylamine hydrochloride was

added to TritonX-100, about 10% of the protein was solubilized (**Figure 2.26., E**). TritonX-100 and ethylammonium chloride seemed to extract about ~30% of the protein (**Figure 2.26., F**).

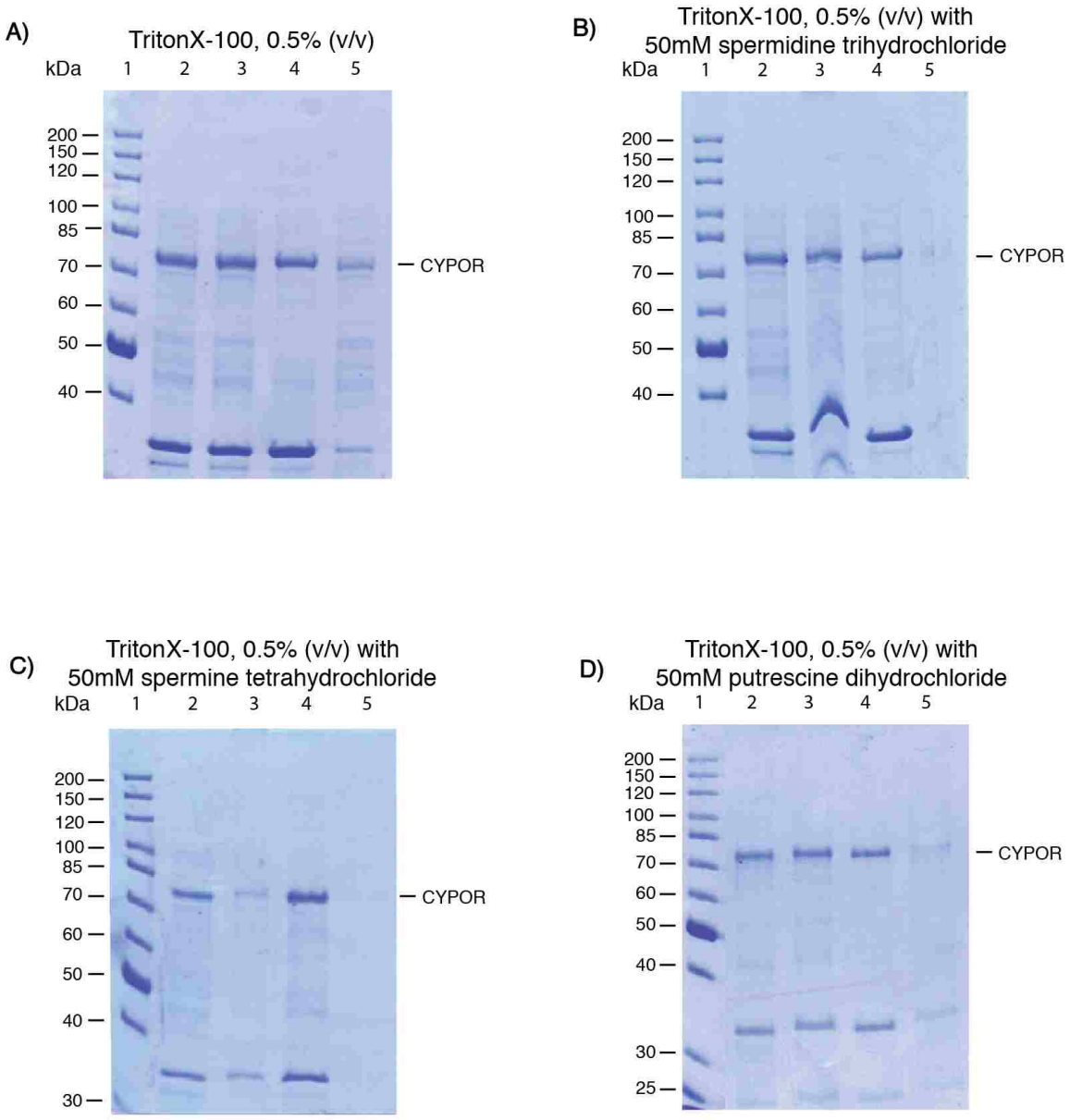

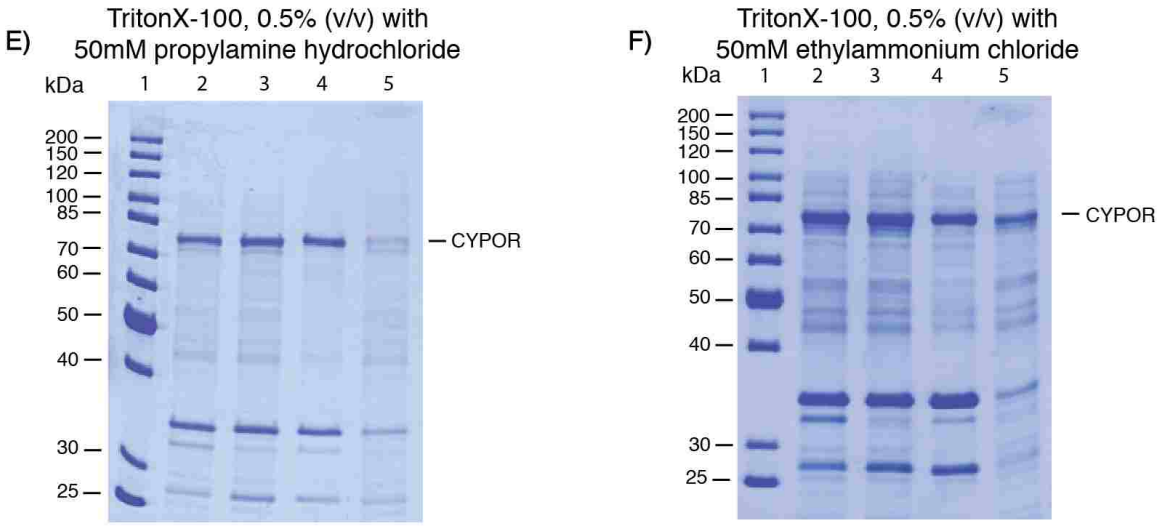

Figure 2.26. SDS-PAGE gels for solubilization of full-length CYPOR by TritonX-100 (**A**) and this detergent combined with additives. Lane assignments are the same as those in **Figure 2.23.** The 78 kDa band in these gels indicates the presence of full-length CYPOR. The additives used are spermidine trihydrochloride (**B**), spermine tetrahydrochloride (**C**), putrescine dihydrochloride (**D**), propylamine hydrochloride (**E**), and ethylammonium chloride (**F**).

It was thought that the gel that represents TritonX-100 with ethylammonium chloride (**Figure 2.26., F**) was overloaded. Thus, the extraction process with TritonX-100 and this additive was repeated using the same total cell lysate, and the results are shown in **Figure 2.27.** Again, extraction with TritonX-100 was used as a reference. Since it was confirmed from previous gels that detergents and additives did not affect the stability of the protein, a sample for gel electrophoresis was not taken after overnight incubation of Pellet 2 with the detergent. In this gel, the addition of ethylammonium chloride, in fact, neither enhanced nor reduced TritonX-100 ability to solubilize the protein.

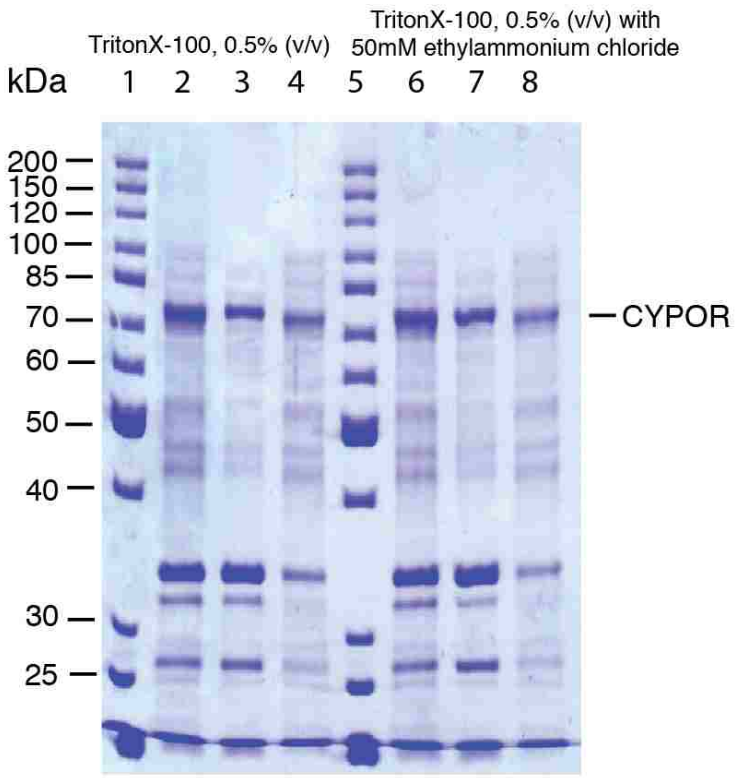

Figure 2.27. Repeated SDS-PAGE gel for solubilization of full-length CYPOR by TritonX-100 and this detergent combined with ethylammonium chloride. **Lanes 1** and **5** contain the PageRuler Unstained Protein Ladder. **Lanes 2** and **6** are the total cell lysate before overnight incubation with TritonX-100 alone or this detergent with ethylammonium chloride, respectively. **Lanes 3** and **7** indicate the amount of the un-solubilized full-length CYPOR, while **lanes 4** and **8** signify the amount of the solubilized protein.

2.5 DISCUSSION

A conventional protocol calls for TritonX-100 to solubilize full-length CYPOR. The major impediment, however, is that the amount of the solubilized protein by TritonX-100 is relatively low for NMR analysis. The extraction efficiency of the protein by this detergent has been ~10%.[45,44] Therefore, large expression volumes are typically required to achieve the desired yield of the protein. This can be difficult to achieve considering the limited capacities of the centrifuges and shakers in the lab. Thus, the goal

of this project was to optimize the extraction and solubilization of full-length CYPOR from the *E. coli* membrane using a variety of detergents and additives. The extraction efficiency of the four sets of detergents was judged by the amount of the protein in Supernatant 3 after overnight incubation of Pellet 2 with the solubilization buffer.

The extent of extraction of full-length CYPOR by the TritonX-series detergents was similar. Yet, to some extent, TritonX-114 was the most effective in extracting the protein followed by TritonX-100 and then TritonX-405, which was the least effective. This was in agreement to what was hypothesized based on the hydrophilicity of these detergents and their HLB numbers. TritonX-114 is less hydrophilic (lower HLB) and has a fewer number of the ethylene oxide units. Thus, its hydrophobic character overcomes its hydrophilicity. Therefore, this detergent bound strongly to the hydrophobic region of the protein and solubilized ~15% of it. TritonX-405, on the other hand, is more hydrophilic (higher HLB) and has a larger number of the ethylene oxide units. Because of the strong hydrophilic character of TritonX-405, it bound less strongly to the hydrophobic region of the protein and solubilized less than 10% of it. TritonX-100 has an intermediate value of HLB, and the number of its ethylene oxide units falls in between the other two detergents. Thus, its hydrophilic and hydrophobic characters contribute equally to the detergent's ability in extracting the protein. This "balance" between the hydrophilic and hydrophobic properties of TritonX-100 enabled it to extract ~10% of the protein.

The results obtained from this set of detergents were also in agreement to those achieved by Slinde et al. in 1976. This group used a variety of TritonX- series detergents with different HLB numbers and ethylene oxide units to solubilize multiple membrane

proteins. They found that TritonX-114 solubilized 91% of cytochrome *b*-561, and that TritonX-100 solubilized 93% of cytochrome b_5 and 88% of mitochondrial *b* cytochromes as well as cytochrome *c* oxidase. In that study, TritonX-405 extracted only 70%, 25%, 3%, and 0% of each of these proteins, respectively.[51] The amount of the solubilized proteins in Slinde's study is obviously higher than that of the solubilized full-length CYPOR in this project. This disparity can be attributed to variations in the membrane composition, where these proteins are embedded and the extent of the hydrophobic interactions they make with these membranes.

In this project, full-length CYPOR is embedded in the *E. coli* membrane, while the proteins solubilized in Slinde's study were obtained from membranes of different organs. Examples of these organs include bovine kidney cortex, bovine liver, and bovine adrenal glands. The composition of these mammalian cells' membrane is different from that of bacterial cells where full-length CYPOR is embedded. Cytochrome *b*-561 is bound to the chromaffin granule membrane. The mitochondrial *b*-type cytochromes and cytochrome *c* oxidase are bound to the mitochondrial membrane.[51] Since these proteins are bound to different membranes, their solubilization by the same detergents was different. In regard to the second rational, de Pinto et al. reported in 1989 that the mitochondrial porin from bovine heart was highly solubilized by detergents with low HLB values. However, the other membrane proteins from the same source were greatly solubilized by detergents with high HLB values.[64] From this study, it can be concluded that full-length CYPOR is more tightly bound to the membrane compared to those solubilized in Slinde's study. Thus, its extraction by the same detergents was more challenging.

The non-ionic detergents, TritonX-100, TWEEN20, and Brij35 solubilized full-length CYPOR to different extents. TritonX-100 and Brij35 solubilized similar amounts of the protein, while TWEEN20 did not solubilize much of it, and most of the protein was left in the pellet. This was opposite to the expectations based on the CMC values of these detergents. TWEEN20 with its low CMC was expected to bind strongly to the protein and extract most of it out of the membrane. TritonX-100 with its higher CMC was expected to keep most of the protein in the pellet. Brij35 with its intermediate CMC was anticipated to solubilize an average amount of the protein that falls between those solubilized by TritonX-100 and TWEEN20.

In reality, TWEEN20 extracted less than 5% of the protein, while TritonX-100 and Brij35 extracted ~10% of it. One possible explanation for these unpredicted results would be that the solubilization conditions used in this project were not optimal for TWEEN20. In other words, this detergent may require a specific temperature, pH, and ionic strength conditions for the efficient solubilization of full-length CYPOR. The solubilization buffer conditions used in this project were not optimized for TWEEN20 but for the stability of full-length CYPOR. Furthermore, the experimental conditions used in this project might have altered the CMC value of TWEEN20. Generally, the CMC value of a detergent is dependent on the solubilization buffer conditions, particularly its ionic strength.[40]

The combination of TritonX-100 and CHAPS detergents did not enhance solubilization of the protein. In fact, the extraction efficiency of TritonX-100 by itself was higher than that when it was mixed with CHAPS. Looking at the SDS-PAGE results for this set of detergents (**Figure 2.25.**), CHAPS appears to have hindered TritonX-100

from extracting the protein. These findings contradict the notion that CHAPS can perturb the membrane structure.[57] It was expected that this detergent with its zwitterionic properties would increase the amount of the protein extracted by TritonX-100. In reality, TritonX-100 combined with CHAPS solubilized ~5% of the protein, and TritonX-100, by itself, solubilized ~10% of it.

Furthermore, these results were opposite to those of Everberg et al. who found that the combination of Zwittergent 3-10 and TritonX-114 was as efficient in solubilizing mitochondrial membrane proteins as SDS.[56] One reason that can account for the discrepancy between these results and those obtained in this project is the different solubilization buffer conditions. Everberg's group used a Tris-HCl buffer (10 mM) at a pH of 9.0, but in this project, the phosphate buffer (25 mM) at a pH of 7.2 (KEG buffer) was used. The pH of the solubilization buffer greatly affects solubility and stability of the extracted proteins.[40] Another reason that can account for this disparity is that Everberg et al. extracted membrane proteins from the mitochondrial membrane of yeast *Saccharomyces cerevisiae*. In this project, full-length CYPOR is a recombinant protein that was extracted from the *E. coli* membrane. This observation confirms that the membrane composition of *E. coli* bacterial cells is different from that of yeast *Saccharomyces cerevisiae*.

The addition of alkyl and polyamines to the solubilization buffer containing TritonX-100 resulted in different amounts of the solubilized full-length CYPOR. The amount of the solubilized protein by this detergent combined with spermidine trihydrochloride, spermine tetrahydrochloride, or putrescine dihydrochloride additives was diminished. In fact, spermine tetrahydrochloride completely hindered the ability of

TritonX-100 in extracting the protein. Propylamine hydrochloride and ethylammonium chloride neither inhibited nor enhanced extraction of the protein by TritonX-100. It was expected that the cationic character of these additives would interact with the anionic phosphate groups of the phospholipid bilayer of the membrane.[38] Consequently, this would disrupt packing of the membrane, and the lipid bilayer would be destabilized. However, this observation was not proved for the additives used in this study. This indicates that extraction by alkyl and polyamines does not rely on a common mechanism but rather on specific interactions with a particular membrane protein.

It is worth to mention that a notable precipitation occurred in the SDS-PAGE gel electrophoresis samples prepared with spermidine trihydrochloride or spermine tetrahydrochloride additives. This explains the low loading observed in **lane 3** of their corresponding gels (**Figure 2.26. B** and **C**). The neutral effect of propylamine hydrochloride and ethylammonium chloride raised questions on whether higher concentrations of these additives would solubilize more of the protein. In this study, all of the additives were used at a final concentration of 50 mM but a higher concentration (like 100 mM) was not attempted.

The solubilization results from the set of alkyl and polyamine additives did not agree with those documented in Yasui's study in 2010. This group found that spermidine trihydrochloride added to the solubilization buffer containing CHAPS, TritonX-100, or sodium cholate enhanced solubilization of polygalacturonic acid synthase by ~9.9-fold. It also enhanced solubilization of NADH-dependent cytochrome c reductase and γ-glutamyl transpeptidase by ~2.5-fold and > 3-fold, respectively.[38] In this project, CYPOR

extraction by TritonX-100 combined with this additive or other alkyl and polyamines was not enhanced.

The discrepancy between Yasui's results and those gained in this work can be attributed to the different membrane composition where the proteins are embedded. Yasui et al. extracted polygalacturonic acid synthase, NADH-cytochrome c reductase, and γ-glutamyl transpeptidase from the membrane of Golgi apparatus, ER, and the plasma membrane of Azuki beans, correspondingly.[38] In this project, full-length CYPOR was extracted from bacterial cells.

2.6 CONCLUSIONS

A broad varition of detergents and additives were screened to optimize the extraction and solubilization of full-length CYPOR. None of these compounds were better in extracting the protein than TritonX-100. This is in contrast to the previous successes of other research groups who enahnced solubilization of various membrane proteins using the same compounds. This confirms that the selection of detergents and solubilization buffer conditions have to be experimentally optimized for a specific membrane protein.[38] Also, it is worth mentioning that full-length CYPOR is a eukaryotic protein, which was produced in this project in *E. coli* using a recombinant plasmid DNA construct. Typically, eukaryotic proteins are more difficult to exract from the *E. coli* membranes compared to their prokayrotic counterparts.[65]

From this project, it is confirmed that there is no correlation between the CMC and HLB values of detergents with the extent of full-length CYPOR solubilization. Since no major improvements were observed for solubilization of the protein, it is proposed that

all of the available and non-aggregated full-length CYPOR was extracted from the membrane. The un-sobluilize protein must be present in an unusual and un-extractable form in the membrane. Therefore, more attention has to be turned to optimizing the expression conditions of full-length CYPOR rather than its extraction with detergents to obtain the desired yield of the protein.

Chapter 3

NMR SPECTROSCOPY OF SOLUBLE CYPOR CONSTRUCT: DETERMINATION OF SITE-SPECIFIC ASSIGNMENTS

3.1 INTRODUCTION

A. Overview

In this chapter, mutants of CYPOR are produced to determine site-specific assignments. To appreciate the effect of such mutations in the protein, this chapter will start with a literature review on disease-related CYPOR mutants.

B. Studies on Mutant CYPOR

It is widely known that mutations in the amino acid sequence of a protein can alter its structure and function.[66] The effect of a mutation depends on its type and location in the sequence.[67] CYPOR, like any protein in the human body, is subjected to mutations that can modify its stability and function. As mentioned in chapter 1 of this thesis, the main function of CYPOR is to deliver two electrons to CYPs and other electron acceptors.[9] When CYPs receive these electrons, they catalyze detoxification of drugs, metabolism of steroids, and activation of procarcinogens.[68] Thus, if a mutated CYPOR dysfunctions, electron transfer to CYPs and other electron acceptors is impaired. Consequently, CYPs cannot catalyze many physiological reactions, causing diseases.[69]

The question that arises is what exactly goes wrong in the mutated CYPOR? The answer can be found in the several studies that were done on mutant forms of the N-terminally truncated protein lacking its membrane-anchoring region. This form of the

protein will be referred to as the "soluble CYPOR" in the following text. The first example was the work done by Xia et al. who investigated the effect of two mutations found in the human CYPOR of the Antley-Bixler Syndrome (ABS) patients.[70] This syndrome is characterized by midface hypoplasia and fracture of femora;[70] mortality rates in the neonatal period was reported to be 80%.[71] In these ABS patients, valine 492 amino acid (V492) was mutated to glutamate (E) forming the V492E mutation. Also, arginine 457 (R457) was mutated to histidine (H) resulting in the R457H mutation. These mutations where found in the FAD/NADP(H) domain of CYPOR (**Figure 3.1.**).

As discussed before, CYPOR is composed of three main domains (**Figure 3.1., A**): the FMN domain (where FMN binds), the connecting domain, and the FAD/NADP(H) domain (where FAD and $NADP^+$ bind). FAD interacts with the amino acids that line its binding site in the FAD/NADP(H) domain of CYPOR (**Figure 3.1., B**). The isoalloxazine ring of this cofactor is sandwiched between the tryptophan 679 (W679) at the *re*-face and tyrosine 459 (Y459) at the *si*-face. The dimethyl benzene of this ring is less than 4 Å away from that of the FMN. The pyrimidine side of the ring interacts with the carbonyl groups of isoleucine 474 (I474), cysteine 475 (C475), and valine 477 (V477). The hydroxyl groups of the ribitol moiety of FAD form hydrogen bonds with the carbonyl oxygen and amide nitrogen of tyrosine 458 (Y458). The pyrophosphate region of this cofactor forms salt bridges with the guanidinium group of R457 and hydrogen bonds with the main-chain atoms of threonine 494 (T494), alanine 493 (A493), and valine 492 (V492). The adenine ring of FAD is stacked against the phenolic ring of tyrosine 481(Y481). Mutating R457 and V492 would cause disruptions to these interactions, which would diminish FAD binding to CYPOR.[70]

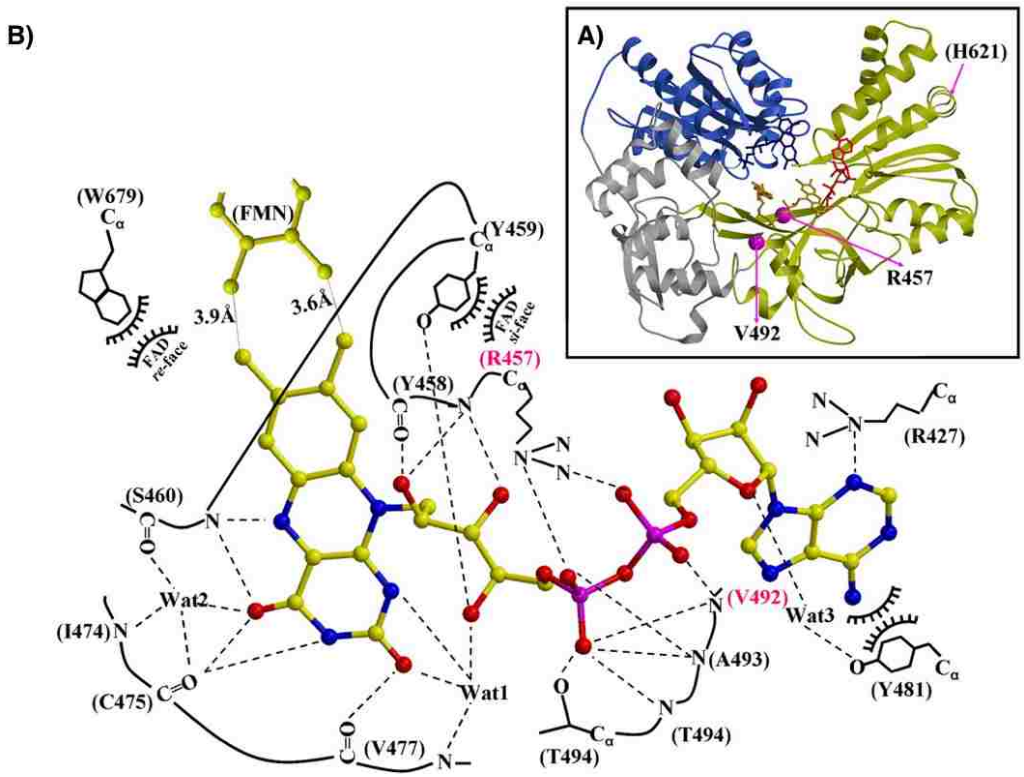

Figure 3.1. Overall structure of CYPOR and the interactions between FAD and the protein. In panel **A**, CYPOR is composed of the FMN domain (blue), the connecting domain (grey), and the FAD/NADP(H) domain (yellow). Cofactors are shown as stick models: FMN (blue), FAD (yellow), and $NADP^+$ (red). Mutation sites in the FAD/NADP(H) domain are marked with pink spheres (V492 and R457). H621 is found in rat but not in the human CYPOR. In panel **B**, FAD interacts with its binding site in the protein via hydrogen bonds and salt bridges (shown as dotted lines) as well as hydrophobic interactions (represented by eye lashes).[70] Illustration taken from reference 70.

Xia et al. aimed to investigate the effect of V492E and R457H mutations on the stability of CYPOR. They expressed, purified, and characterized three soluble forms of this protein: wild-type CYPOR used as a control, CYPOR with the V492E mutation, and another with the R457H mutation. The flavin content, catalytic activity, and structural stability of these isoforms were determined. For flavin analysis, the protein samples were boiled, centrifuged, and the supernatant was analyzed by high performance liquid chromatography (HPLC). It was found that the R457H and V492E CYPOR mutants

contained 35% and less than 5% of the wild-type FAD content, respectively. Both mutants, however, contained nearly the FMN content of the wild-type protein.[70]

The catalytic activity of these isoforms was determined using the cytochrome c reduction assay. Reduction of cytochrome c by CYPOR isoforms resulted in an absorbance at 550 nm, which was increasing with time. The R457H mutant had 31% of the wild-type reductase activity, while the V492E mutant had 0.6% of that activity.[70] However, upon the addition of exogenous FAD, the R457H and V492E mutants regained 69% and 89% of the wild-type activity, respectively.[70]

The structural stability of these CYPOR isoforms was assessed by subjecting them to a limited trypsin digestion. The digestion pattern was analyzed by SDS-PAGE (**Figure 3.2.**). Since this work was done on the soluble form of the protein, a band at 72 kDa was expected. The wild type CYPOR was stable up to 4 hours after trypsin treatment, while the V492E mutant was cleaved into two major fragments (bands a and b in the gel) within 15 minutes. This mutant was unstable and was completely digested within 60 minutes. On the other hand, the R457H mutant was digested within 15 minutes, and most of it remained intact for 4 hours after trypsin treatment. When FAD was added to both mutants, they were stable up to 4 hours like the wild-type protein.[70]

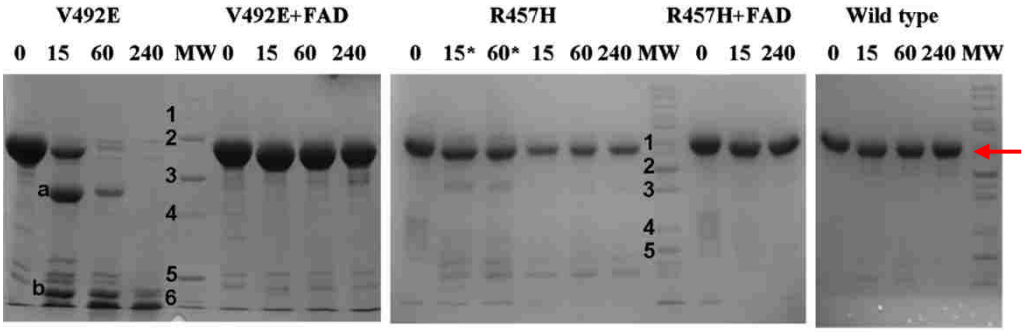

Figure 3.2. SDS-PAGE analysis of trypsin digestion of the wild type, theV492E, and the R457H CYPOR isoforms. A protein band at 72 kDa (red arrow) is expected for these soluble proteins.[70] Figure taken from reference 70.

Xia et al. concluded that the V492E and R457H mutations disrupted the interactions between FAD and its binding site in CYPOR, and this diminished its binding to the protein. Consequently, CYPOR lost its activity and stability. However, the mutant CYPOR isoforms regained their cytochrome c reductase activity and stability upon the addition of exogenous FAD.[70]

Another study was done by Marohnic et al. in 2010 who investigated a mutation in the human CYPOR of the congenital adrenal hyperplasia patients. This disorder is characterized by amenorrhea (absence of menstruation), infertility,[72] and lack of cortisol and aldosterone production.[73] In contrast to the previous study, this mutation was found in the FMN domain of CYPOR, where tyrosine 181 (Y181) was mutated to aspartate (D) leading to the Y181D mutation.[74] **Figure 3.3.** shows that the structures of the FMN domain in rat and human CYPOR proteins overlap. In this domain, Y181 (Y178 in rat) forms hydrophobic and aromatic interactions with the isoalloxazine ring of the bound FMN. Mutating this residue to aspartate removes these interactions and introduces a strong negative charge from the carboxylic side chain of the new residue. This reduces FMN binding to CYPOR.[74]

Marohnic et al. examined the physical properties of the Y181D mutation in the soluble human CYPOR. They analyzed the protein's flavin content and cytochrome c reductase activity and compared these values to those of the wild-type protein. In this study, the purified wild-type CYPOR was green because of the yellow oxidized FAD and the blue FMN semiquinone. However, the purified Y181D mutant was yellow, and this indicated an alteration to its flavin content. To investigate the nature of the flavins in these CYPOR isoforms, UV-visible absorbance spectra (λ = 250–900 nm) were recorded

for the wild-type, its oxidized form, and the Y181D mutant CYPOR proteins (**Figure 3.4.**). The broad peak around 600 nm, which is characteristic of the FMN semiquinone was present in the wild-type CYPOR but not in its oxidized form or the mutant protein. This confirmed that the mutant CYPOR contained the oxidized FMN.[74]

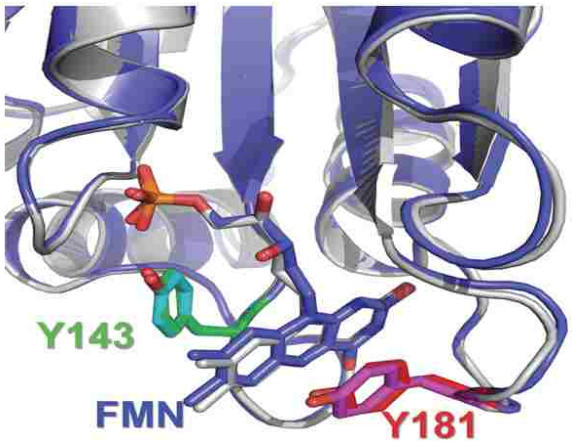

Figure 3.3. Overlay of the FMN domain of rat and human CYPOR proteins. The human Y181 (red) is orthologous to rat Y178 (magenta). Both form hydrophobic interactions with the isoalloxazine ring of FMN.[74] The human Y143 (green) is orthologous to rat Y140 (cyan). Both are positioned at the *re*-face of the FMN isoalloxazine ring. Diagram taken from reference 74.

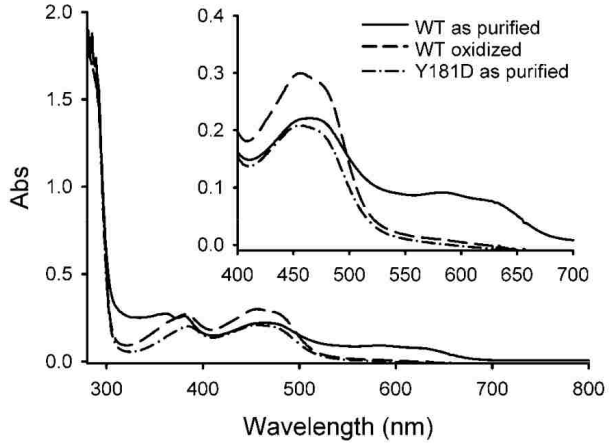

Figure 3.4. UV-visible absorbance spectra of CYPOR. The broad absorption band at 500-700 nm for the FMN semiquinone is present in the wild-type protein but not in its oxidized or the Y181D mutant forms.[74]Adapted from reference 74.

HPLC elution profiles of the wild-type and the Y181D mutant CYPOR isoforms were recorded (**Figure 3.5.**). The standard FAD and FMN had retention times of ~ 4.7 and 7.4 minutes, respectively. The wild-type CYPOR contained both flavins at a ~1:1 ratio. The Y181D mutant, however, had FMN and FAD to ~10% and ~95 % of the protein concentration, respectively.[74] Regarding the cytochrome c reductase activity, the wild-type protein exhibited a catalytic efficiency (k_{cat}/K_m^{NADPH}) of 220 $min^{-1}\mu M^{-1}$, whereas the mutant reaction rates were beneath the limits of detection. Upon the addition of FMN to the Y181D mutant, it gained 159% of the wild-type protein catalytic efficiency. From these observations, Marohnic et al. concluded that CYPOR requires a bound FMN to exhibit the cytochrome c reductase activity.[74] In the Y181D mutant, FMN binding was compromised because of the loss of hydrophobic and aromatic interactions between this cofactor and its binding site in the protein.

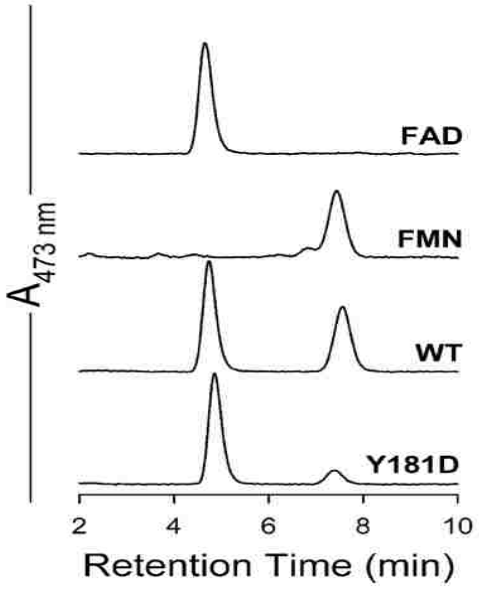

Figure 3.5. HPLC elution profiles of CYPOR flavins. The standard FAD and FMN elute at 4.7 and 7.4 minutes, respectively. The wild-type protein has a ~1:1 ratio of the flavins. The Y181D mutant lacks FMN and has a normal amount of FAD.[74]Adapted from reference 74.

In summary, a common theme for all mutations that caused dysfunction of CYPOR was that they were localized in the interior of the protein. Thus, the amino-acid changes perturbed CYPOR packing or binding of the flavins, resulting in a loss of function.

C. Solution Nuclear Magnetic Resonance (NMR) of Proteins

UV-visible spectroscopy, HPLC analysis, and reduction assays are routinely used to biochemically characterize CYPOR. These techniques give an insight into the overall activity and stability of the protein, but they do not provide site-resolved information on its structure and dynamics. The solution nuclear magnetic resonance (NMR) spectroscopy allows to obtain such information at high resolution. This technique exploits the magnetic dipole moments of nuclei with spin ½ isotopes such as ^{1}H, ^{13}C, ^{15}N and ^{31}P.[75] These isotopes can be introduced at the desired locations within the protein of interest without disturbing its structure and function. Thus, they can act as site-specific reporters of the protein dynamics.[75] Since solution NMR is sensitive to the structural changes of proteins, it can provide details on protein folding and the catalytic turnover of enzymes.[75] These details are extracted from the chemical shift changes of the NMR signals as the protein binds to its ligand or changes its conformations.[76]

Despite its ability to give highly-resolved structural information on proteins, solution NMR has its own limitations. First, the proteins to be analyzed must be soluble in solution and must not aggregate.[77] Besides, this technique requires a high concentration of the protein sample (0.1-5 mM) due to the low characteristic energy of the magnetic spin transitions.[75] Furthermore, the fast transverse relaxation of ^{1}H, ^{15}N,

and ^{13}C nuclei by dipole-dipole coupling (DD) and chemical shift anisotropy (CSA) limits structural determination by solution NMR spectroscopy to small proteins.[78] Large proteins tumble slowly in solution, and this enhances interactions between the spins in the protein. This leads to a fast transverse relaxation with a short relaxation time (T_2),[79] resulting in signal broadening and spectral overlap.[80] As the static magnetic field increases, this overall relaxation increases as well.[78] In order to extend the size limit of solution NMR to large proteins, Pervushin et al. proposed the use of the transverse relaxation-optimized spectroscopy (TROSY).[78]

D. TROSY and Methyl-TROSY

TROSY utilizes the fact that DD and CSA relaxation mechanisms can interfere with each other leading to a decrease in the transverse relaxation rates of nuclear spins.[78] In a conventional heteronuclear NMR experiment such as ^{1}H-^{13}C heteronuclear single quantum correlation (^{1}H-^{13}C HSQC), scalar coupling between the spins is used to establish correlations between them. This coupling also splits the signals from each nucleus into multiplets with different relaxation properties.[79] TROSY retains only the slower relaxing component of the multiplet while discarding the other faster relaxing components.[79] In other words, the TROSY pulse scheme is designed in a way that the long-lived coherences are chosen and isolated from those that relax fast.[81] This results in the formation of narrower lines in the NMR spectra and higher sensitivity.[79]

The TROSY effect can be observed on methyl groups (Methyl-TROSY), which relax via cross-correlated relaxation.[81] In addition, methyl groups rotate fast about their symmetry axis, and this leads to the narrow proton and carbon spectral line widths.[82,83]

To introduce ^{13}C-labled methyl groups at the surface of the protein, a solvent-exposed thiol group of a free cysteine residue is reacted with ^{13}C-methyl-methanethiosulfoante (^{13}C-MMTS). This results in the formation of ^{13}C-methylthiocysteine (^{13}C-MTC) (**Scheme 3.1.**).[84] Thus, through site-directed mutagenesis, it is possible to introduce ^{13}C-methyl probes at any desired location in the protein.

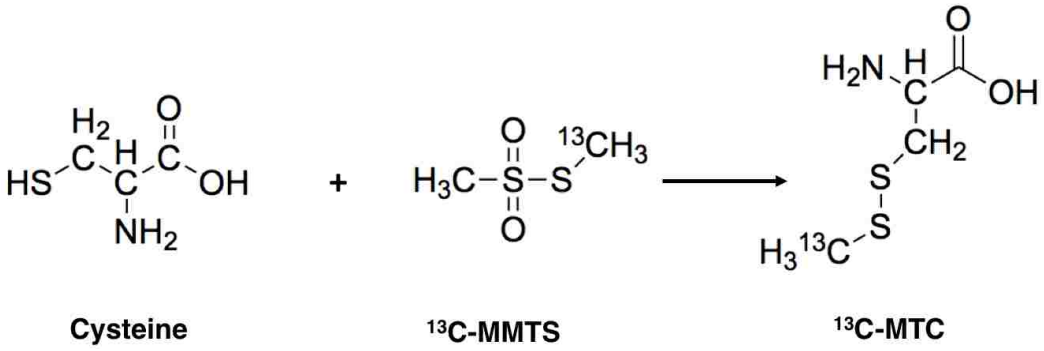

Scheme 3.1. Reaction of ^{13}C-MMTS with a cysteine residue in the protein to produce ^{13}C-MTC.

3.2 GOAL AND PLAN

It is important to understand the redox cycle of CYPOR, and its conformational transitions and interactions with CYP proteins. The effective approach to obtain highly-resolved data on CYPOR dynamics and its structural changes is through the use of solution NMR spectroscopy. To probe particular structural details of CYPOR, the ^{13}C-methyl probes may be placed at crucial sites in the protein. Such sites may be located in CYPOR, where they sense the changes in the redox states of its flavins or the interactions between the protein and CYPs. The NMR spin transitions are sensitive to the changes in the environment that CYPOR experiences in its catalytic cycle. These changes are reflected in chemical shift perturbations for these signals, which are directly recorded in

an NMR experiment. Because of the large molecular weight and extrinsic labeling strategy, methyl assignments in CYPOR may only be obtained through site-directed mutagenesis. To make the assignment of many sites feasible, the soluble form of the protein that lacks the first 56 residues (**Δ**56) at its N-terminus was used instead of the full-length protein.

The main goal of this project was to perform NMR analysis on the oxidized state of CYPOR in order to obtain methyl resonance assignments of the protein. These assignments will be indispensable in the following study of the protein's function, structure, and dynamics using the methyl-TROSY approach. The ^{1}H-^{13}C HSQC experiment was used to obtain NMR signals for the Q157C/Q517C and the Q157C/N271C **Δ**56 CYPOR mutants. This experiment was expected to give strong NMR signals for the labeled sites in the protein. The second objective of this work was based on the NMR spectral results reported by Galiakhmetov et al.[60] This group performed ^{1}H-^{13}C heteronuclear multiple quantum correlation (^{1}H-^{13}C HMQC) experiments on several **Δ**56 CYPOR mutants. The spectra contained a major broad peak in the middle (the middle peak). Accordingly, this project aimed to develop a protocol for the production of an NMR protein sample that gives highly-resolved spectra without the presence of the middle peak. A ^{1}H-^{13}C HMQC spectrum of the Q157C/N271C **Δ**56 CYPOR was recorded and compared with that of the Q157C/Q517C mutant protein.

To create CYPOR specifically labeled at its surface with ^{13}C-methyl groups, the cysteine-less construct[11] of the protein was used. This construct lacks all of its seven native cysteine residues, and site-specific mutations were introduced to create cysteines at the desired locations. In previous work, the native glutamine 157 (Q157), asparagine 271

(N271), and glutamine 517 (Q517) in CYPOR were mutated to cysteines (**Figure 3.6.**). This established the Q157C mutation in the FMN domain as well as the N271C and Q517C mutations in the FAD/NADP(H) domain of the protein. The overall result was two plasmid constructs, one codes for the Q157C/Q517C Δ56 CYPOR, and another codes for the Q157C/N271C mutant proteins. Then, these mutant surface-exposed cysteine residues were reacted with ^{13}C-MMTS introducing extrinsic ^{13}C methyl groups for the assignment of methyl signals. The resulting MTC residues have a similar geometry to methionine and give a strong signal in a methyl-TROSY NMR experiment.

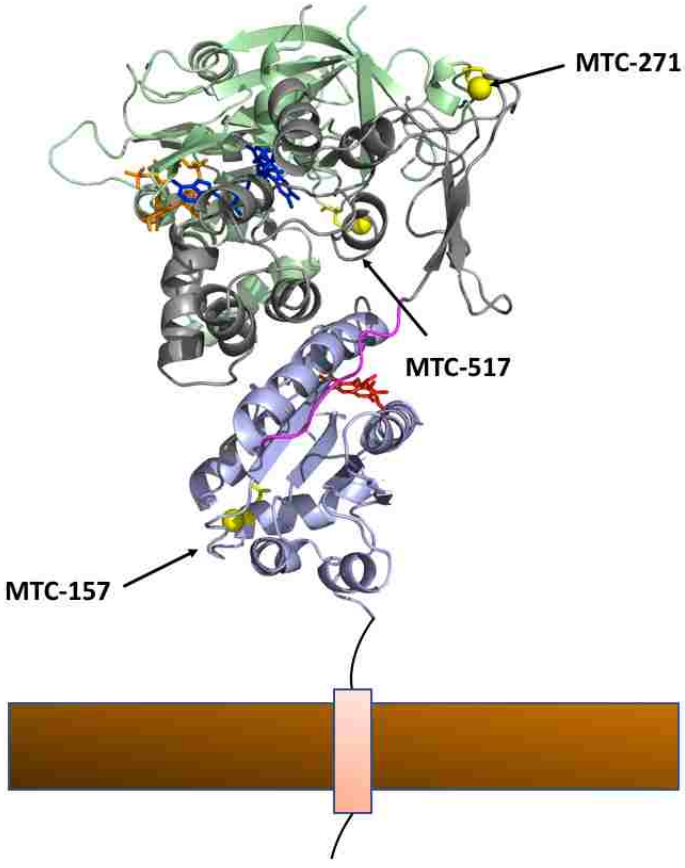

Figure 3.6. Localization of methyl probes on a model for membrane-bound CYPOR. MTC-157 is in the FMN domain, while MTC-271 and MTC-517 are in the FAD/NADP(H) domain of the protein.

It is worth mentioning that these surface-localized mutations are distant from the flavins and do not perturb the protein structure. Thus, it was expected that these mutations would not affect CYPOR functions. However, this was directly tested by analysis of the flavin content and the reductase activity of the Δ56 CYPOR mutants. Expression, purification, and characterization of this protein are illustrated using the data for the Q157C/Q517C Δ56 CYPOR. The Q157C/N271C mutant samples were prepared and characterized similarly unless otherwise indicated. Both CYPOR constructs will be referred to as "Δ56 CYPOR" for the presentation and discussion of these data.

3.3 EXPERIMENTAL

A. Reagents, Chemicals, and Biochemicals

Some of the chemicals and reagents that were used in this project are listed in **Table 2.2.**, while the rest are listed in **Table 3.1.** Purified water from Branstead Water Mixed Bed Deionizer Filter was used when needed for dilutions and preparation of solutions. Yeast extract (5 g), NaCl (5 g), and trypton (10 g) were used to prepare the LB medium, and these reagents along with the kanamycin sulfate antibiotic (Kan) (30 ug/mL) and granulated agar (3 g) were used to prepare the Kan-LB agar plates. Overexpression of Δ56 CYPOR was induced by the addition of IPTG. Riboflavin 5'-Phosphate was added to the LB medium to enrich it for culture growth. NaCl (137 mM), potassium chloride (KCl) (2.7 mM), sodium phosphate dibasic (Na_2HPO_4) (10 mM), and KH_2PO_4 (1.8 mM) were used to prepare the phosphate-buffered saline (PBS) at a pH of 7.4. These reagents were also used to prepare the NMR buffer. TCEP and PMSF were used in cell lysis.

Protein purification by nickel affinity chromatography was done with the His60 Ni Superflow resin. PBS (pH 7.4), glycerol (5% v/v), and TCEP (0.5 mM) were used to prepare the equilibration buffer for this purification. In addition to these reagents, imidazole (20 mM and 500 mM) was added to make the wash and elution buffers, respectively. The pH of these buffers was adjusted to 7.4. The Ni-column equilibration buffer was also used to dialyze the column's eluate (except that the 0.5 mM TCEP reducing agent was replaced with 1 mM DTT) The second affinity chromatography was done with the 2'5'ADP Sepharose^{TM} 4B resin. PBS (pH 7.4), glycerol (5% v/v), and DL-Dithiothreitol (DTT) (1 mM) were used to prepare the equilibration, wash and elution buffers. Along with these reagents, adenosine 2' (3')-monophosphate mixed isomers (AMP) (20 mM) was added to the elution buffer. The pH of all of these buffers was adjusted to 7.4. The 2'5'ADP Sepharose^{TM} 4B equilibration buffer without the 5% v/v glycerol was used to dialyze the column's eluate. Size-exclusion chromatography (SEC) was carried out using the Superose 6 Increase column packed with Superose 6 resin. PBS (pH 7.4) and DTT (1 mM) were used to prepare the mobile phase equilibration buffer at a pH of 7.4.

Potassium ferricyanide $K_3[Fe(CN)_6]$ was used to oxidize the protein. Potassium phosphate (50 mM) at a pH of 7.5 along with EDTA (1 mM) were used to prepare the ^{13}C-MMTS reaction buffer (MRB). ^{13}C-MMTS in DMSO was used for labeling the cysteine residues in the protein. Deuterium oxide (D_2O) was added to the protein before recording the NMR spectra.

The reagents used to prepare samples for SDS-PAGE gel electrophoresis were the same as those used in the first project (**Table 2.2.**). The Coomassie (Bradford) Protein

Assay Kit was used to measure the concentration of the protein. K_2HPO_4, cytochrome c from horse heart, and β-nicotinamide adenine dinucleotide 2'-phosphate reduced tetrasodium salt hydrate (NADPH) were used in the cytochrome c reduction assay. Also, NADPH was used to reduce the Δ56 CYPOR protein. Phosphodiesterase l from *Crotalus adamanteus* venom (PDE) was used for the flavin content determination in the protein.

The expression vectors based on pET28a, which code for the mutant proteins were gifts from Dr. Jung-Ja Kim, MCW. *E. coli* strains of DH5α and C41 (DE3) were used for plasmid amplification and protein expression, respectively.

Chemical / Reagent	**Manufacturer**	**Catalog Number**
Kanamycin sulfate (Kan)	Sigma Aldrich	K4000-25G
Riboflavin 5'-Phosphate	Nutritional Biochemicals Corporation	1-1123
Potassium chloride (KCl)	Fisher Scientific	P217-3
Sodium phosphate dibasic (Na_2HPO_4)	Sigma Aldrich	S0876-1KG
His60 Ni Superflow resin	Clontech lab	635660
Imidazole	Sigma Aldrich	I-0125
2'5'ADP Sepharose™ 4B resin	GE Healthcare Life Sciences	17070001
DL-Dithiothreitol	Sigma Aldrich	D0632-25G
Adenosine 2'(3')-monophosphate mixed isomers (AMP)	Sigma Aldrich	A3013-5G
Superose 6 Increase column packed with Superose 6 resin	GE Healthcare Life Sciences	29-0915-96
Potassium ferricyanide $K_3[Fe(CN)_6]$	Sigma Aldrich	702587-50G
S-methyl-^{13}C-methanethiosulfonate (^{13}C-MMTS)	Sigma Aldrich	723401-10.00MG
Deuterium oxide (D_2O)	Cambridge Isotope Laboratories	DLM-4-99.8-1000
Coomassie (Bradford) Protein Assay Kit	Pierce	23200
Cytochrome c from horse heart	Fisher Scientific	50-247-464

β-nicotinamide adenine dinucleotide 2'-phosphate reduced tetrasodium salt hydrate (NADPH)	Sigma Aldrich	N1630-25MG
Phosphodiesterase l from *Crotalus adamanteus* venom (PDE)	Sigma Aldrich	P3243-1VL

Table 3.1. Manufacturers and catalog numbers for the chemicals and reagents used in this project (project 2).

B. Plasmid, Cell Growth, and Expression of Δ56 CYPOR

The kanamycin-resistant pET28a plasmid, which contains the His-tagged Δ56 CYPOR genes (~72 kDa) was amplified in *E. coli* DH5α competent cells. Then, it was extracted and purified using the Omega bio-tek E.Z.N.A. Plasmid Mini Kit I, (Q-spin) following the manual's protocol.

For protein expression, the plasmid was transformed into *E. coli* C41 (DE3) competent cells using a heat shock at 42ºC for 40 seconds in the VWR 1224 Digital Water Bath. The transformed *E. coli* cells were incubated with LB medium in a culture tube. They were grown at 220 rpm and 37ºC for 1 hour in the New Brunswick Stackable Incubator Shaker I2500 and I2500 KC. A 100 uL of the cell suspension was plated on a Kan-LB agar plate and was incubated at 37ºC overnight in the Precision Incubator. The next day, a single colony from the plate was inoculated into room-temperature sterile LB medium containing Kan (30 ug/mL). This starter culture was shaken at 220 rpm and 37ºC for 3 hours. Later, the larger culture was prepared by transferring the starter culture into a larger volume of sterile LB medium with Kan (30 ug/mL). This culture was grown in the shaker at 220 rpm and 37ºC overnight.

On the following day, the OD_{600} of the overnight culture was measured using the Varian Cary 50 Bio UV-Visible Spectrophotometer. Then, this overnight culture was transferred to a sterile LB medium containing Kan (30 ug/mL) in order to make the expression culture. This culture was shaken at 220 rpm and 37^{o}C for ~3 hours until the cells reached OD_{600} of ~ 0.7- 0.9 au. Later, the growth culture was cooled on ice and was further shaken at room temperature for 10 minutes in the New Brunswick G25 Shaker Incubator. Then, small portions from that culture were taken to represent the non-induced cell culture. To the rest of the cells, IPTG (0.5 mM) and riboflavin 5'-Phosphate (0.5 uM) were added in order to induce overexpression of the Δ56 CYPOR. OD_{600} was measured for the non-induced and induced cell cultures before shaking them at 220 rpm and 18^{o}C overnight.

C. Purification and Dialysis

In morning of the following day, OD_{600} was checked for the overnight cell cultures to ensure reaching OD_{600} of ~ 3-6 au. The cells were harvested by centrifugation at 5,000 g and 4^{o}C for 15 minutes in the Sorvall LYNX 4000 Superspeed Centrifuge. The cell pellet was suspended in PBS (pH 7.4) (25 mL per 1 L of the original cell culture) along with PMSF (1 mM) and TCEP (0.1 mM). The cells were broken by sonicating the cell suspension on ice at 50% duty cycle, power setting of 6 for 30 seconds in the VWR Branson 450 Sonifier. This was followed by incubating the cell suspension on ice, and the sonication step was repeated 3 times. Following that, the cell lysate was centrifuged at 10,000 g and 4^{o}C for 40 minutes in the Eppendorf™ 5810R Centrifuge.

The supernatant from the cell lysate contained Δ56 CYPOR along with other soluble proteins. Thus, it was purified via nickel-affinity chromatography using the His60 Ni Superflow column, pre-equilibrated with the Ni-column equilibration buffer. The supernatant was passed through the column, and the flow-through fractions were collected. Contaminant proteins that non-specifically and weakly bound to the column were removed with the Ni-column wash buffer. The resulting wash fractions were collected. After that, Δ56 CYPOR was eluted from the column by the Ni-column elution buffer, and the elution fractions were collected. In order to remove imidazole from the Ni-column eluate, it was dialyzed overnight against the column's equilibration buffer (after replacing the 0.5 mM TCEP with 1 mM DTT). This was done using a regenerated cellulose dialysis tubing 3,500 MWCO (Fisher Scientific).

On the next day, the dialyzed eluate was passed through the 2'5'-ADP Sepharose 4B column, pre-equilibrated with the equilibration buffer for this column. The flow through fractions were collected to capture the excess unbound protein. Then, the column was washed with its corresponding wash buffer, and the wash fractions were collected. The protein was eluted from the column using the column's elution buffer. Then, it was concentrated with the Amicon Ultra-15 Centrifugal Filter Device 10,000 MWCO (Merck Millipore**)** to a final volume of 10 mL. Afterwards, the sample was dialyzed overnight against PBS (pH 7.4) containing 1 mM DTT. On the following day, the dialyzed protein sample was passed through the Superose 6 Increase column, which was equilibrated with the mobile phase equilibration buffer. SEC (gel filtration) was carried out at a flow rate of 0.5 mL/min using the Shimadzu liquid chromatography equipped with an SPD-m20A diode array detector. SEC was only performed on the Q157C/Q517C Δ56 CYPOR but

not on the Q157C/N271C mutant protein. The purity of Δ56 CYPOR was analyzed by SDS- PAGE powered by Invitrogen Life Technology PowerEase 500 at 135 V, 90 mA, and 12.5 W for 95 minutes.

D. NMR Sample Preparation and NMR Spectroscopy

The SEC eluate was concentrated with Vivaspin ®2 Centrifugal Concentrator 10,000 MWCO (Sartorius) to a final volume of 0.5 mL. Then, this sample was treated with a 4-fold molar excess of $K_3[Fe(CN)_6]$ in order to fully oxidize the protein. The concentration of $K_3[Fe(CN)_6]$ was determined by specific absorption at ε (340 nm) = 6220 $M^{-1}cm^{-1}$.[85] UV-visible spectra were recorded to ensure the absence of the semiquinone absorption band at 600 nm. The sample was dialyzed against the MRB buffer overnight using the Slide-A-Lyzer Dialysis Cassettes 3,500 MWCO, 0.5-3 mL (ThermoFisher Scientific).

On the next day, a few microliters of this sample were placed aside for characterization of Δ56 CYPOR. To the rest of the protein, a 1.5-fold molar excess of the stock solution of ^{13}C-MMTS in DMSO (100 mM) was added. The mixture was incubated at 4^{o}C for 3 hours. Unreacted ^{13}C-MMTS was removed by dialysis against the NMR buffer overnight. Afterwards, the dialyzed sample was concentrated to a final volume of 300 uL and was degassed under vacuum for 1 hour. Then, D_2O was added to 10% (v/v) for the NMR spectrometer lock.

NMR measurements were carried out at 20^{o}C in Shigemi tube on the 600 MHz Varian VNMR-S spectrometer with the Cold Probe. ^{1}H-^{13}C HSQC spectra were recorded for the Δ56 CYPOR mutants. Along with this, a ^{1}H-^{13}C HMQC spectrum was recorded

for the Q157C/N271C Δ56 CYPOR but not for the Q157C/Q517C mutant protein. In addition, a ^{1}H-^{13}C HSQC spectrum was recorded for the reduced Q157C/N271C Δ56 CYPOR; this construct was reduced by the addition of a 4-fold molar excess of NADPH. All of the NMR spectra were processed with NMRPipe[86] and Sparky.[87]

Figure 3.7. demonstrates an overview of the ^{1}H-^{13}C HSQC and ^{1}H-^{13}C HMQC pulse sequences that were used in this project. The ^{1}H-^{13}C HSQC pulse sequence (**Figure 3.7., A**) starts with the equilibrium magnetization on the ^{1}H spin, which is flipped into the transverse plane by an x-axis 90^{o} pulse. During period **A**, two x-axis 180^{o} pulses are applied on the ^{1}H and ^{13}C spins. The time delays (τ_1) before and after the application of these pulses are equivalent. This allows for the ^{1}H spin magnetization to evolve via scalar coupling but not via chemical shift. In period **B**, subsequent 90^{o} pulses are applied on the ^{1}H and ^{13}C spins, but one is applied along the y-axis and the other along the x-axis, respectively. This results in the transfer of the anti-phase magnetization component from the ^{1}H spin to that of ^{13}C. Then,^{13}C spin magnetization evolves for t_1 via its chemical shift (period **C**). During this period, the x-axis 180^{o} pulse on the ^{1}H spin refocuses the J-coupling evolution. The x-axis 90^{o} pulses on both spins during period **D** transfer the anti-phase magnetization back to the ^{1}H spin. Then, two x-axis 180^{o} pulses are applied on the ^{1}H and ^{13}C spins with τ_1 before and after the application of these pulses (period **E**). This spin echo converts the anti-phase magnetization into an in-phase, which is detected during t_2 using the broadband ^{13}C spin decoupling.[88]

The ^{1}H-^{13}C HMQC pulse sequence (**Figure 3.7., B**) starts with an x-axis 90^{o} pulse on the ^{1}H spin, which flips the equilibrium magnetization of this spin into the transverse plane. This magnetization becomes anti-phase during τ (period **A**). The x-axis 90^{o} pulse

on the ^{13}C spin (period **B**) converts this anti-phase magnetization into a heteronuclear multiple quantum coherence. This coherence evolves for t_1 (period **C**). Then, the x-axis 90° pulse on the ^{13}C spin (period **D**) converts the multiple quantum coherence into an anti-phase magnetization on the ^{1}H spin. This magnetization evolves into an in-phase magnetization during τ (period **E)**. During t_2, ^{1}H spin is decoupled from that of ^{13}C, and the signal is detected.

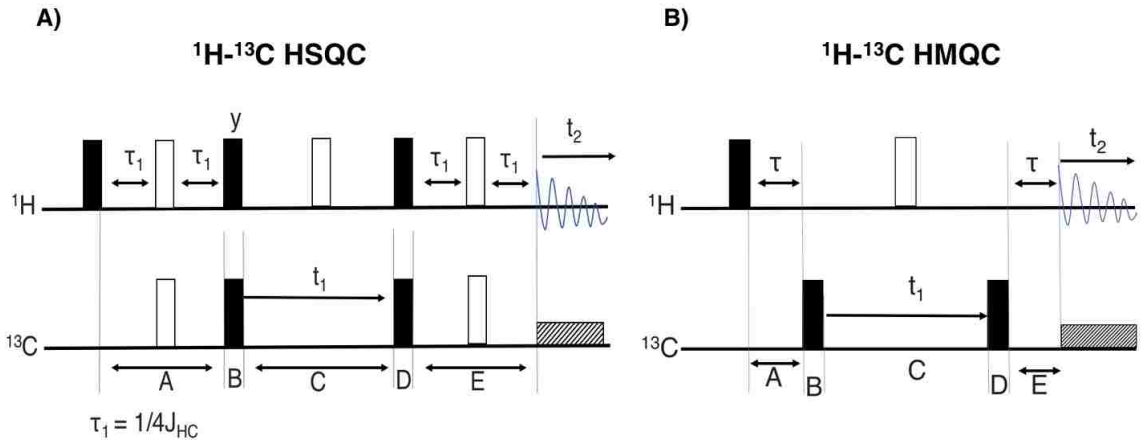

Figure 3.7. ^{1}H-^{13}C HSQC and ^{1}H-^{13}C HMQC pulse sequences. ^{1}H-^{13}C HSQC (**A**) and ^{1}H-^{13}C HMQC (**B**) experiments have similar pulse sequences. The unlabeled black and white rectangles represent x- axis 90° and 180° pulses, respectively. The black rectangles that are labeled with "y" indicate 90° pulses applied along the y axis. The time delay τ_1 is equal to 1/4 J_{HC}, while τ can acquire any time duration. The time, t_1, indicates the evolution time of the magnetizations, while t_2 is the duration of signal detection. The stippled boxes represent decoupling of the ^{13}C spin from that of ^{1}H. The wiggling line denotes signal detection.

E. Cytochrome c Assay

The reduction activity of Δ56 CYPOR was determined using the NADPH-P450 reductase assay.[89] This assay is based on the use of cytochrome c, which accepts electrons from NADPH via CYPOR without being re-oxidized *in vitro*. The rate at which CYPOR reduces cytochrome c is measured in this assay. Reduction of the protein is

monitored by an increase in its absorbance at 550 nm (A_{550}). The reaction mixture containing cytochrome c (40 uM), Δ56 CYPOR (0.1 uM), and K_2HPO_4 (273 mM) at a pH of 7.7 was prepared in a 1 mL optical cell. The A_{550} reading was recorded to establish the baseline absorbance. Next, to initiate the reaction, NADPH (100 uM) was added, and the components in the optical cell were rapidly mixed. The A_{550} for this reaction mixture was recorded as a function of time for 5 minutes. The total activity of the protein was determined using **Equation 3.1.** Its specific activity was calculated using **Equation 3.2.**

$$Total\ \ activity = \frac{\Delta A_{550}/_{min}}{0.021\ mM^{-1}cm^{-1}}$$

Equation 3.1. Calculation of the total activity of Δ56 CYPOR. This calculation gives the amount of cytochrome c (in nmol) that is reduced per minute. ΔA_{550} is the change in absorbance at 550 nm. The value of 0.021 $mM^{-1}cm^{-1}$ is the molar extinction coefficient of the reduced cytochrome c.[90]

$$Specific\ activity = Total\ activity \div 0.1$$

Equation 3.2. Calculation of the specific activity of Δ56 CYPOR. This calculation gives the amount of cytochrome c (in nmol) that is reduced per min per nmol of Δ56 CYPOR. The value of 0.1 is the amount of Δ56 CYPOR in nmol; this value can vary depending on the number of nmoles of the reductase used in the assay.

F. Flavin Content

The stoichiometry of the bound FAD and FMN in Δ56 CYPOR was determined using fluorescence measurements.[90] This method utilizes the fact that fluorescence of FMN is 10-fold higher than that of FAD. The PDE enzyme catalyzes the conversion of FAD into FMN and adenosine monophosphate (AMP). Therefore, the addition of PDE to a mixture of FAD and FMN will result in a fluorescence increase reporting on the fraction of FAD in the sample.[90] To release the flavins, Δ56 CYPOR (~5 uM) was

denatured by incubating it at a 100ºC for 15 minutes. The sample was chilled on ice for 5 minutes. The denatured protein was removed by centrifugation at 16,000 g and 4ºC for 10 minutes in the Eppendorf Centrifuge 5415D.

The supernatant was transferred to a 3 mm Starna quartz cell. Emission spectra of the supernatant were recorded before and after a 15-minute treatment with PDE (3 mU/uL) using Horiba PTI QM40 fluorometer. **Table 3.2.** shows the parameters that were used for the fluorometer settings. The molar ratio of FAD and FMN in the protein was determined using **Equation 3.3.** This equation is based on the use of the fluorescence values of the flavins before (F_o) and after treatment with PDE (F_{fin}). To examine the effect of protein denaturation on fluorescence of the flavins, UV-visible absorbance spectra were recorded before and after heating the protein.

Parameter	**Value**
λ_{ex}	450 nm
$\lambda_{emission}$	460-610 nm
Excitation slit	2 nm
Emission slit	2 nm

Table 3.2. The Horiba PTI QM40 fluorometer settings. Fluorescence of the flavins in **Δ**56 CYPOR was determined using the above settings in the fluorometer.

$$r = \frac{\left(10 \times \left(\frac{F_{fin}}{F_o}\right) - 10\right)}{10 - \left(\frac{F_{fin}}{F_o}\right)}$$

Equation 3.3. Calculation of the molar ratio (r) of FAD and FMN in **Δ**56 CYPOR. This ratio is determined using fluorescence of the flavins at 525 nm before (F_o) and after (F_{fin}) treatment with PDE. The value of 10 is the ratio of the quantum yield of the flavins.[90]

3.4 RESULTS

Protein expression. The overnight starter, induced, and non-induced cell cultures were growing at an expected rate (**Table 3.3.**). The overnight starter culture grew to a high density (OD_{600} = 3.4), and it was inoculated into fresh LB medium. During growth for three hours, the cells reached OD_{600} of 1.0 at which they were induced for overexpression of Δ56 CYPOR with IPTG. When the cells reached OD_{600} of 5.1, the protein overexpression was confirmed by SDS-PAGE of the cell lysate from the non-induced and induced cell cultures **(Figure 3.8.**).

The amount of the protein in the non-induced cell lysate (**Figure 3.8., lane 2**) was lower than that in the induce one (**Figure 3.8., lane 3**). This was confirmed by the intensity of the 72 kDa band, which was less intense for the non-induced cells (**lane 2**) compared to that of the induced ones (**lane 3**). This observation confirmed that the protein was overexpressed after inducing *E. coli* cells with IPTG. Following cell lysis and centrifugation, Δ56 CYPOR was present in the supernatant of the induced cell lysate along with other soluble proteins (**Figure 3.9.**). This supernatant contained many protein bands along with that of the Δ56 CYPOR (**Figure 3.9., lane 2**).

Sample	**OD_{600}, $\frac{au}{mL.cm}$**
Overnight starter culture	3.4
Average growth at the start	0.1
Average growth after 1 hour	0.1
Average growth after 2 hours	0.5
Average growth after 3 hours	1.0
Average growth of induced cells before overnight	1.4
Average growth of non-induced cells before overnight	1.5

Average growth of induced cells after overnight	5.1
Average growth of non-induced cells after overnight	4.7

Table 3.3. OD_{600} values of the cell cultures. The concentration of bacterial cells in the overnight starter, induced, and non-induced cultures is signified by their OD_{600}.

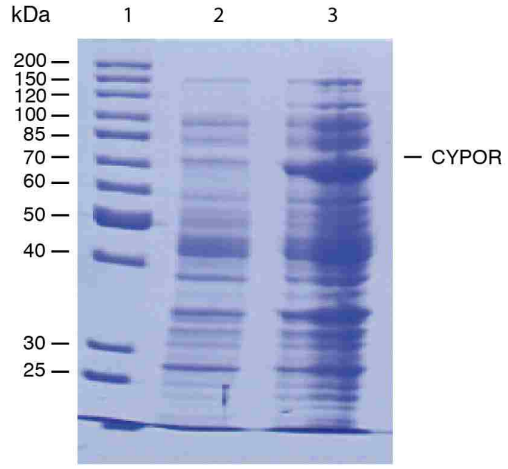

Figure 3.8. SDS-PAGE gel for overexpression of Δ56 CYPOR. **Lane 1** denotes the PageRuler Unstained Protein Ladder. The presence of Δ56 CYPOR is confirmed by the 72 kDa band. This band is less intense in the non-induced cell lysate (**lane 2**) compared to that of the induced one (**lane 3**).

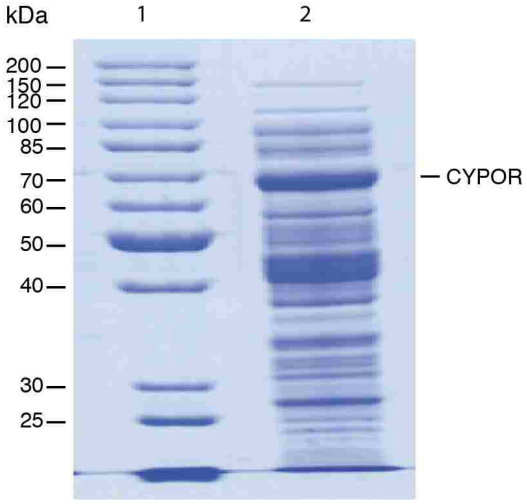

Figure 3.9. SDS-PAGE gel for the induced cell lysate supernatant. **Lane 1** is the PageRuler Unstained Protein Ladder. The 72 kDa band for Δ56 CYPOR is present in this supernatant along with bands for other soluble proteins (**lane 2**).

Protein purification. The Δ56 CYPOR protein was purified by affinity and size-exclusion chromatography. In nickel affinity purification (**Figure 3.10.**), the protein was retained in the column by its 6 histidine residues. The rest of the soluble proteins passed through the column and were collected in the flow through fractions (**Figure 3.10.**, **lanes 2-4**). It is worth to mention that the column was overloaded with the protein. This was clear from the presence of the 72 kDa band in **lanes 3** and **4** of **Figure 3.10.** Thus, the second and third flow through fractions were stored at -80ºC for later purification of the protein when needed. The column was washed to remove non-specific proteins, which bound to the column. These proteins were collected in the wash fractions (**Figure 3.10., lanes 5-7**). The desired His-tagged protein was eluted from the column, and the elution fractions were collected (**Figure 3.10., 8-10**). The 72 kDa band was not seen in **lane 10**. This denoted that the protein eluted successfully from the column, and it was present in the elution fractions 8 and 9.

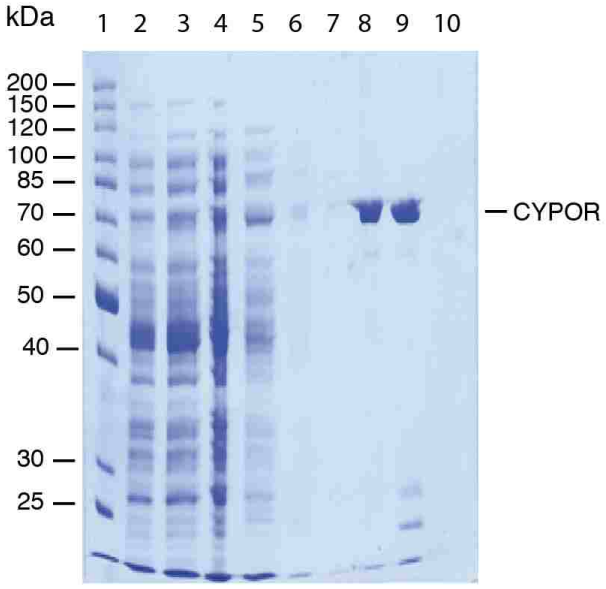

Figure 3.10. SDS-PAGE gel for nickel-affinity purification of Δ56 CYPOR. **Lane 1** is the PageRuler Unstained Protein Ladder. **Lanes 2-4** are the flow through fractions from

the column. **Lanes 5-7** and **8-10** are the column's wash and elution fractions, correspondingly. The Δ56 CYPOR protein band is around 72 kDa.

The Nickel-column eluate was dialyzed to remove excess imidazole and was passed through the 2',5'- ADP Sepharose 4B resin to further purify the protein (**Figure 3.11.**). Upon loading the eluate, the flow through fractions were collected (**Figure 3.11., lanes 2-4**). The presence of only one protein band in these lanes signified that the protein was relatively pure at the beginning. Then, the column was washed, and the wash fractions were collected (**Figure 3.11., lanes 5-7**). There was one protein band in **lane 5** and no bands in **lanes 6** and **7**. These results clearly indicated that very few non-specific proteins bound to the column. The Δ56 CYPOR eluted from the column, and the elution fractions were collected (**Figure 3.11., lanes 8-10**).

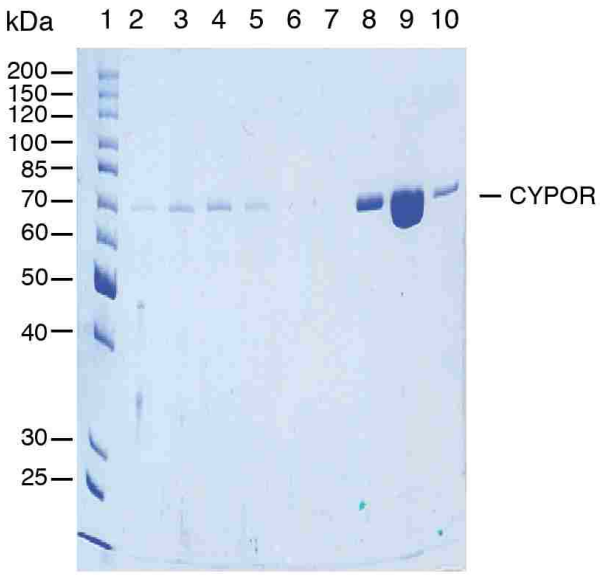

Figure 3.11. SDS-PAGE gel for ADP-affinity purification of Δ56 CYPOR. Lane assignments are the same as those in **Figure 3.10.** The Δ56 CYPOR band is around 72 kDa.

The intense 72 kDa protein band that was observed in **lane 9** of **Figure 3.11.** signified that most of Δ56 CYPOR was present in the second elution fraction. It is important to mention that five elution fractions were collected from the 2',5'- ADP Sepharose 4B column. However, the last two fractions did not contain any protein band (data not shown). Thus, it was concluded that the protein was collected successfully in the first three elution fractions.

The purity and stability of Δ56 CYPOR were increased by passing the protein through the Superose 6 Increase column. This step separated the protein from proteases, which would otherwise degrade it. SEC purification was performed only on the Q157C/Q517C Δ56 CYPOR but not on the Q157C/N271C mutant protein. **Figure 3.12.** shows the HPLC elution profile of the protein.

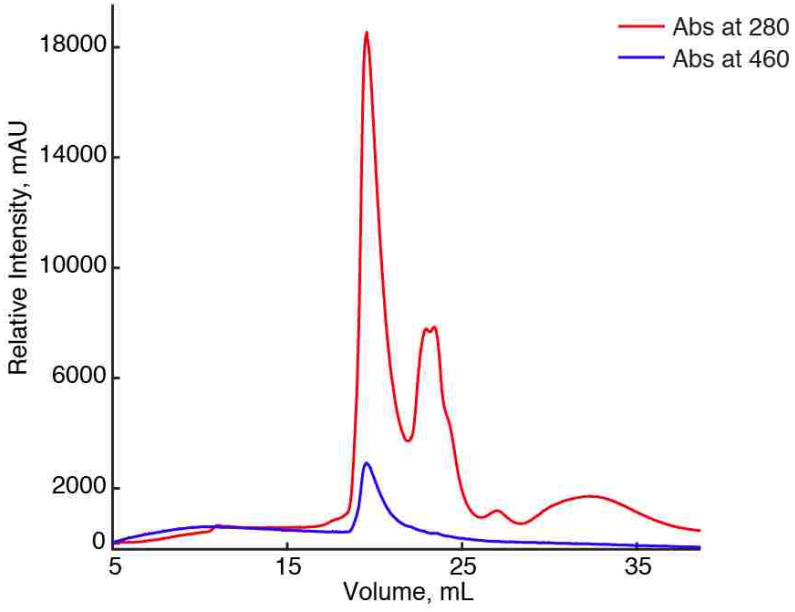

Figure 3.12. HPLC elution profile of the Q157C/Q517C Δ56 CYPOR. The presence of the protein is detected by absorption of tyrosine and tryptophan at 280 nm (red trace) and by absorption of the flavins at 460 nm (blue trace).

As indicated in **Figure 3.12.**, the void volume of the SEC column is 10.5 mL, and the absence of absorption bands in this volume confirmed that the protein did not aggregate. The protein eluted after about 20 mL passed through the column. This was clear from the absorption of tyrosine and tryptophan amino acids at 280 nm as well as absorption of the flavins at 460 nm. It is worth to mention that there was a small absorption band at 280 nm after about 30 mL passed through the column. This was probably due to degraded forms of the Q157C/Q517C Δ56 CYPOR.

Protein oxidation. To ensure the oxidation state of Δ56 CYPOR, a UV-visible absorption spectrum was recorded for the protein after treatment with $K_3[Fe(CN)_6]$ (**Figure 3.13.**). Typically, the oxidized flavins give UV-visible absorption bands with maxima at 380 nm and 450 nm.[1] The semiquinone flavins, however, have an absorption maximum around 585 nm. In this spectrum, the absence of the 585 nm absorption band and the presence of the 380 nm and 450 nm bands confirmed that the protein was oxidized.

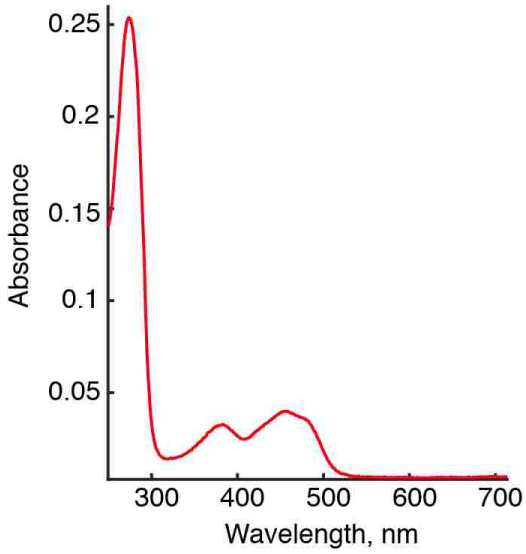

Figure 3.13. UV-visible absorption spectrum of the flavins in the oxidized Δ56 CYPOR. The flavins have 380 nm and 450 nm absorption maxima in the oxidized protein. The 585 nm absorption band for the semiquinone flavins is absent in this spectrum.

Activity measurements. The activity of Δ56 CYPOR was determined by measuring the rate at which it reduces cytochrome c. The change in absorbance at 550 nm (ΔA_{550}) was monitored over 5 minutes (**Figure 3.14.**). The ΔA_{550} between 75 and 200 seconds was used in **Equations 3.1. and 3.2.** to calculate the reductase activity (See Appendix for calculations). It is important to note that activity measurements were done once on the Q157C/Q517C Δ56 CYPOR because of the insufficient amount of cytochrome c available. However, measurements on the Q157C/N271C mutant were done in a triplicate. It was expected that the error in the Q157C/Q517C mutant would be similar to that of the Q157C/N271C Δ56 CYPOR.

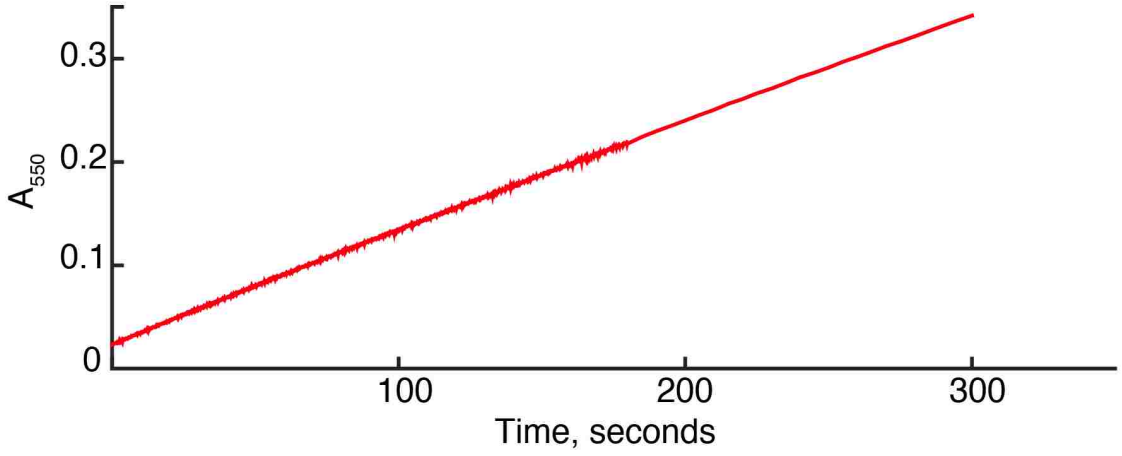

Figure 3.14. NADPH- cytochrome c reductase activity of Δ56 CYPOR. Cytochrome c reduction is detected by measuring the A_{550} as a function of time in seconds.

The rate of the reductase activity of the Q157C/Q517C Δ56 CYPOR was calculated to be 3.03 nmol of cytochrome c reduced per minute. With this, the specific activity of this mutant was found to be 30.3 nmol of cytochrome c reduced per minute per

1 nmol of the Q157C/Q517C Δ56 CYPOR. These values corresponded to 1.01% of the wild-type reductase activity. The activity of the Q157C/N271C mutant protein was found to be 3.1 ± 0.2 nmol of cytochrome c reduced per minute. Thus 31 ± 2 nmol of cytochrome c was reduced per minute per 1 nmol of the Q157C/N271C Δ56 CYPOR. This resulted in 1.02 ± 0.06 % of the wild-type reductase activity.

The effect of ^{13}C-MMTS labeling on the protein activity was determined for the Q157C/N271C mutant protein. The rate of cytochrome c reduction by the ^{13}C-MMTS - labeled Q157C/N271C Δ56 CYPOR was found to be 2.9 ± 0.5 nmol of cytochrome c reduced per minute. This corresponded to 29 ± 5 nmol of cytochrome c reduced per minute per 1 nmol of the Q157C/N271C Δ56 CYPOR. Hence, this mutant had 1.0 ± 0.2 % of the wild-type reductase activity. The calculated error for the Q157C/N271C mutant activity measurements are the standard deviations from three replicates.

Flavin content. To determine the flavin content in Δ56 CYPOR, the protein was denatured by heating it at 100ºC. This resulted in a slight shift of its UV-visible absorbance spectrum towards the lower limit compared to the one before heating (**Figure 3.15.**). However, absorption of the oxidized flavins at 380 nm and 450 nm remained relatively the same before and after heating the protein.

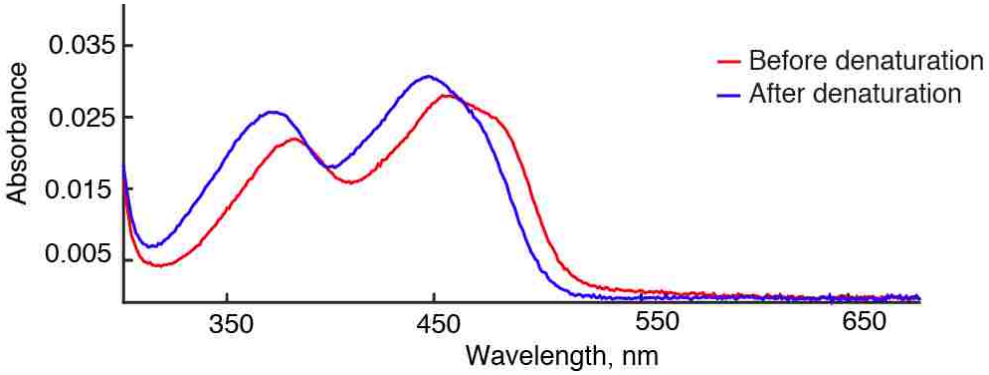

Figure 3.15. UV-visible absorbance spectra of Δ56 CYPOR flavins. Absorbance of the oxidized flavins at 380 nm and 450 nm is relatively the same before (red trace) and after (blue trace) denaturing the protein with heat.

Fluorescence of the released flavins at ~525 nm was determined before and after treating the protein with PDE. **Figure 3.16.** shows that the maximum fluorescence of the flavins at ~525 nm in the Q157C/Q517C Δ56 CYPOR before the PDE treatment (F_o) was 5.7492 x 10^4. The fluorescence after the PDE treatment (F_{fin}) was 1.12522 x 10^5. The molar ratio of the flavins in Δ56 CYPOR was determined using **Equation 3.3.** (see Appendix for calculations).

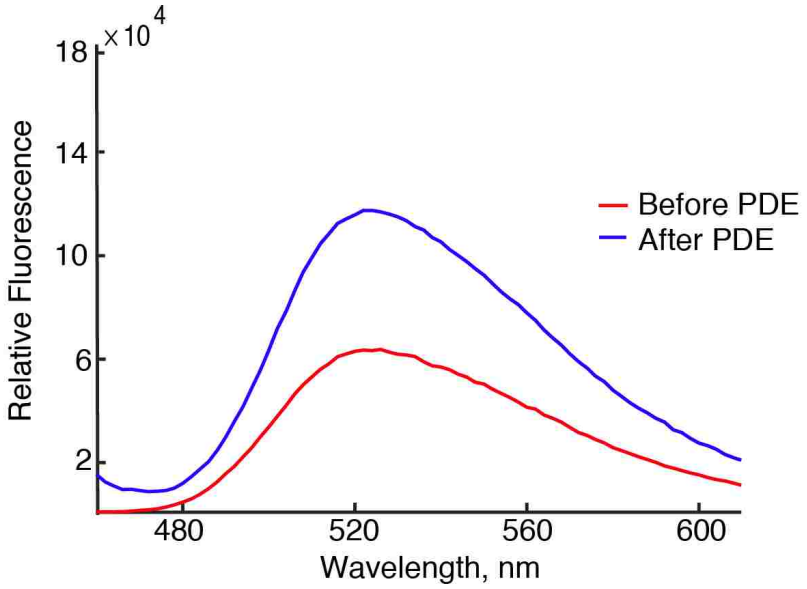

Figure 3.16. Fluorescence of Δ56 CYPOR flavins. The maximum fluorescence of the flavin solution at 525 nm before treating it with PDE (red trace) is 5.7492 x 10^4. The fluorescence increases up to 1.12522 x 10^5 after treating the solution with PDE (blue trace).

It was found that the Q157C/Q517C Δ56 CYPOR had 1.1 ± 0.1 mole of each of FAD and FMN because fluorescence of the flavin's solution increased by 1.87 ± 0.08-fold. Besides, the Q157C/N271C Δ56 CYPOR was found to contain 0.8 ± 0.1 of each of

the flavins because fluorescence of the flavin solution increased by 1.70 ± 0.08-fold. These values indicate that ~ 20% of the Q157C/N271C Δ56 CYPOR lost its FMN. In these results, the ratios represent the moles of FMN: FAD (mole: mole), and the calculated error for the flavin content in the Δ56 CYPOR constructs is the standard deviation from three replicates.

NMR spectroscopy. ^{1}H-^{13}C HSQC spectra of the ^{13}C-MMTS-labled Δ56 CYPOR constructs were acquired at 20°C (**Figure 3.17.**). The spectrum of the Q157C/Q517C mutant protein (**Figure 3.17., A**) contained peaks for MTC-157 and MTC-517. Similarly, the spectrum for the Q157C/N271C construct (**Figure 3.17., B**) had peaks for MTC-157 and MTC-271. The resonance positions of MTC-157 and MTC-517 were known from previous measurements.[60] The resonance position for MTC-271, however, is new in this study.

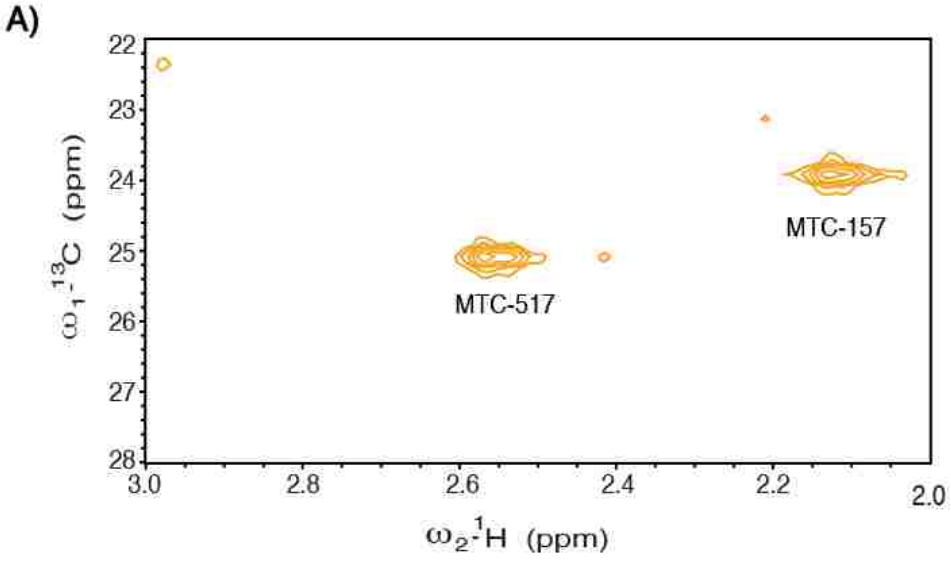

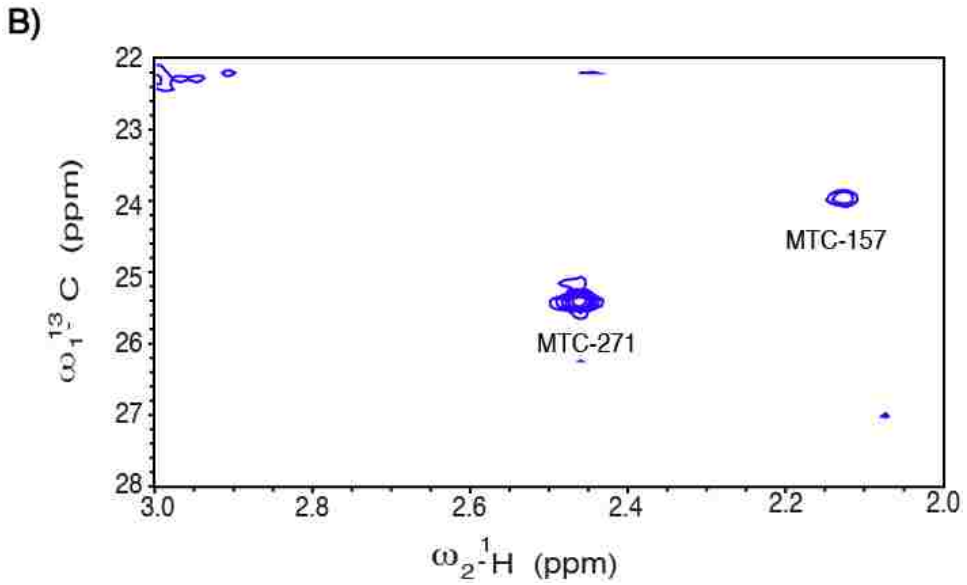

Figure 3.17. ^{1}H-^{13}C HSQC spectra of Δ56 CYPOR mutants, Q157C/Q517C (**A**) and Q157C/N271C (**B**).

To establish the assignment of MTC-271 residue, the ^{1}H-^{13}C HSQC spectra in **Figure 3.17.** were overlaid (**Figure 3.18.**); the resonance position of MTC-271 in the Q157C/N271C Δ56 CYPOR construct (blue) was found to be 2.46 ppm ^{1}H, 25.42 ppm ^{13}C. These chemical shifts are different from those of MTC-157 and MTC-517 in the Q157C/Q517C Δ56 CYPOR construct (orange).

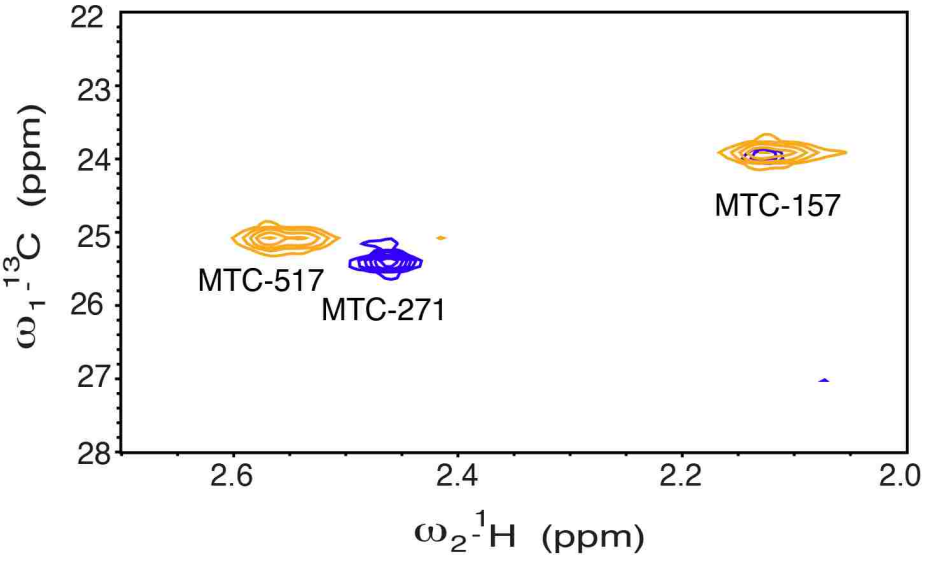

Figure 3.18. Overlay of ^{1}H-^{13}C HSQC spectra of Δ56 CYPOR mutants. MTC signals for the Q157C/Q517C (orange) and the Q157C/N271C (blue) constructs.

It is worth noting that the MTC signals for the Q157C/N271C mutant were weak as shown in **Figure 3.17., B**. To increase the intensity of these signals, an additional 1.5-fold molar excess of ^{13}C-MMTS was added to the Q157C/N271C protein sample. After overnight incubation at 4^{o}C, a ^{1}H-^{13}C HSQC spectrum was recorded again for this mutant. **Figure 3.19.** shows an overlay of the ^{1}H-^{13}C HSQC spectra of the Q157C/N271C construct with the excess ^{13}C-MMTS (green) and without excess of this reagent (blue). As expected, the MTC signals became stronger and more intense upon the addition of excess^{13}C-MMTS. A strong signal for free ^{13}C-MMTS produced a ridge of artifacts at 2.71-2.75 ppm ^{1}H, along the entire ^{13}C-dimension yet did not interfere with the observation of MTC signals from the protein.

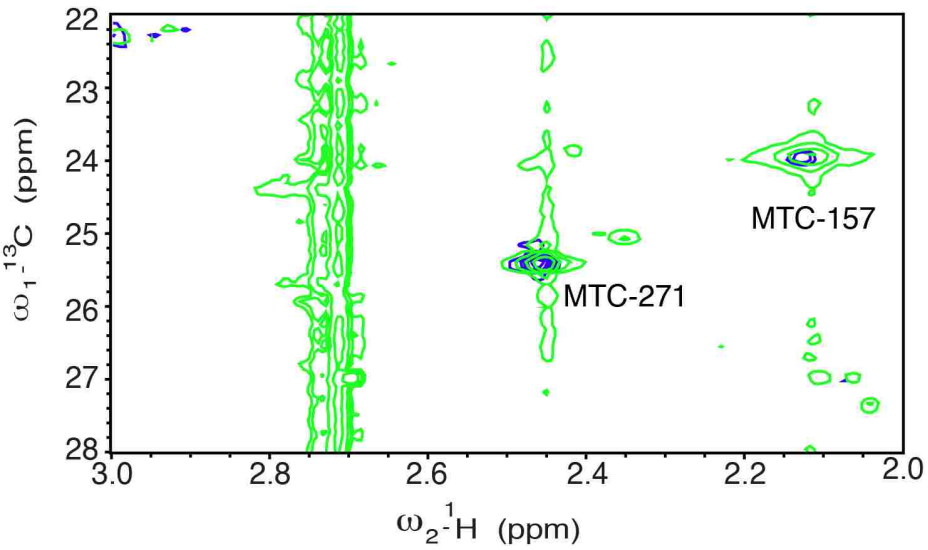

Figure 3.19. Overlay of ^{1}H-^{13}C HSQC spectra of the Q157C/N271C Δ56 CYPOR before (blue) and after (green) the additional ^{13}C-MMTS.

In the earlier report from Galiakhmetov et al., the ^{1}H-^{13}C HMQC spectrum of the Q157C/Q517C Δ56 CYPOR mutant contained a broad peak in the middle near 2.35 ppm ^{1}H, 25.01 ppm ^{13}C (**Figure 3.20., A**). **Figure 3.17.** demonstrates that the ^{1}H-^{13}C HSQC spectra of both protein preparations did not have this artifact any more. To confirm the absence of this peak in the Q157C/N271C Δ56 CYPOR in a methyl-TROSY experiment, a ^{1}H-^{13}C HMQC spectrum was recorded for this mutant (**Figure 3.20., B**). The size of the contours in the ^{1}H-^{13}C HMQC spectra in **Figure 3.20.** are different because these spectra were recorded using different number of increments and resolution settings. The spectrum in **Figure 3.20., A** was collected with a lower number of increments and resolution compared to the one in **Figure 3.20., B**.

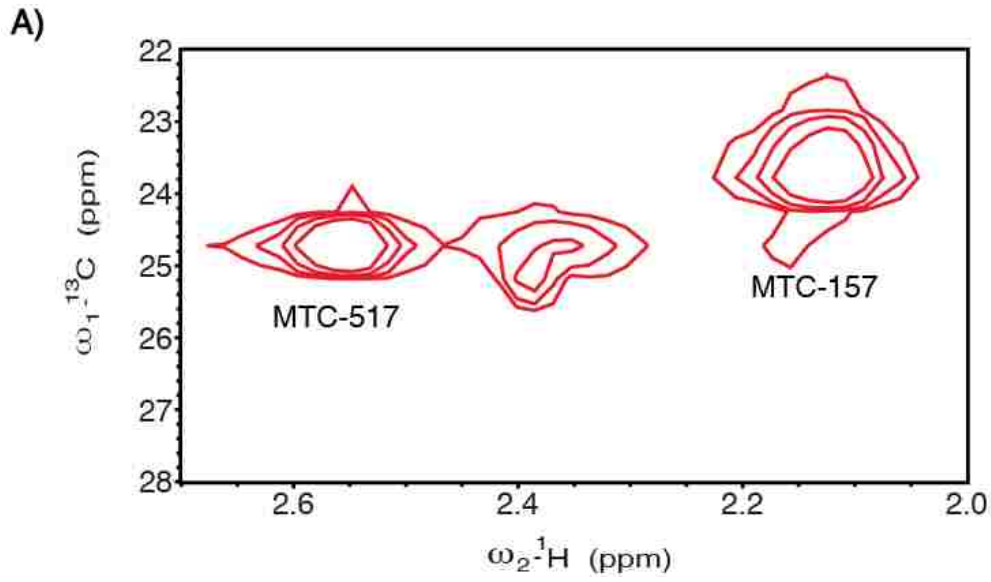

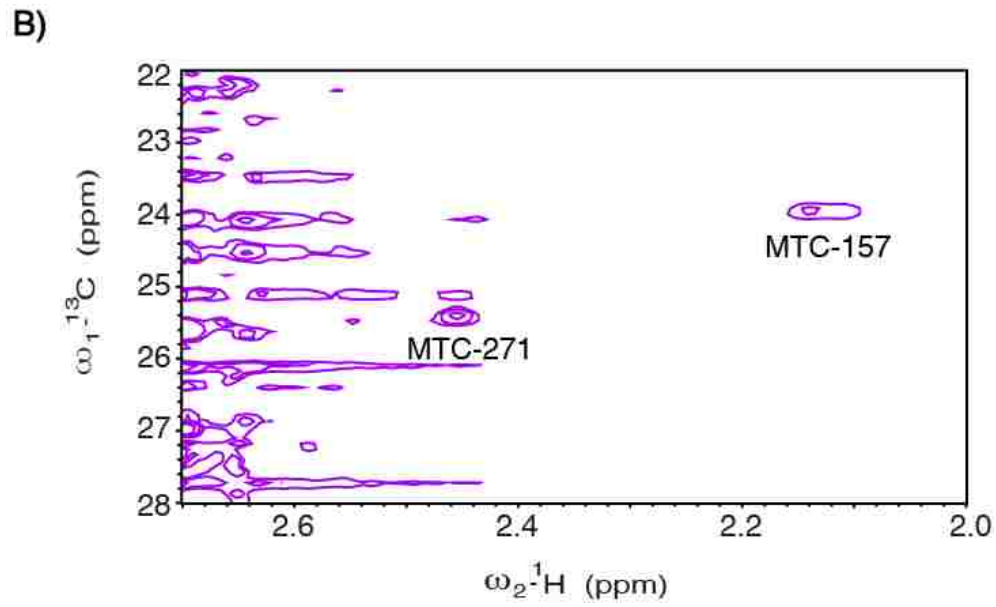

Figure 3.20. ^{1}H-^{13}C HMQC spectra of Δ56 CYPOR. The Q157C/Q517C construct (**A**) from Galiakhmetov et al.,[60] and the Q157C/N271C mutant protein from this study (**B**).

The response of methyl signals to the redox state of the Q157C/N271C Δ56 CYPOR construct was evaluated. A ^{1}H-^{13}C HSQC spectrum was recorded for MTC-157 and MTC-271 in the reduced form of the this mutant and was compared with that of the oxidized protein. **Figure 3.21.** illustrates an overlay of the ^{1}H-^{13}C HSQC spectra for the Q157C/N271C construct in the oxidized (green) and reduced (maroon) states. As shown in this figure, the ^{1}H and ^{13}C chemical shifts for MTC-271 are similar regardless of the redox state of the protein. However, the ^{1}H and ^{13}C chemical shifts for MTC-157 shift to the left upon reduction of the protein.

The observations from **Figure 3.21.** can be explained by the distance that separates these methyl groups from the flavins in Δ56 CYPOR (**Figure 3.22.**). MTC-271 is 28.6 Å away from FAD (**Figure 3.22., A**), whereas MTC-157 is 16.5 Å away from FMN (**Figure 3.22., B**). It is hypothesized that MTC-271 is less sensitive to the redox state of FAD because it is faraway. Thus, it does not sense the changes in the surrounding

environment after reducing the protein. MTC-157, on the other hand, is more sensitive to the redox state of FMN because it is close to it. Thus, it senses the changes in the surrounding environment when FMN is reduced.

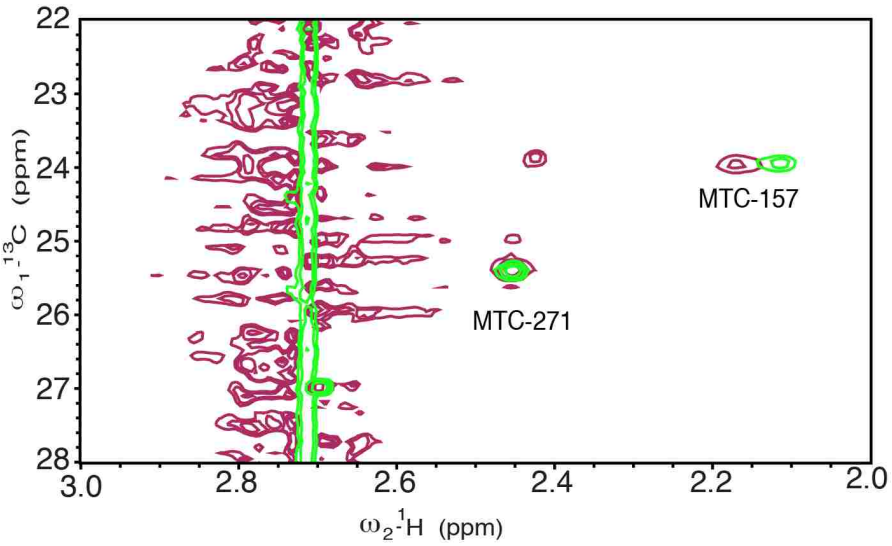

Figure 3.21. Overlay of ^{1}H-^{13}C HSQC spectra of the Q157C/N271C Δ56 CYPOR in the oxidized (green) and reduced (maroon) states.

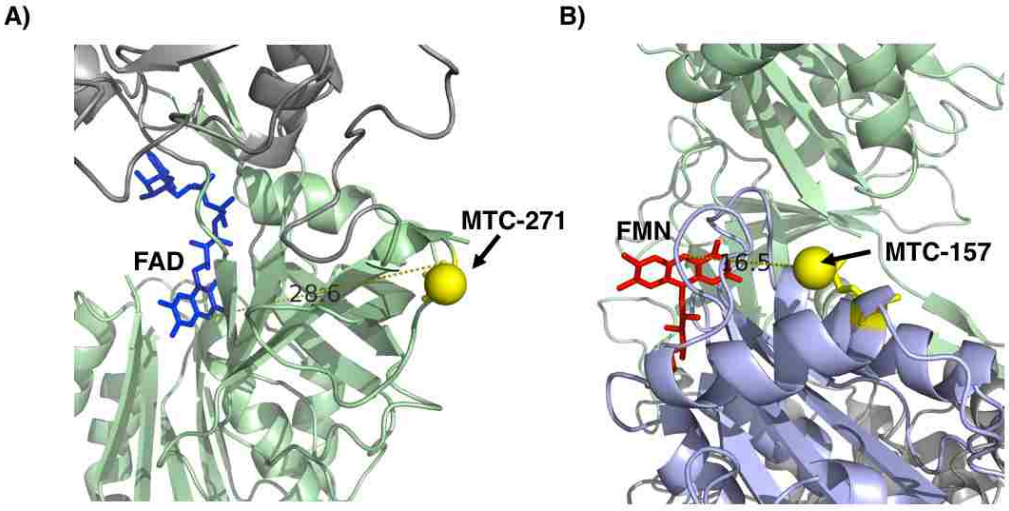

Figure 3.22. Distance between the MTC signals of the Q157C/N271C Δ56 CYPOR and the flavins in the protein. MTC-271 is 28.6 Å away from FAD (**A**), while MTC-157 is 16.5 Å away from FMN (**B**).

3.5 DISCUSSION

The goal of this project was to obtain new methyl assignments of the soluble form of CYPOR. This will enable future studies aimed at better understanding the structure and dynamics of the CYPOR-CYP complex. ^{1}H-^{13}C-HSQC spectra were acquired to establish the MTC-271 resonance assignment. Besides, the project aimed to understand the nature of the middle peak in the ^{1}H-^{13}C-HMQC spectrum of the Q157C/Q517C construct. For this part, a ^{1}H-^{13}C-HMQC spectrum was recorded for the Q157C/N271C **Δ**56 CYPOR and was compared with that of the Q157C/Q517C mutant protein from Galiakhmetov et al.[60] The flavin content in the **Δ**56 CYPOR mutants was not altered, but their reductase activity was greatly diminished.

In regard to the cytochrome c reductase activity of **Δ**56 CYPOR, the Q157C/Q517C mutant exhibited 1.01% of the wild-type reductase activity. Similarly, the Q157C/N271C **Δ**56 CYPOR had 1.02 ± 0.06 % of the wild-type protein activity. Guengerich et al mentioned that a typical activity for NADPH-cytochrome c reductase is when 1 nmol of the protein reduces 3,000 nmol of cytochrome c. In this project, 30.3 nmol of cytochrome c was reduced per minute per 1 nmol of the Q157C/Q517C **Δ**56 CYPOR. Also, 31 ± 2 nmol of cytochrome c was reduced per minute per 1 nmol of the Q157C/N271C construct. This is consistent with the fact that these **Δ**56 CYPOR constructs lack all of their seven-native cysteine amino acids. One of these cysteines is Cys 630, which was previously shown to be critical for CYPOR function.[11,91] Shen et al. mutated this residue to alanine and observed a 49-fold decrease in the enzymatic activity of CYPOR. Cys 630 interacts with NADPH and FAD, and functions as an electron acceptor and donor to FAD.[91] Thus, it was expected that the electron transfer was

obliterated in the cysteine-less constructs of CYPOR used in this project. Hence, cytochrome c was not efficiently reduced by the proteins, and absorbance of the reduced cytochrome c at 550 nm was diminished.

Furthermore, ^{13}C-MMTS labeling of the Q157C/N271C Δ56 CYPOR decreased the reductase activity from 1.02 ± 0.06 % to 1.0 ± 0.2 % of the wild-type protein activity. One possible explanation for this observation is that the interaction between ^{13}C-MMTS and the mutant cysteines in Δ56 CYPOR altered the structure of the protein. This affected its binding and interaction with cytochrome c, resulting in a less efficient electron transfer to cytochrome c.

To determine the flavin content in the Δ56 CYPOR constructs, the proteins were denatured by heat. This slightly shifted the UV-visible absorbance of their flavins towards the lower limit. A good explanation for this observation is that the flavins sensed the changes in their surrounding environment upon heating the proteins. Before heating these constructs, their flavins were bound and buried inside them. After heating, however, they were released into the solution. Yet, denaturing Δ56 CYPOR did not alter the oxidation state of these flavins. This was clear from the 380 nm and 450 nm absorption bands of the oxidized flavins before and after heating the protein constructs. Following that, fluorescence of the flavins' solution in the Q157C/Q517C and the Q157C/N271C Δ56 CYPOR mutants was determined before and after treating them with PDE. Fluorescence of the flavin solution of the Q157C/Q517C construct increased by 1.87 ± 0.08-fold upon the addition of PDE. This indicated that the protein contained some amount of FAD, which was digested by PDE into FMN and AMP. The molar ratio of the flavins in this construct was calculated to be 1.1 ± 0.1 mole of each of FAD and FMN.

This is similar to the flavin content of the wild-type protein which contains one molecule each of FAD and FMN.[92]

The addition of PDE to the flavin solution of the Q157C/N271C construct increased its fluorescence by 1.70 ± 0.08-fold. This denoted that the protein contained some amount of FAD that was digested by PDE into FMN and AMP. The molar ratio of the flavins in this construct was calculated to be 0.8 ± 0.1 mole of each of FAD and FMN. This construct had a lower amount of FMN; probably around 20% of the protein lost its FMN. This observation can be attributed to the fact that the Q157C/N271C construct was not passed through SEC, so it was not very stable, and it lost some of its FMN content. Overall, the surface-localized mutations in the Δ56 CYPOR constructs did not disrupt the interactions between the proteins and their bound flavins.

To create a detailed view of the structural changes in CYPOR in the course of its redox cycle and interaction with CYP proteins, highly-resolved NMR spectra are required. These spectra may be obtained using site-specific methyl labels. Recording ^{1}H-^{13}C HSQC spectra for the two forms of Δ56 CYPOR (the Q157C/Q517C and the Q157C/N271C) allowed to confirm the NMR assignments of MTC-157 and MTC-517. Also, these spectra allowed to establish the new assignment of MTC-271 in the oxidized CYPOR. Furthermore, it was observed that ^{13}C methyl labeling with ^{13}C-MMTS is not always efficient while using the standard protocol described in the literature. The labeling efficiency can be improved by adding the labeling agent directly to the NMR sample. The ^{13}C-MMTS signal is well resolved from the MTC spectral window and minimally interferes with the measurements. Last but not least, it was found that the unidentified "middle peak" that was previously reported in several ^{13}C- MMTS- labeled CYPOR

samples is, indeed, an artifact of sample preparation. The labeling protocol reported in this thesis allowed to prepare NMR samples of the Q157C/Q517C and the Q157C/N271C Δ56 CYPOR that did not contain the middle peak resonance. NMR spectra of these mutants only featured the specific signals from MTC.

3.6 CONCLUSIONS

In this project, a new assignment of MTC-271 was established in the oxidized form of CYPOR. Highly-resolved NMR spectra of the Q157C/Q517C and the Q157C/N271C mutants lacked the middle peak confirming that this peak is an artifact. It was demonstrated that the Q157C, N271C, and Q517C mutations in Δ56 CYPOR did not alter its flavin content. However, cytochrome c reduction activity of this protein was significantly lowered compared to that of the wild-type Δ56 CYPOR. This is probably due to the fact that the CYPOR constructs used in this project lack all of their seven native cysteine residues including Cys 630, which is essential for CYPOR function. In addition, ^{13}C-MMTS labeling lowered the activity of Δ56 CYPOR compared to the unlabeled protein. This is possibly due to alterations in the interactions between Δ56 CYPOR and cytochrome c. The new NMR assignment for the N271 residue in Δ56 CYPOR is a successful step towards obtaining more assignments for important sites in the protein. This may be transferred to the full-length ^{13}C-MMTS labeled CYPOR constructs in lipid nanodisks in the future work.

Chapter 4

FUTURE WORK

4.1 INTRODUCTION

Several vital projects can be established based on the findings and conclusions of this thesis. Future plans will approach the problem of full-length CYPOR extraction and solubilization differently. Rather than using detergents to solubilize the protein, other amphiphiles and organic compounds can be used. These compounds should bind tightly to the protein without denaturing it, and they should stabilize it in aqueous solutions. If one of these alternatives extracts the desired yield of the protein, NMR studies on full-length CYPOR will no longer be a challenge.

In regard to the soluble form of CYPOR, it is important to acquire NMR assignments of other residues in this protein to extend our understanding of its dynamics. These residues should be located in CYPOR, where they act as faithful reporters of the structural changes it undergoes during its catalytic cycle. These residues are proposed to be located in the three domains of CYPOR; this will vary and enrich the acquired NMR data.

4.2 DETERGENT ALTERNATIVES

As discussed previously, solubilization of membrane proteins in aqueous solutions is commonly facilitated by detergents.[21] There are some drawbacks for using these amphiphiles in extraction and solubilization of membrane proteins. First, the concentration of detergents in the solubilization buffer must be higher than their CMC.[93]

This prevents dissociation of the detergent monolayer around the hydrophobic region of membrane proteins and protects them from aggregation.[93] Nevertheless, some of solubilized membrane proteins may be inactivated under this high detergent concentration.[93] Another disadvantage is that many membrane proteins are resistant to solubilization and isolation by the available detergents. An example is cytochrome c oxidase, which is not solubilized easily in many of the TritonX-series detergents.[51] To circumvent these challenges with detergents, less destabilizing compounds can be used to handle membrane proteins in aqueous solutions.[22] This part of chapter 4 introduces three classes of alternative compounds that can be used, in the future, to extract full-length CYPOR. Extraction by these compounds may yield higher amounts of the solubilized protein than those obtained by TritonX-100.

The first alternative compounds to discuss in this chapter are the amphipoles (APols). These are short amphipathic polymers, which have a hydrophilic backbone that is randomly attached to hydrophobic chains.[94] These chains allow APols to form multiple points of attachment along the hydrophobic region of membrane proteins.[94] Hence, these polymers can bind tightly to these regions with a high affinity and a small dissociation constant.[93] **Figure 4.1.** features the structure of one of the commonly used APols, which is polyacrylate-based (A8-35).[95] This is an anionic polymer, which has a hydrophilic polyacrylate backbone that is randomly attached, via amide bonds, to isopropyl and octylamines.[94] An A8-35 APol has a mass of 8 kDa, and 35% (mol/mol) of its carboxyl groups are in the sodium carboxylate form. The other carboxyl groups are attached to octylamines and isopropylamines at percentages of 25% and 40% (mol/mol), respectively.[96]

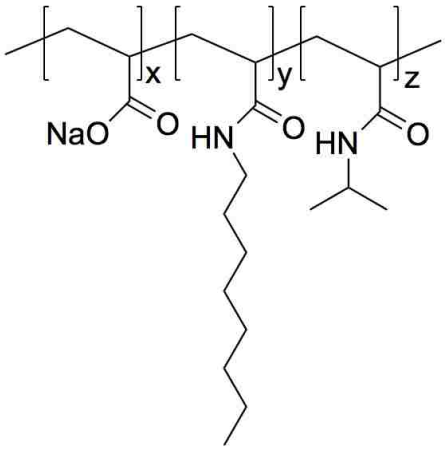

x = 0.35, y = 0.25, z = 0.40

Figure 4.1. Structure of a polyacrylate-based APol (A8-35). The carboxyl groups of this APol are in three forms: 35% in the sodium carboxylate form, 25% are bound to octylamines, and 40% of them are bound to isopropylamines.[96] Percentages represent the mol/mol ratio. The structure was constructed using the ChemDraw molecular editor.

The second type of synthetic compounds to discuss are the tripod amphiphiles (TPAs). These compounds contain a tetra-substituted carbon atom, which is connected to one hydrophilic and three lipophilic chains.[97] This quaternary carbon acts as a rigid center, which restricts flexibility of TPAs.[98] This is opposite to the conventional detergents which have long and flexible hydrocarbon chains. The size and feature of each hydrophilic and hydrophobic chain can be manipulated. This tunes the behavior of TPAs and allows them to adapt to any local variations in membrane proteins that they interact with. It is hypothesized that the appropriate choice of the hydrophobic chains can optimize the interactions of TPAs with the hydrophobic region of membrane proteins.[49]

Figure 4.2. shows the structure of an N-oxide TPA, which has a neutral N-oxide polar moiety and three lipophilic chains.[22]

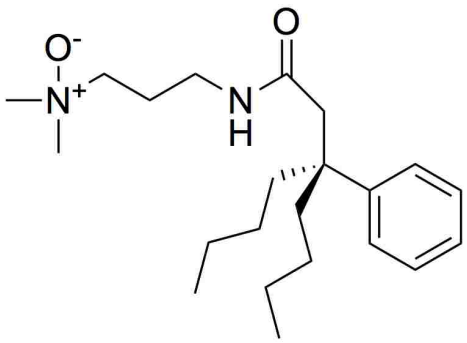

Figure 4.2. Structure of N-oxide TPA. This TPA has a quaternary carbon which is connected to a neutral N-oxide hydrophilic chain and three hydrophobic chains.[49] The structure was built using the ChemDraw molecular editor.

The last type of alternative compounds to discuss in this chapter are the non-detergent sulfobetaines (NDSBs). These compounds have a hydrophilic group that is similar to that of the zwitterionic detergents, but they have a very short hydrophobic tail. Due to their small hydrophobic region, NDSBs cannot form micelles. Thus, they can be easily removed by dialysis.[99] Several types of NDSBs were able to efficiently solubilize proteins without denaturing them, so they could increase the extraction yield of several proteins.[100] **Figure 4.3.** shows the structure of NDSB 201 which has a positively-charged pyridinium and a negatively-charged sulfonate along with a short hydrophobic chain.[100,101]

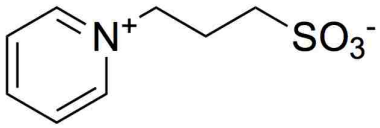

Figure 4.3. Structure of NDSB 201. This compound has a cationic pyridinium and a negatively-charged sulfonate along with a short hydrophobic tail.[100,101] The structure was constructed using the ChemDraw molecular editor.

4.3 OTHER MUTANTS

In chapter 3, characterization and NMR analysis were performed on the Q157C/Q517C and the Q157C/N271C Δ56 CYPOR constructs. The Q157C residue is in the FMN domain of CYPOR, and it is proposed to be sensitive to the redox states of FMN. The Q517C amino acid is in the FAD/NADP(H) domain of the protein, and it is expected to be sensitive to the redox states of FAD and FMN. Also, the N271C residue is in the FAD/NADP(H) domain but distant from FAD, therefore, serves as both a redox control (not affected by reduction) and a membrane-proximity probe with different distances to the membrane in the open and closed conformations of CYPOR.

Understanding the kinetics, thermodynamics, and structural changes of CYPOR may be improved through investigating a series of mutant CYPOR isoforms with methyl probes placed in different locations. This requires a judicious selection of candidate residues in CYPOR to be mutated to cysteines following a few basic criteria. First, these residues must be solvent exposed to allow ^{13}C-MMTS access to the cysteine thiols. Second, the wild-type residue side chain must not be charged and must be similar in size to the cysteine amino acid. This ensures that the overall charge and structure of the protein remains intact, so its stability and catalytic activity remain similar to those of the wild-type protein. Furthermore, these native amino acids should be sensitive to the redox state of the protein or its structural changes. This may be derived from consideration of their distances to the flavins and changes in the environment upon domain closing and opening. With these considerations in mind, five more native residues in the protein are proposed to be sites for the five new methyl signals in methyl-TROSY (**Figure 4.4.**).

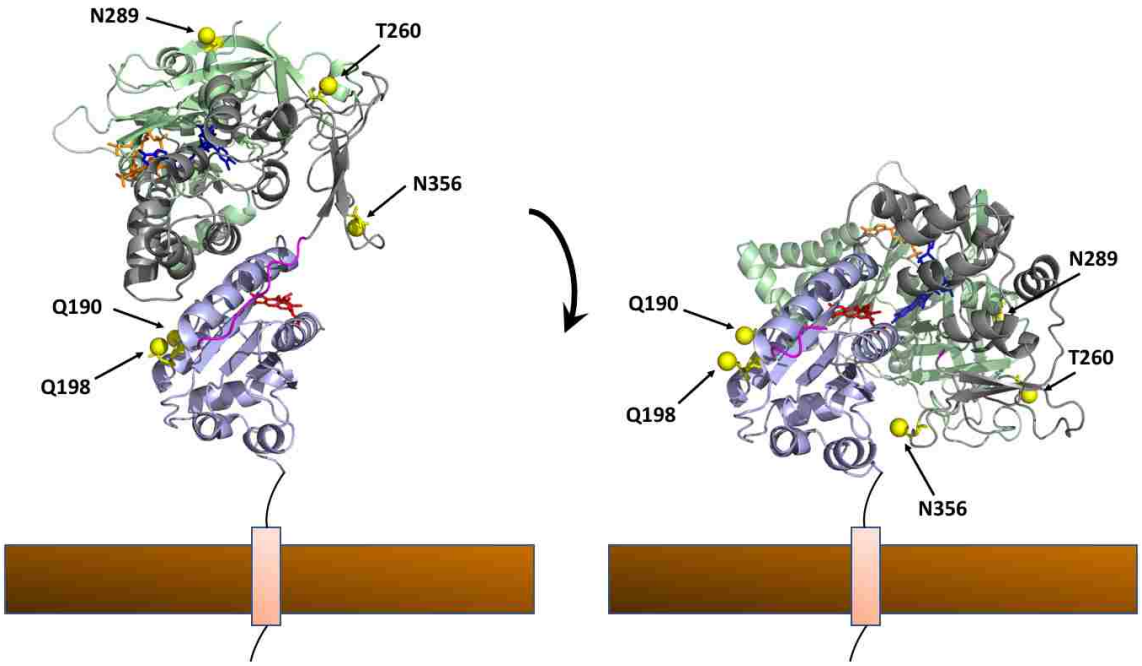

Figure 4.4. Selected wild-type residues in CYPOR for NMR signal assignment. The proposed residues are: Q190 and Q198 in the FMN domain, T260 and N356 in the connecting domain, and N289 in the FAD/NADP(H) domain. Sites of the residues are shown in the open (left) and closed (right) conformations of CYPOR.

The Q190 and Q198 residues are in the FMN domain of CYPOR. The Q190 amino acid is proposed to be sensitive to the redox states of FMN, while Q198 changes its orientation when CYPOR shifts between its conformations. Thus, it is anticipated that the Q198 residue senses the changes in environment during the open and closed transitions of the protein. The T260 and N356 residues are in the connecting domain of CYPOR. The T260 amino acid can serve as a sensor of CYPOR domain motion. The N356 residue is very close to the CYPOR-CYP reaction interface. Thus, this residue may give information about the electron transfer process between these proteins when they interact with each other. Finally, N289 is in the FAD/NADP(H) domain of CYPOR, and it is expected to be sensitive to the redox states of FAD.

4.4 CONCLUSIONS

In summary, this thesis work demonstrates the current findings of research on the full-length and soluble forms of CYPOR. The overall goal of this thesis is to expand the knowledge on CYPOR dynamics, structure, conformational changes, and electron transfer in its membrane-bound and soluble forms. This goal requires, first, improving the yields of the extracted membrane-bound full-length CYPOR by, possibly, using the alternative compounds mentioned in this chapter. Second, it is important to further expand the methyl resonance assignment list for CYPOR to enable more informative methyl-TROSY experiments. In the final stage, it should be possible to produce an NMR sample for CYPOR NMR studies with high-yields and multiple important mutations incorporated in the same protein construct. Using several samples with different subsets of mutants will allow to dramatically increase the information content of NMR measurements. This will enable in-depth structural studies of CYPOR in the course of its functional cycle.

BIBLIOGRAPHY

(1) Waskell, L.; Kim, J. J. P. In *Cytochrome P450: Structure, Mechanism, and Biochemistry, Fourth Edition*; 2015; pp 33–68.

(2) Hubbard, P. a; Shen, a L.; Paschke, R.; Kasper, C. B.; Kim, J. J. *J. Biol. Chem.* **2001**, *276* (31), 29163–29170.

(3) Huang, W. C.; Ellis, J.; Moody, P. C. E.; Raven, E. L.; Roberts, G. C. K. *Structure* **2013**, *21* (9), 1581–1589.

(4) Wang, M.; Roberts, D. L.; Paschke, R.; Shea, T. M.; Masters, B. S. S.; Kim, J.-J. P. *Proc. Natl. Acad. Sci.* **1997**, *94* (16), 8411–8416.

(5) Berg, J. M.; Tymoczko, J. L.; Stryer, L.; Stryer, L. W.H. Freeman, 2002.

(6) Iyanagi, T.; Xia, C.; Kim, J. J. P. *Arch. Biochem. Biophys.* **2012**, *528* (1), 72–89.

(7) Sancho, J. *Cell. Mol. Life Sci.* **2006**, *63* (7–8), 855–864.

(8) Batie, C. J.; Kamin, H. *J. Biol. Chem.* **1981**, *256* (15), 7756–7763.

(9) Frances, O.; Fatemi, F.; Pompon, D.; Guittet, E.; Sizun, C.; Pérez, J.; Lescop, E.; Truan, G. *Biophys. J.* **2015**, *108* (6), 1527–1536.

(10) Hedison, T. M.; Hay, S.; Scrutton, N. S. *FEBS J.* **2015**, *282* (22), 4357–4375.

(11) Xia, C.; Hamdane, D.; Shen, A. L.; Choi, V.; Kasper, C. B.; Pearl, N. M.; Zhang, H.; Im, S. C.; Waskell, L.; Kim, J. J. P. *J. Biol. Chem.* **2011**, *286* (18), 16246–16260.

(12) Meunier, B.; de Visser, S. P.; Shaik, S. *Chem. Rev.* **2004**, *104* (9), 3947–3980.

(13) Porter, T. D.; Coon, M. J. *J. Biol. Chem.* **1991**, *266* (21), 13469–13472.

(14) Kovrigina, E. A.; Pattengale, B.; Xia, C.; Galiakhmetov, A. R.; Huang, J.; Kim, J. J. P.; Kovrigin, E. L. *Biochemistry* **2016**, *55* (43), 5973–5976.

(15) Vincent, B.; Morellet, N.; Fatemi, F.; Aigrain, L.; Truan, G.; Guittet, E.; Lescop, E. *J. Mol. Biol.* **2012**, *420* (4–5), 296–309.

(16) Watson, H. *Essays Biochem.* **2015**, *59* (10), 43–69.

(17) Alberts, B.; Johnson, A.; Lewis, J.; Raff, M.; Roberts, K.; Walter, P. 2002.

(18) Rawlings, A. E. *Biochem. Soc. Trans.* **2016**, *44* (3), 790–795.

(19) Hedin, L. E.; Illergård, K.; Elofsson, A. *J. Proteome Res.* **2011**, *10* (8), 3324–3331.

(20) Krogh, a; Larsson, B.; von Heijne, G.; Sonnhammer, E. L. *J. Mol. Biol.* **2001**, *305* (3), 567–580.

(21) Arachea, B. T.; Sun, Z.; Potente, N.; Malik, R.; Isailovic, D.; Viola, R. E. *Protein Expr. Purif.* **2012**, *86* (1), 12–20.

(22) Chae, P. S.; Laible, P. D.; Gellman, S. H. *Mol. Biosyst.* **2009**, *6* (1), 89–94.

(23) Seddon, A. M.; Curnow, P.; Booth, P. J. *Biochim. Biophys. Acta - Biomembr.* **2004**, *1666* (1–2), 105–117.

(24) Bhairi, S. M.; Mohan, C. *Calbiochem* **2001**, 41.

(25) Popot, J.-L. *Annu. Rev. Biochem.* **2010**, *79* (1), 737–775.

(26) Garavito, R. M.; Ferguson-Miller, S. *J. Biol. Chem.* **2001**, *276* (35), 32403–32406.

(27) Kragh-Hansen, U.; Le Maire, M.; Møller, J. V. *Biophys. J.* **1998**, *75* (6), 2932–2946.

(28) Wiktor, M.; Hartley, O.; Grzesiek, S. *Biophys. J.* **2013**, *105* (11), 2586–2597.

(29) Rabilloud, T. *Methods Mol. Biol.* **2009**, *528*, 259–267.

(30) Anatrace. Detergents and their uses in membrane protein Science https://www.anatrace.com/Technical-Documentation/Catalogs/Anatrace-Detergents-Booklet-FINAL (accessed Jan 31, 2018).

(31) Neugebauer, J. M. *Methods Enzymol.* **1990**, *182* (C), 239–253.

(32) Linke, D. *Methods Enzymol.* **2009**, *463* (C), 603–617.

(33) Uniqema. *Society* **2004**, *37* (10), 1390–1393.

(34) Berger, B. W.; García, R. Y.; Lenhoff, A. M.; Kaler, E. W.; Robinson, C. R. *Biophys. J.* **2005**, *89* (1), 452–464.

(35) PIERCE. Remove detergent from protein samples https://fscimage.fishersci.com/webimages_FSC/downloads/pierce_detergent.pdf (accessed Mar 10, 2018).

(36) Duquesne, K.; Sturgis, J. N. *Methods Mol. Biol.* **2010**, *601*, 205–217.

(37) Le Maire, M.; Champeil, P.; Møller, J. V. *Biochim. Biophys. Acta - Biomembr.* **2000**, *1508* (1–2), 86–111.

(38) Yasui, K.; Uegaki, M.; Shiraki, K.; Ishimizu, T. *Protein Sci.* **2010**, *19* (3), 486–493.

(39) Kalipatnapu, S.; Chattopadhyay, A. *IUBMB Life* **2005**, *57* (7), 505–512.

(40) Hjelmeland, L. M. *Methods Enzymol.* **1990**, *182* (C), 253–264.

(41) Tribet, C.; Diab, C.; Dahmane, T.; Zoonens, M.; Popot, J. L.; Winnik, F. M. *Langmuir* **2009**, *25* (21), 12623–12634.

(42) Murataliev, M. B.; Feyereisen, R.; Walker, F. A. *Biochim. Biophys. Acta - Proteins Proteomics* **2004**, *1698* (1), 1–26.

(43) Aigrain, L.; Pompon, D.; Truan, G. *Biochem. J.* **2011**, *435* (1), 197–206.

(44) Shen, A. L.; Porter, T. D.; Wilson, T. E.; Kasper, C. B. *J. Biol. Chem.* **1989**, *264* (13), 7584–7589.

(45) Porter, T. D.; Wilson, T. E.; Kasper, C. B. *Arch. Biochem. Biophys.* **1987**, *254* (1), 353–367.

(46) Parikh, a; Guengerich, F. P. *Protein Expr. Purif.* **1997**, *9* (3), 346–354.

(47) Cavanagh, J.; Fairbrother, W.; Palmer III, A.; Rance, M.; Skelton, N. 2007; Vol. 2nd.

(48) Lichtenberg, D.; Ahyayauch, H.; Alonso, A.; Goñi, F. M. *Trends Biochem. Sci.* **2013**, *38* (2), 85–93.

(49) Chae, P. S.; Guzei, I. A.; Gellman, S. H. *J. Am. Chem. Soc.* **2010**, *132* (6), 1953–1959.

(50) Chae, P. S.; Kruse, A. C.; Gotfryd, K.; Rana, R. R.; Cho, K. H.; Rasmussen, S. G. F.; Bae, H. E.; Chandra, R.; Gether, U.; Guan, L.; et al. *Chem. - A Eur. J.* **2013**, *19* (46), 15645–15651.

(51) Slinde, E.; Flatmark, T. *BBA - Biomembr.* **1976**, *455* (3), 796–805.

(52) Storm, D. R.; Field, S. O.; Ryan, J. *J. Supramol. Struct.* **1976**, *4* (2), 221–231.

(53) Kerwin, B. A. *J. Pharm. Sci.* **2008**, *97* (8), 2924–2935.

(54) Deechongkit, S.; Wen, J.; Narhi, L. O.; Jiang, Y.; Park, S. S.; Kim, J.; Kerwin, B. A. *J. Pharm. Sci.* **2009**, *98* (9), 3200–3217.

(55) Umbreit, J. N.; Strominger, J. L. *Proc. Natl. Acad. Sci. U. S. A.* **1973**, *70* (10), 2997–3001.

(56) Everberg, H.; Leiding, T.; Schiöth, A.; Tjerneld, F.; Gustavsson, N. *J. Chromatogr. A* **2006**, *1122* (1–2), 35–46.

(57) Cladera, J.; Ricaud, J.-L.; Verde, J. V.; DuNach, M. *Eur. J. Biochem.* **1997**, *243* (3), 798–804.

(58) Chattopadhyay, A.; Harikumar, K. G. *FEBS Lett.* **1996**, *391* (1–2), 199–202.

(59) Herrera, F. E.; Garay, A. S.; Rodrigues, D. E. *J. Phys. Chem. B* **2014**, *118* (14), 3912–3921.

(60) Galiakhmetov, A. R.; Kovrigina, E. A.; Xia, C.; Kim, J.-J. P.; Kovrigin, E. L. *J. Biomol. NMR* **2018**, *70* (1), 21–31.

(61) Protein Purification - Extraction and Clarification - Solubilisation of membrane proteins - EMBL https://www.embl.de/pepcore/pepcore_services/protein_purification/extraction_clarification/solubilisation_membrane_proteins/ (accessed Mar 10, 2018).

(62) Szymczyk, K.; Taraba, A. *J. Therm. Anal. Calorim.* **2016**, *126* (1), 315–326.

(63) Kile, D. E.; Chiou, C. T. *Environ. Sci. Technol.* **1989**, *23* (7), 832–838.

(64) de PINTO, V.; BENZ, R.; PALMIERI, F. *Eur. J. Biochem.* **1989**, *183* (1), 179–187.

(65) Lantez, V.; Nikolaidis, I.; Rechenmann, M.; Vernet, T.; Noirclerc-Savoye, M. *Eng. Life Sci.* **2015**, *15* (1), 39–50.

(66) Schaefer, C.; Rost, B. *BMC Genomics* **2012**, *13* (Suppl 4), S4.

(67) Faivre, L.; Collod-Beroud, G.; Loeys, B. L.; Child, A.; Binquet, C.; Gautier, E.; Callewaert, B.; Arbustini, E.; Mayer, K.; Arslan-Kirchner, M.; et al. *Am. J. Hum. Genet.* **2007**, *81* (3), 454–466.

(68) Hasemann, C. A.; Kurumbail, R. G.; Boddupalli, S. S.; Peterson, J. A.; Deisenhofer, J. *Structure* **1995**, *3* (1), 41–62.

(69) Marohnic, C. C.; Huber Iii, W. J.; Patrick Connick, J.; Reed, J. R.; McCammon, K.; Panda, S. P.; Martásek, P.; Backes, W. L.; Masters, B. S. S. *Arch. Biochem. Biophys.* **2011**, *513* (1), 42–50.

(70) Xia, C.; Panda, S. P.; Marohnic, C. C.; Martásek, P.; Masters, B. S.; Kim, J.-J. P. *Proc. Natl. Acad. Sci. U. S. A.* **2011**, *108* (33), 13486–13491.

(71) Lahiri, S.; Ghoshal, B.; Nandi, D. *J. Clin. Neonatol.* **2012**, *1* (1), 46.

(72) Witchel, S. F. *Steroids* **2013**, *78* (8), 747–750.

(73) Speiser, P. W. *F1000Research* **2015**.

(74) Marohnic, C. C.; Panda, S. P.; McCammon, K.; Rueff, J.; Masters, B. S. S.; Kranendonk, M. *Drug Metab. Dispos.* **2010**, *38* (2), 332–340.

(75) Kleckner, I. R.; Foster, M. P. *Biochim. Biophys. Acta - Proteins Proteomics* **2011**, *1814* (8), 942–968.

(76) Opella, S. J.; Marassi, F. M. *Arch. Biochem. Biophys.* **2017**, *628*, 92–101.

(77) Clore, G. M.; Gronenborn, A. M. *Science* **1991**, *252* (5011), 1390–1399.

(78) Pervushin, K.; Riek, R.; Wider, G.; Wuthrich, K. *Proc. Natl. Acad. Sci.* **1997**, *94* (23), 12366–12371.

(79) Foster, M. P.; McElroy, C. A.; Amero, C. D. *Biochemistry* **2007**, *46* (2), 331–340.

(80) Clore, G. M.; Gronenborn, A. M. *Prog. Nucl. Magn. Reson. Spectrosc.* **1991**, *23* (1), 43–92.

(81) Tugarinov, V.; Hwang, P. M.; Ollerenshaw, J. E.; Kay, L. E. *J. Am. Chem. Soc.* **2003**, *125* (34), 10420–10428.

(82) Gardner, K. H.; Rosen, M. K.; Kay, L. E. *Biochemistry* **1997**, *36* (6), 1389–1401.

(83) Kay, L. E.; Bull, T. E.; Nicholson, L. K.; Griesinger, C.; Schwalbe, H.; Bax, A.; Torchia, D. A. *J. Magn. Reson.* **1992**, *100* (3), 538–558.

(84) Religa, T. L.; Ruschak, A. M.; Rosenzweig, R.; Kay, L. E. *J. Am. Chem. Soc.* **2011**, *133* (23), 9063–9068.

(85) Fruscione, F.; Sturla, L.; Duncan, G.; Van Etten, J. L.; Valbuzzi, P.; De Flora, A.; Di Zanni, E.; Tonetti, M. *J. Biol. Chem.* **2008**, *283* (1), 184–193.

(86) Delaglio, F.; Grzesiek, S.; Vuister, G. W.; Zhu, G.; Pfeifer, J.; Bax, A. *J. Biomol. NMR* **1995**, *6* (3), 277–293.

(87) Goddard, Td.; Kneller, D. G. *Univ. California, San Fr.* **2004**, *14*, 15.

(88) Keeler, J. 2nd ed.; Wiley: United Kingdom, 2010.

(89) Guengerich, F. P.; Martin, M. V.; Sohl, C. D.; Cheng, Q. *Nat. Protoc.* **2009**, *4* (9), 1245–1251.

(90) Aliverti, A.; Curti, B.; Vanoni, M. A. *Methods Mol. Biol.* **1999**, 9–24.

(91) Shen, A. L.; Sem, D. S.; Kasper, C. B. *J. Biol. Chem.* **1999**, *274* (9), 5391–5398.

(92) Gutierrez, A.; Paine, M.; Wolf, C. R.; Scrutton, N. S.; Roberts, G. C. K. *Biochemistry* **2002**, *41* (14), 4626–4637.

(93) Popot, J. L.; Berry, E. A.; Charvolin, D.; Creuzenet, C.; Ebel, C.; Engelman, D. M.; Flötenmeyer, M.; Giusti, F.; Gohon, Y.; Hervé, P.; et al. *Cell. Mol. Life Sci.* **2003**, *60* (8), 1559–1574.

(94) Champeil, P.; Menguy, T.; Tribet, C.; Popot, J. L.; le Maire, M. *J. Biol. Chem.* **2000**, *275* (25), 18623–18637.

(95) Popot, J.-L.; Althoff, T.; Bagnard, D.; Banères, J.-L.; Bazzacco, P.; Billon-Denis, E.; Catoire, L. J.; Champeil, P.; Charvolin, D.; Cocco, M. J.; et al. *Annu. Rev. Biophys.* **2011**, *40* (1), 379–408.

(96) Zoonens, M.; Catoire, L. J.; Giusti, F.; Popot, J.-L. *Proc. Natl. Acad. Sci. U. S. A.* **2005**, *102* (25), 8893–8898.

(97) Yu, S. M.; McQuade, D. T.; Quinn, M. A.; Hackenberger, C. P. R.; Gellman, S. H.; Krebs, M. P.; Polans, A. S. *Protein Sci.* **2000**, *9* (12), 2518–2527.

(98) McQuade, D. T.; Quinn, M. A.; Yu, S. M.; Polans, A. S.; Krebs, M. P.; Gellman, S. H. *Angew. Chem. Int. Ed.* **2000**, *39* (4), 758–761.

(99) Vuillard, L.; Rabilloud, T.; Goldberg, M. E. *Eur. J. Biochem.* **1998**, *256* (1), 128–135.

(100) Goldberg, M. E.; Expert-Bezançon, N.; Vuillard, L.; Rabilloud, T. *Fold. Des.* **1996**, *1* (1), 21–27.

(101) Wangkanont, K.; Forest, K. T.; Kiessling, L. L. *Protein Expr. Purif.* **2015**, *115*, 19–25.

APPENDIX

- **The standard deviation equation used to calculate error in the measurements:**

$$SD = \sqrt{\frac{\Sigma\,(x - \bar{x})^2}{n - 1}}$$

- **Calculation of cytochrome c (cyt c) reduction by Q157/Q517 Δ56 CYPOR (Δ56 CYPOR)**

$$\Delta Abs_{550}(au) = 0.24017076 - 0.10780818 = \ 0.13236258\ au$$

$$\Delta Time\ (seconds) = 200.0500031 - \ 75.05000305 = 125.0000001\ seconds$$

$$\Delta Time\ (minutes) = (125.0000001 seconds) \times \left(\frac{1 minute}{60\ seconds}\right)$$
$$= 2.083333334\ minutes$$

$$\frac{\Delta Abs_{550}}{\Delta Time\ (minutes)} = \frac{0.13236258\ au}{2.083333334\ minutes} = 0.063534038\ au/min$$

$$Total\ activity\ = \frac{{}^{\Delta Abs_{550}}/_{\Delta Time\ (minutes)}}{0.021\ mM^{-1}cm^{-1}} = \frac{0.063534038\ au/min}{0.021\ mM^{-1}cm^{-1}} =$$
$$3.025\ \frac{{}^{au}/_{min}}{mM^{-1}cm^{-1}} = 3.03\ nmol\ of\ cyt\ c\ reduced/min$$

$$Specific\ activity = Total\ activity \div 0.1$$

= 3.03 nmol of cyt c reduced /min ÷0.1 nmol of Δ56 CYPOR
= 30.3 nmol of cyt c reduced / min / 1 nmol of Δ56 CYPOR

$$Percent\ activity\ of\ \Delta 56\ CYPOR =$$

$$\frac{Specific\ activity\ of\ \Delta 56\ CYPOR}{Specific\ activity\ of\ wild - type\ \ CYPOR} \times 100$$

$$= \frac{30.3\ nmol\ cyt\ c/min/1\ nmol\ protein}{3{,}000\ nmol\ cyt\ c\ /min/\ 1\ nmol\ protein} \times 100 = 1.01\ \%$$

- **Calculation of cytochrome c reduction by Q157C/N271C Δ56 CYPOR (Δ56 CYPOR) before and after ^{13}C-MMTS labeling**

  - **Before labeling**

    (1) *sample* 1*:*

    $\Delta Abs_{550}(au) = 0.2446118 - 0.1076667 = 0.1369451\ au$

    $\Delta Time\ (seconds) = 200.056244 - 75.09375 = 124.96249\ seconds$

    $$\Delta Time\ (minutes) = (\ 124.96249\ seconds) \times \left(\frac{1\ minute}{60\ seconds}\right) = 2.0827082\ minutes$$

    $$\frac{\Delta Abs_{550}}{\Delta Time\ (minutes)} = \frac{0.1369451\ au}{2.0827082\ \ minutes} = 0.06575337\ au/min$$

    $$Total\ activity = \frac{\Delta Abs_{550}/_{\Delta Time\ (minutes)}}{0.021\ mM^{-1}cm^{-1}} = \frac{0.06575337\ au/min}{0.021\ mM^{-1}cm^{-1}}$$

    = 3.131 $\frac{au/_{min}}{mM^{-1}cm^{-1}}$ *= 3.13 nmol of cytochrome c reduced / min*

    $Specific\ activity = \ Total\ activity \div 0.1$
    = 3.13 nmol of cyt c reduced / min/0.1 nmol of Δ56 CYPOR
    =31.3 nmol of cyt c reduced/min/1 nmol of Δ56 CYPOR

    $$Percent\ activity\ of\ \Delta 56\ CYPOR = \frac{Secific\ activity\ of\ \Delta 56\ CYPOR}{Specific\ activity\ of\ wild-type\ \ CYPOR} \times 100$$
    $$= \frac{31.3\ nmol\ cyt\ c\ reduced/min/1\ \ nmol\ of\ \Delta 56\ CYPOR}{3{,}000 nmol\ cyt\ c\ /min 1 nmol\ protein} \times 100$$
    $= 1.04\ \%$

    (2) sample 2:

    $\Delta Abs_{550}(au) = 0.25836003 - 0.11765455 = 0.14070548\ au$

    $\Delta Time\ (seconds) = 200.056244 - 75.09375 = 124.96249\ seconds$

    $$\Delta Time\ (minutes) = (\ 124.96249\ seconds) \times \left(\frac{1\ minute}{60\ seconds}\right) = 2.0827082\ minutes$$

$$\frac{\Delta Abs_{550}}{\Delta Time\ (minutes)} = \frac{0.14070548\ au}{2.0827082\ \ minutes} = 0.067558902\ au/min$$

$$Total\ activity = \frac{\Delta Abs_{550}/\Delta Time\ (minutes)}{0.021\ mM^{-1}cm^{-1}} = \frac{0.067558901\ au/min}{0.021\ mM^{-1}cm^{-1}}$$

$= 3.217 \frac{au/min}{mM^{-1}cm^{-1}}$ *= 3.22 nmol of cytochrome c reduced / min*

$Specific\ activity = Total\ activity \div 0.1$
= 3.22 nmol of cyt c reduced / min/0.1 nmol of Δ56 CYPOR
=32.2 nmol of cyt c reduced/min/1 nmol of Δ56 CYPOR

$$Percent\ activity\ of\ \Delta 56\ CYPOR = \frac{Secific\ activity\ of\ \Delta 56\ CYPOR}{Specific\ activity\ of\ wild-type\ \ CYPOR} \times 100$$

$$= \frac{32.2\ nmol\ cyt\ c\ reduced/min/1\ \ nmol\ of\ \Delta 56\ CYPOR}{3{,}000 nmol\ cyt\ c\ /min 1 nmol\ protein} \times 100$$
$= 1.07\ \%$

(3) sample 3:

$$\Delta Abs_{550}(au) = 0.23446098 - 0.10999635 = 0.12446463\ au$$

$$\Delta Time\ (seconds) = 200.056244 - 75.09375 = 124.96249\ seconds$$
$$\Delta Time\ (minutes) = (\ 124.96249\ seconds) \times \left(\frac{1\ minute}{60\ seconds}\right)$$
$$= 2.0827082\ minutes$$

$$\frac{\Delta Abs_{550}}{\Delta Time\ (minutes)} = \frac{0.12446463\ au}{2.0827082\ \ minutes} = 0.059760955\ au/min$$

$$Total\ activity = \frac{\Delta Abs_{550}/\Delta Time\ (minutes)}{0.021\ mM^{-1}cm^{-1}} = \frac{0.059760955\ au/min}{0.021\ mM^{-1}cm^{-1}}$$

$= 2.845 \frac{au/min}{mM^{-1}cm^{-1}}$*= 2.85 nmol of cyt c reduced / min*

$Specific\ activity = Total\ activity \div 0.1$
= 2.85 nmol of cyt c reduced / min/0.1 nmol of Δ56 CYPOR
=28.5 nmol of cyt c reduced/min/1 nmol of Δ56 CYPOR

$$Percent\ activity\ of\ \Delta 56\ CYPOR = \frac{Secific\ activity\ of\ \Delta 56\ CYPOR}{Specific\ activity\ of\ wild-type\ \ CYPOR} \times 100$$
$$= \frac{28.5\ nmol\ cyt\ c\ reduced/min/1\ \ nmol\ of\ \Delta 56\ CYPOR}{3{,}000 nmol\ cyt\ c\ /min 1 nmol\ protein} \times 100$$
$$= 0.950\ \%$$

Average total activity = 3.06 nmol of cyt c reduced / min
Standard deviation of total activity = 0.19
Reported result for total activity before ^{13}C-MMTS labeling = 3.1 ± 0.2

Average specific activity = 30.6 nmol of cytochrome c reduced / min / 1 nmol of Δ56 CYPOR
Standard deviation of specific activity = 1.9
Reported result for specific activity before ^{13}C-MMTS labeling = 31 ± 2

Average percent activity of wild-type Δ56 CYPOR = 1.02 %
Standard deviation of percent activity of wild-type Δ56 CYPOR = 0.06
Reported result for percent activity of wild-type Δ56 CYPOR before ^{13}C-MMTS labeling = 1.02 ± 0.06 %

- **After labeling**

(1) *sample* 1*:*

$$\Delta Abs_{550}(au) = 0.19503616 - 0.08283733 = 0.11219883\ au$$

$$\Delta Time\ (seconds) = 200.056244 - 75.09375 = 124.96249\ seconds$$

$$\Delta Time\ (minutes) = (\ 124.96249\ seconds) \times \left(\frac{1\ minute}{60\ seconds}\right)$$
$$= 2.0827082\ minutes$$

$$\frac{\Delta Abs_{550}}{\Delta Time\ (minutes)} = \frac{0.11219883\ \ au}{2.0827082\ \ minutes} = 0.053871603\ au/min$$

$$Total\ activity = \frac{\Delta Abs_{550}/_{\Delta Time\ (minutes)}}{0.021\ mM^{-1}cm^{-1}} = \frac{0.053871603\ \ au/min}{0.021\ mM^{-1}cm^{-1}}$$
$$= 2.565 \frac{au/_{min}}{mM^{-1}cm^{-1}} = 2.57\ nmol\ of\ cytochrome\ c\ reduced\ /\ min$$

$$Specific\ activity = \ Total\ activity \div 0.1$$

= 2.57 nmol of cyt c reduced / min/0.1 nmol of Δ56 CYPOR
=25.7 nmol of cyt c reduced/min/1 nmol of Δ56 CYPOR

$$\textit{Percent activity of } \Delta 56\ CYPOR = \frac{Secific\ activity\ of\ \Delta 56\ CYPOR}{Specific\ activity\ of\ wild-type\ \ CYPOR} \times 100$$
$$= \frac{25.7\ nmol\ cyt\ c\ reduced/min/1\ \ nmol\ of\ \Delta 56\ CYPOR}{3{,}000 nmol\ cyt\ c\ /min 1 nmol\ protein} \times 100$$
$$= 0.856\ \%$$

(2) *sample 2:*

$$\Delta Abs_{550}(au) = 0.22763531 - 0.07644556 = 0.15118975\ au$$

$$\Delta Time\ (seconds) = 200.056244 - 75.09375 = 124.96249\ seconds$$

$$\Delta Time\ (minutes) = (124.96249\ seconds) \times \left(\frac{1\ minute}{60\ seconds}\right)$$
$$= 2.0827082\ minutes$$

$$\frac{\Delta Abs_{550}}{\Delta Time\ (minutes)} = \frac{0.15118975\ au}{2.0827082\ \ minutes} = 0.072592838\ au/min$$

$$Total\ activity = \frac{\Delta Abs_{550}/_{\Delta Time\ (minutes)}}{0.021\ mM^{-1}cm^{-1}} = \frac{0.072592838\ au/min}{0.021\ mM^{-1}cm^{-1}}$$
=3.456 $\frac{au/_{min}}{mM^{-1}cm^{-1}}$ *= 3.46 nmol of cytochrome c reduced / min*

$$Specific\ activity = \ Total\ activity \div 0.1$$
= 3.46 nmol of cyt c reduced / min/0.1 nmol of Δ56 CYPOR
=34.6 nmol of cyt c reduced/min/1 nmol of Δ56 CYPOR

$$\textit{Percent activity of } \Delta 56\ CYPOR = \frac{Secific\ activity\ of\ \Delta 56\ CYPOR}{Specific\ activity\ of\ wild-type\ \ CYPOR} \times 100$$
$$= \frac{34.6\ \ nmol\ cyt\ c\ reduced/min/1\ \ nmol\ of\ \Delta 56\ CYPOR}{3{,}000 nmol\ cyt\ c\ /min 1 nmol\ protein} \times 100$$
$$= 1.15\ \%$$

(3) *sample 3:*

$$\Delta Abs_{550}(au) = 0.21828732 - 0.09837032 = 0.119917\ au$$

$$\Delta Time\ (seconds) = 200.056244 - 75.09375 = 124.96249\ seconds$$

$$\Delta Time\ (minutes) = (\ 124.96249\ seconds) \times \left(\frac{1\ minute}{60\ seconds}\right)$$
$$= 2.0827082\ minutes$$

$$\frac{\Delta Abs_{550}}{\Delta Time\ (minutes)} = \frac{0.119917\ au}{2.0827082\ minutes} = 0.0575774\ au/min$$

$$Total\ activity = \frac{\Delta Abs_{550}/\Delta Time\ (minutes)}{0.021\ mM^{-1}cm^{-1}} = \frac{0.0575774\ au/min}{0.021\ mM^{-1}cm^{-1}}$$

$=2.741\frac{au/min}{mM^{-1}cm^{-1}}$ *= 2.74 nmol of cytochrome c reduced / min*

$Specific\ activity = Total\ activity \div 0.1$
= 2.74 nmol of cyt c reduced / min/0.1 nmol of Δ56 CYPOR
=27.4 nmol of cytc reduced/min/1 nmol of Δ56 CYPOR

$$Percent\ activity\ of\ \Delta 56\ CYPOR = \frac{Secific\ activity\ of\ \Delta 56\ CYPOR}{Specific\ activity\ of\ wild-type\ \ CYPOR} \times 100$$
$$= \frac{27.4\ \ nmol\ cyt\ c\ reduced/min/1\ \ nmol\ of\ \Delta 56\ CYPOR}{3{,}000 nmol\ cyt\ c\ /min 1 nmol\ protein} \times 100$$
$$= 0.913\ \%$$

Average total activity = 2.92 nmol of cytochrome c reduced / min
Standard deviation of total activity = 0.47
Reported result for total activity after ^{13}C-MMTS labeling = 2.9 ± 0.5

Average specific activity = 29.2 nmol of cytochrome c reduced / min
Standard deviation of specific activity = 4.7
Reported result for specific activity after ^{13}C-MMTS labeling = 29 ± 5

Average percent activity of wild-type Δ56 CYPOR = 0.973 %
Standard deviation of percent activity of wild-type Δ56 CYPOR = 0.15
Reported result for percent activity of wild-type Δ56 CYPOR after ^{13}C-MMTS labeling = 1.0 ± 0.2 *%*

- **Calculations of the flavin content in Q157C/Q517C Δ56 CYPOR**

(1) sample (1):

$$F_o = 6.3282 \times 10^4$$
$$F_{fin} = 1.17503 \times 10^5$$

$$r = \frac{\left(10 \times \left(\frac{F_{fin}}{F_o}\right) - 10\right)}{10 - \left(\frac{F_{fin}}{F_o}\right)} = \frac{\left(10 \times \left(\frac{1.17503 \times 10^5}{6.3282 \times 10^4}\right) - 10\right)}{10 - \left(\frac{1.17503 \times 10^5}{6.3282 \times 10^4}\right)} = \frac{8.5681}{8.1431}$$
$$= 1.0521$$

$$Fluoresence\ increase\ in\ \Delta\ \text{CYPOR} = \frac{1.17503 \times 10^5}{6.3282 \times 10^4}$$
$$= 1.8568 \text{ fold increase}$$

So, increase by ~ 1.86 -fold

(2) sample (2):

$$F_o = 5.7492 \times 10^4$$
$$F_{fin} = 1.12522 \times 10^5$$

$$r = \frac{\left(10 \times \left(\frac{F_{fin}}{F_o}\right) - 10\right)}{10 - \left(\frac{F_{fin}}{F_o}\right)} = \frac{\left(10 \times \left(\frac{1.12522 \times 10^5}{5.7492 \times 10^4}\right) - 10\right)}{10 - \left(\frac{1.12522 \times 10^5}{5.7492 \times 10^4}\right)} = \frac{9.5717}{8.0428}$$
$$= 1.1900$$

$$Fluoresence\ increase\ in\ \Delta\ \text{CYPOR} = \frac{1.12522 \times 10^5}{5.7492 \times 10^4}$$
$$= 1.9571 \text{ fold increase}$$

So, increase by ~ 1.96-fold

(3) sample (3):

$$F_o = 5.5562 \times 10^4$$
$$F_{fin} = 9.9939 \times 10^4$$

$$r = \frac{\left(10 \times \left(\frac{F_{fin}}{F_o}\right) - 10\right)}{10 - \left(\frac{F_{fin}}{F_o}\right)} = \frac{\left(10 \times \left(\frac{9.9939 \times 10^4}{5.5562 \times 10^4}\right) - 10\right)}{10 - \left(\frac{9.9939 \times 10^4}{5.5562 \times 10^4}\right)} = \frac{7.9869}{8.2013}$$
$$= 0.97385$$

$$Fluoresence\ increase\ in\ \Delta\ \text{CYPOR} = \frac{9.9939 \times 10^4}{5.5562 \times 10^4}$$
$$= 1.7986 \text{ fold increase}$$

So, increase by ~ 1.80-fold

Average "r" = 1.071
Standard deviation of "r" = 0.10
Reported result "r" = 1.1± 0.1

Average increase in fluorescence = 1.87
Standard deviation of increase in fluorescence = 0.08
Reported result increase in fluorescence = 1.87± 0.08

- **Calculations of the flavin content in Q157C/N271C Δ56 CYPOR**

(1) sample (1):

$F_o = 8.4526 \times 10^4$
$F_{fin} = 1.5177 \times 10^5$

$$r = \frac{\left(10 \times \left(\frac{F_{fin}}{F_o}\right) - 10\right)}{10 - \left(\frac{F_{fin}}{F_o}\right)} = \frac{\left(10 \times \left(\frac{1.5177 \times 10^5}{8.4526 \times 10^4}\right) - 10\right)}{10 - \left(\frac{1.5177 \times 10^5}{8.4526 \times 10^4}\right)} = \frac{7.9554}{8.2044}$$
$$= 0.96965$$

$$Fluoresence\ increase\ in\ \Delta\ \text{CYPOR} = \frac{1.5177 \times 10^5}{8.4526 \times 10^4}$$
$$= 1.7955 \text{ fold increase}$$

So, increase by ~ 1.80-fold

(2) sample (2):

$F_o = 9.8639 \times 10^4$
$F_{fin} = 1.6626 \times 10^5$

$$r = \frac{\left(10 \times \left(\frac{F_{fin}}{F_o}\right) - 10\right)}{10 - \left(\frac{F_{fin}}{F_o}\right)} = \frac{\left(10 \times \left(\frac{1.6626 \times 10^5}{9.8639 \times 10^4}\right) - 10\right)}{10 - \left(\frac{1.6626 \times 10^5}{9.8639 \times 10^4}\right)} = \frac{6.8554}{8.3144}$$
$$= 0.82452$$

$$Fluoresence\ increase\ in\ \Delta\ \text{CYPOR} = \frac{1.6626 \times 10^5}{9.8639 \times 10^4}$$
$$= 1.6855 \text{ fold increase}$$

So, increase by ~ 1.69-fold

(3) sample (3):

$$F_o = 1.0656 \times 10^5$$
$$F_{fin} = 1.7352 \times 10^5$$

$$r = \frac{\left(10 \times \left(\frac{F_{fin}}{F_o}\right) - 10\right)}{10 - \left(\frac{F_{fin}}{F_o}\right)} = \frac{\left(10 \times \left(\frac{1.7352 \times 10^5}{1.0656 \times 10^5}\right) - 10\right)}{10 - \left(\frac{1.7352 \times 10^5}{1.0656 \times 10^5}\right)} = \frac{6.2837}{8.3716}$$
$$= 0.75059$$

$$Fluoresence\ increase\ in\ \Delta\ \text{CYPOR} = \frac{1.7352 \times 10^5}{1.0656 \times 10^5}$$
$$= 1.6283 \text{ fold increase}$$

So, increase by ~ 1.63-fold

Average "r" = 0.84825
Standard deviation of "r" = 0.111
Reported result "r" = 0.8 ± 0.1

Average increase in fluorescence = 1.70
Standard deviation of increase in fluorescence = 0.084
Reported result increase in fluorescence = 1.70± 0.08

- Manuscript submitted to the Protein Expression and Purification journal. Below is the link to the editor and reviewer comments once available.

  - **Manuscript Title:** Extraction of a recombinant full-length NADPH-cytochrome P450 oxidoreductase from bacterial membranes: effect of detergents and additives

  - **URL for the Submitted Manuscript to the Protein Expression and Purification Journal**:

http://www.evise.com/profile/api/navigate/PREP?resourceUrl=%2Fco-author%2F%3Fdgcid%3Dinvite_email_coauthoroutreach10465928%23%2FPREP%2Fsubmission%2FPREP_2018_110

- **URL to the Deposited Manuscript**:

https://www.biorxiv.org/content/early/2018/03/08/279216